

**PH.D. DISSERTATION**

**Urban Energy Information Modeling: A framework to  
quantify the thermodynamic interactions between the  
natural and the built environment that affect building  
energy consumption**

**Shalini Ramesh**

Center for Building Performance and Diagnostics  
School of Architecture, Carnegie Mellon University  
Pittsburgh, Pennsylvania, United States

August 11, 2017

**Doctoral Committee**

**Khee Poh Lam**, PhD, Professor, FRIBA (Chair)

School of Architecture, Carnegie Mellon University

**Kristen Kurland**, Teaching Professor of School of Architecture & Information Systems  
and Public Policy

School of Architecture & H. John Heinz III College, Carnegie Mellon University

**Steve Kardinal Jusuf**, PhD, CEng (UK) MCIBSE, LEED Green Associate,

Assistant Professor

Sustainable Infrastructure Engineering, Singapore Institute of Technology

**Mikako Harada**, PhD, AEC Workgroup Technical Lead and Americas Manager

Autodesk, Inc.

## Copyright Declaration

---

I hereby declare that I am the sole author of this thesis.

I authorize Carnegie Mellon University, Pittsburgh, PA, USA to lend this thesis to other institutions or individuals for the purpose of scholarly research.

I authorize Carnegie Mellon University, Pittsburgh, PA, USA to reproduce this thesis by photocopying or by other means, in total or in part, at the request of other institutions or individuals for the purpose of scholarly research.

Copyright © 2017 Shalini Ramesh. All rights reserved.

*Dedicated to my beloved parents,  
my fiancée David Stover and  
my friends Joerose Tharakan and Sanah Sabharwal*

## Acknowledgement

The successful completion of this doctoral dissertation is and will always be one of the most important achievements in my life. I would like to express my gratitude to the following people that have made this possible.

First and foremost, I would like to give my deepest gratitude to my Thesis Advisor and Committee Chair - Professor Khee Poh Lam. For the past six years, he has been an extraordinary mentor not only for my research but also enhancing my teaching skills, domain expertise and most importantly, setting the bar high to produce quality work. His in-depth knowledge of the current industry trends opened several opportunities for me to present my work as well as gain industry experience. I am grateful to continue collaborating with him and his team after graduation through my role in my job.

I would like to thank my PhD committee member – Professor Kristen Kurland from the School of Architecture and Information Systems & Public Policy. I not only learned how to utilize GIS above and beyond the realm of the most commonly used arenas today, but was also able to establish an integrated approach between the field of urban scale energy simulation and GIS. I would like to specially thank Kristen for her moral support and encouragement during the final and hardest stage of my dissertation.

I would like to thank my PhD committee member – Professor Steve Kardinal Jusuf from Singapore Institute of Technology. His expert knowledge in the microclimate modeling domain helped me formulate the scope of my thesis. In addition, he was also extremely instrumental in providing focused technical feedback for my thesis document.

I would like to thank my PhD committee member – Mikako Harada, from Autodesk, Inc. Her comments and suggestions over the past three years has helped me think about the importance and real-world implications of my research.

Additionally, I would like to express my gratitude to Xiaoshan Yang, Assistant Professor at Nanjing Technological University. His support and time provided a solid foundation to the development of my thesis objectives.

I would like to give my sincere gratitude to Jason Wirick, Sarah States, John Buck, Chao Ding and Bertrand Lasternas who have helped with my case-study at the Phipps Center for Sustainable Landscapes. The case-study measurement data would not have been possible without their support and time.

I would like to give my special thanks to Nisha Shanmugaraj and Juliann Reineke from the CMU Global Communications Center who provided valuable comments and writing guidance throughout my thesis writing.

Special thanks to my amazing batch mates and colleagues at the Intelligent workplace: Darlene Covington Davis, Surekha Tetali, Haopeng Wang, Erica Cochran, Weili Xu, Adrian Chong, Omer T. Karaguzel, Zhiang Zhang, Nina Baird, Rohini Srivastava, Flore Marion, and Latina Awomolo.

Lastly, this journey would not have been possible without the strength, support and encouragement from my parents - Ramesh Kalyan and Usha Ramesh, my partner - David Stover and my two best friends - Sanah Sabharwal and Joerose Tharakan.

## Abstract

By 2050, the world's population is expected to reach 9.7 billion, with over half living in urban settlements (United Nations, 2015). Planning and designing new urban developments and improving existing infrastructure will create or reshape urban landscapes and will carry significant implications for energy consumption, infrastructure costs, and the urban microclimate on a larger scale. Researchers and industry professionals must recognize how changes in land use affect the urban microclimate and, therefore, building energy consumption. Built environment and microclimate studies commonly involve modeling or experimenting with mass and energy exchanges between natural and the built environment. Current methods to quantify these exchanges include the isolated use of microclimate and building energy simulation tools. However, current urban planning and building design processes lack a holistic and seamless approach to quantifying all thermodynamic interactions between natural and built environments; nor is there a method for communicating and visualizing the simulated building energy data. This dissertation has developed a coupling method to quantify the effects of the urban microclimate on building energy consumption. The coupling method was tested on a medium-sized office building and applied to a design case, a redevelopment project in Pittsburgh, PA. Three distinct approaches were used.

First, to develop the coupling method, a study was conducted to quantify the importance of accurate microclimate model initialization for achieving simulation results that represent measured data. This initialization study was conducted for 24 cases in the Pittsburgh climate. The initialization study developed a rule-based method for estimating the number of ENVI-met simulations needed to predict the microclimate for an annual period.

Second, a coupling method was developed to quantify these microclimate effects on building energy consumption. The Center for Sustainable Landscapes (CSL) building was used as a test-case for this coupling method to measure improvement in predicting building heating and cooling energy consumption. Results show that the coupling method, more than the TMY3 weather data used for energy simulations, can improve building energy consumption predictions for the winter and summer months.

Third, to demonstrate industry implications, the coupling method was applied to a design case, the Lower Hill District Redevelopment, Pittsburgh, PA. Comparing the decoupled energy model and TMY3 weather data revealed a high degree of variation in the heating and cooling energy consumption. Overall results reinforced the hypothesis that building surface level coupling is not essential if the energy model accounts for the microclimate effects.

A Design Decision Support (DDS) method was also developed as a tool for project stakeholders to communicate high-fidelity simulated energy data.

**Keywords:** urban energy information modeling, urban microclimate, building energy simulation, building energy consumption, design decision support, urban planning, building design

This page is intentionally left blank



# Table of Contents

Copyright Declaration.....	II
Acknowledgement.....	IV
Abstract .....	VI
This page is intentionally left blank.....	VIII
List of Figures.....	XII
List of Tables .....	XVII
<b>Chapter 1: Introduction .....</b>	<b>1</b>
1.1. Background .....	1
1.2. Literature review .....	3
1.2.1. Effects of the urban microclimate on building energy consumption.....	3
1.2.2. Existing methods and tools.....	8
1.2.3. Review of quantitative methods for evaluating microclimate model performance.....	15
1.2.4. Communication and visualization methods for design decision support.....	16
1.3. Summary of literature review and knowledge gap.....	21
1.4. Hypotheses.....	24
1.5. Objectives.....	24
1.6. Dissertation chapter overview .....	25
<b>Chapter 2: Research Method .....</b>	<b>27</b>
2.1. Overview .....	27
2.2. Summary of tools used in the research study .....	27
2.2.1. ENVI-met v4.0 (Microclimate simulation) .....	28
2.2.2. EnergyPlus v8.5 (Building energy simulation) .....	31

2.2.3. Building Controls Virtual Test Bed (BCVTB).....	33
2.3. Method Description .....	34
2.3.1. Automation and modeling of ENVI-met area input model .....	36
2.3.2. ENVI-met microclimate model initialization .....	37
2.3.3. Coupling of urban microclimate model with building energy model .....	39
2.3.4. Visualizing simulated building energy data .....	48
2.4. Summary .....	51

### **Chapter 3: Urban Microclimate Modeling: setup, simulation and model**

<b>performance.....</b>	<b>52</b>
3.1. Overview .....	52
3.2. Case-study for urban microclimate modeling .....	52
3.3. Experimental setup for simulated & measured data comparison .....	55
3.4. Urban microclimate model generation and initialization .....	58
3.5. Comparison of simulated data to measured data .....	63
3.5.1. Analysis of air temperature and relative humidity .....	64
3.5.2. Statistical analysis of simulated with experiment measured air temperature .....	67
3.6. Analysis of ENVI-met model initialization .....	68
3.6.1. Method to derive number of ENVI-met simulations for an annual period....	77
3.6.2. Analysis of simulated and measured façade temperature.....	78
3.7. Summary .....	84

### **Chapter 4: Implementation of coupling method to improve building energy**

<b>consumption predictions .....</b>	<b>86</b>
4.1. Overview .....	86
4.2. Building energy model description.....	86
4.3. Data mapping and exchange between ENVI-met and EnergyPlus .....	89
4.4. Implementation of coupling platform.....	92

4.5. Effects of coupling microclimate data on façade temperature .....	94
4.6. Effects of coupling microclimate on building energy consumption .....	101
4.8. Summary .....	111
<b>Chapter 5: Design case implementation of the coupling method to improve building energy consumption predictions .....</b>	<b>113</b>
5.1. Overview .....	113
5.2. Design case – Lower Hill District mixed-use redevelopment .....	113
5.3. ENVI-met microclimate model and EnergyPlus model description .....	114
5.4. Analysis of Building Energy consumption .....	116
5.5. Visualization Method (Design Decision Support) .....	124
5.6. Importance of the Design Decision Support (DDS) .....	126
5.6. Summary .....	133
<b>Chapter 6: Conclusion.....</b>	<b>134</b>
6.1. Summary of findings .....	134
6.1.1. Hypothesis testing results.....	134
6.2. Industry applicability .....	137
6.3. Limitations .....	140
6.4. Future work .....	141
<b>References.....</b>	<b>144</b>
<b>Appendices.....</b>	<b>156</b>
<b>Appendix A: Analysis of façade temperature for CSL case-study .....</b>	<b>157</b>
<b>Appendix B: Synthesized workflow to implement visualization platform .....</b>	<b>159</b>

## List of Figures

Figure 1. Profile of the urban heat island (UHI) phenomenon (Daniel, 2017) .....	2
Figure 2. Building energy flow paths (Clarke, 2001) .....	7
Figure 3. 3D visualization of real-time measured data using Project Dasher .....	17
Figure 4. 3D CFD flow visualization in SimulationHub.....	18
Figure 5. 2D energy map of block level energy consumption for New York .....	18
Figure 6. 3D City information model developed with ArcGIS Pro .....	19
Figure 7. Autodesk BIM 360 Glue 3D visualization .....	19
Figure 8. Thermodynamic interactions between the built and the natural environment (adapted from ENVI-MET, 2017).....	28
Figure 9. ENVI-met sub-models (Bruse, 2004).....	29
Figure 10. EnergyPlus – Internal modeling elements (DOE).....	32
Figure 11. The BCVTB co-simulation platform .....	34
Figure 12. Overview of thesis method .....	35
Figure 13. Workflow for automating ENVI-met model generation.....	36
Figure 14. Layout of receptors for recording simulated data in ENVI-met .....	40
Figure 15. Variables implemented and the input source in the coupling platform .....	42
Figure 16. Method for coupling ENVI-met microclimate simulation data and EnergyPlus model .....	44

Figure 17. As-built view of the Center for Sustainable Landscapes (Schrag, 2017) ....	53
Figure 18. Location of the CSL Building .....	54
Figure 19. ENVI-met microclimate model of the CSL building .....	55
Figure 20. ENVI-met model receptor points corresponding to the experiment setup ....	56
Figure 21. Equipments used to measure air and façade temperature .....	57
Figure 22. CSL experiment setup along the south façade .....	58
Figure 23. Automation of ENVI-met microclimate model for CSL .....	59
Figure 24. Flowchart indicating ENVI-met simulation input parameters and source (Ramesh and Lam 2015).....	61
Figure 25. Comparison of simulated and measured data for January 20 - 22 .....	68
Figure 26. Comparison of simulated and measured data for February 20 – 22 .....	70
Figure 27. Comparison of simulated and measured data for February 20 – 22 .....	71
Figure 28. Comparison of simulated and measured data for April 13 - 15.....	73
Figure 29. Comparison of simulated and measured data for April 13 - 15.....	73
Figure 30. Comparison of simulated and measured data for June 2 - 4.....	74
Figure 31. Comparison of simulated and measured data for August 15 -17.....	75
Figure 32. Comparison of simulated and measured data for October 4 - 6 .....	76
Figure 33. Schematic layout of 7-node wall and roof construction in ENVI-met (Simon, 2016).....	79
Figure 34. DesignBuilder model of the CSL building .....	87

Figure 35. First floor plan of the CSL building .....	88
Figure 36. Layout of receptors for recording simulated data in ENVI-met for the CSL case-study .....	90
Figure 37. BCVTB module for data extraction and mapping.....	91
Figure 38. BCVTB coupling module for convective and radiative fluxes for the CSL case-study .....	93
Figure 39. Comparison of north façade temperature in the summer .....	94
Figure 40. Comparison of east façade temperature in the summer.....	95
Figure 41. Comparison of south façade temperature in the summer .....	95
Figure 42. Comparison of west façade temperature in the summer.....	96
Figure 43. Comparison of north façade temperature in the winter .....	97
Figure 44. Comparison of south façade temperature in the winter.....	98
Figure 45. Comparison of east façade temperature in the winter.....	98
Figure 46. Comparison of west façade temperature in the winter .....	99
Figure 47. Comparison of building energy consumption in the winter .....	104
Figure 48. Comparison of building energy consumption in the winter .....	104
Figure 49. Comparison of building energy consumption in the summer.....	106
Figure 50. Comparison of building energy consumption in the summer .....	107
Figure 51. Comparison of building energy consumption in a swing period .....	108
Figure 52. Comparison of building energy consumption in a swing period .....	109

Figure 53. Lower Hill District study area (design case) .....	114
Figure 54. Automation of ENVI-met microclimate model for the Lower Hill District	115
Figure 55. ENVI-met model domain for the Lower Hill District design case .....	116
Figure 56. DesignBuilding (EnergyPlus) model of Building G1 .....	116
Figure 57. Comparison of building energy consumption in the winter .....	117
Figure 58. Comparison of building energy consumption in the winter .....	118
Figure 59. Comparison of building energy consumption in a swing period .....	119
Figure 60. Comparison of building energy consumption in a swing period .....	120
Figure 61. Comparison of building energy consumption in the summer .....	121
Figure 62. Comparison of building energy consumption in the summer .....	122
Figure 63. Development of DDS method using ESRI's Web Scene .....	125
Figure 64. Visualization of simulated energy consumption data using ArcGIS Pro and Web Scene .....	128
Figure 65. Visualization of annual and monthly energy consumption data from building level to floor level .....	129
Figure 66. ESRI's Story map provides detail on the energy simulation input parameters .....	130
Figure 67. Story map provides details on the zoning criteria for the Lower Hill District .....	131
Figure 68. Story map provides daylight and shadow analysis for the Lower Hill District .....	132

Figure 69. Industry applicability to implement the coupling method during conceptual design..... 139



## List of Tables

Table 1. Summary of literature review and knowledge gap .....	23
Table 2. ENVI-met model configuration and area file input parameters .....	62
Table 3. Statistical comparison of simulated and weather station measured air temperature and relative humidity .....	64
Table 4. Statistical comparison of simulated and experiment measured air temperature .....	67
Table 5. Comparison of simulated and measured north façade temperature .....	81
Table 6. Comparison of simulated and measured south façade temperature .....	82
Table 7. Percentage difference in heating/cooling energy consumption using TMY3, measured and simulated weather data .....	110
Table 8. Percentage difference in heating/cooling energy consumption using TMY3, measured and simulated weather file .....	123

# Chapter 1: Introduction

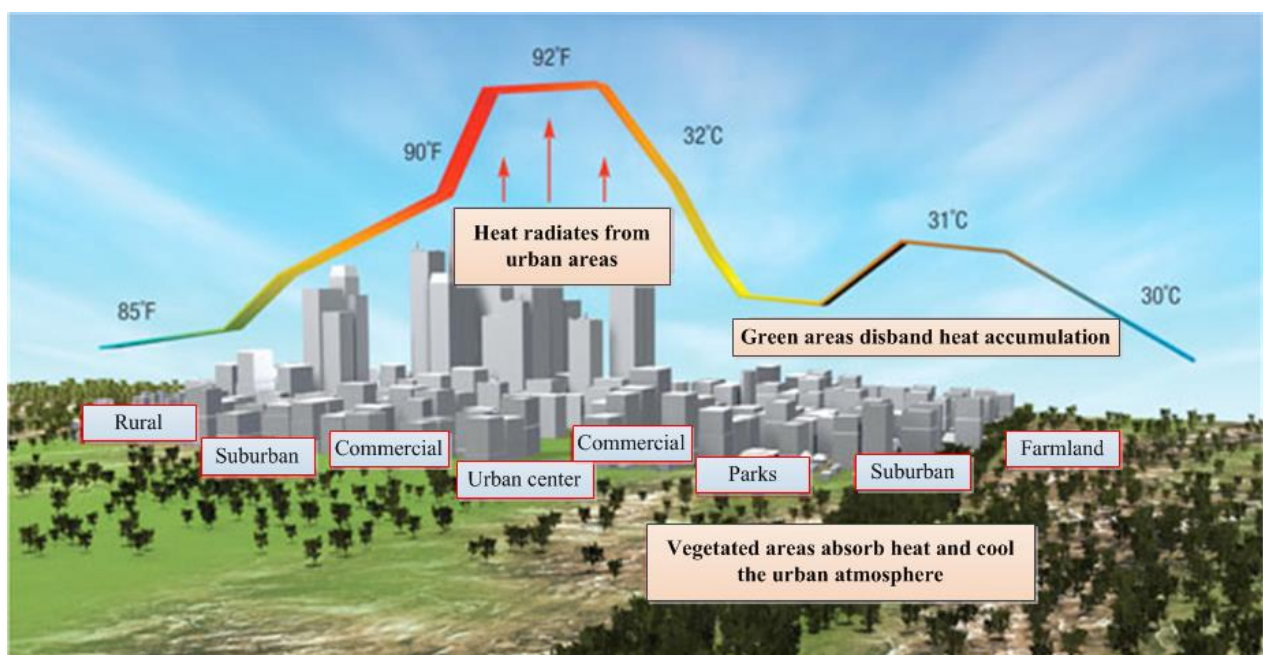
## 1.1. Background

In today's increasingly global and interconnected world, over half of the population (54%) now lives in urban areas, up from 30% in 1950. As reported by the United Nations, the coming decades will bring further profound changes to the size and the spatial distribution of the global population: in 2050, 66% of the world's population is projected to be living in urban spaces. Rapid and unplanned urbanization has serious global impacts that are beginning to affect life on earth, such as climate change leading to higher temperatures; changing landscapes and wildlife habitat; rising sea levels; and increasing risks of storms, droughts, and floods. Impacts of urbanization on the global scale can be realized on city or neighborhood scale in the form of change in urban fabric. Buildings, roads and other infrastructure replace open land and vegetation. Such urban changes negatively affect the environment, mainly by releasing heat and producing pollutants, and modifying the atmosphere's physical and chemical properties. The cumulative effect of these modifications in the urban fabric have amplified the development of urban microclimates giving rise to "urban heat islands" (UHI).

UHIs are characterized by higher urban air temperatures than are found in suburban areas (Figure 1). Numerous factors influence UHIs, as follows (Oke, 1973):

1. Urban street canyons induce radiation trapping. Longwave radiation loss toward the sky is reduced and multiple reflections of shortwave radiation decrease the effective albedo, thus increasing the solar irradiation trapping.

2. Thermal properties of the built environment (building façade, roads, pavements, vegetation) increase the storage of sensible heat in the fabric of a city.
3. A decrease in vegetation reduces evapotranspiration from urban areas.
4. Anthropogenic heat is released from various human activities (transportation, heat rejection from buildings, etc.).
5. Increased longwave irradiation from the warm urban atmosphere causes an urban greenhouse gas effect.



**Figure 1. Profile of the urban heat island (UHI) phenomenon (Daniel, 2017)**

Because of the above-mentioned interactions between the natural and built environments, the microclimate of an area is almost instantly affected. For example, microclimate changes can be observed in air temperature, wind speed, and wind direction.

Conversely, the microclimate of an area has implications for outdoor water use, air quality, and energy use in buildings, thus adversely affecting humans' well-being. The extent of changes in the microclimate greatly depends on such factors as thermal and radiative properties of urban materials, building size and type, and the canyon geometry.

The thermodynamic heat fluxes generated from these interactions affect urban heat transfer and building energy consumption (Yaghoobian and Kleissi, 2012).

According to Architecture 2030 (2017), buildings accounts for approximately 48% of the total energy consumption making them the largest energy consuming sector compared to industrial (24%) or transportation (28%). Therefore, assessing the effects of a changing urban microclimate on building energy consumption is a step toward improving energy predictions that can, in turn, drive energy-efficient design.

## **1.2. Literature review**

For a better understanding of the effects of urban microclimate on building energy consumption and the existing methods for quantifying these effects, previous research studies are reviewed in the following four sections.

### **1.2.1. Effects of the urban microclimate on building energy consumption**

UHIs, which are characterized by higher urban temperatures as compared to suburban areas, are a manifestation of the negative impact of urbanization. Several studies have been conducted in various countries to quantify the temperature differences between rural and urban locations. Many studies have observed that, as a consequence of this modified urban microclimate, buildings in urban areas consume more energy for cooling, though less energy for heating, compared to rural areas. Extensive research has been conducted since the late 1980s in countries with mild climates as well as those with heating and cooling-dominated climates—including Japan, Canada, Greece, UK, USA, Spain, Hong Kong, Sweden, and Singapore—to demonstrate the impact of urban microclimates on energy consumption. Results from a selection of these studies are summarized as follows:

1. In cooling-dominated climates, urban areas experienced cooling load increases and heating load decreases compared to suburban areas. Studies by Santamouris et al. (2001) and Santamouris (2014) in Athens, Greece showed an increase in cooling load and a decrease in heating load owing to higher temperatures in the urban centers. These studies were conducted on commercial office buildings using weather data from stations located in the urban, suburban, and green areas. Weather data from urban versus suburban areas showed that the cooling load for the former increased close to 200%, and the heating load reduced approximately 30–50%. This phenomenon was attributed to high density surroundings, lack of green areas, industrial activity and high vehicle traffic compared to suburban areas. The studies also noted a reduction in natural ventilation potential in the urban centers caused by a decrease in wind velocity.

Rong (2006) examined heating and cooling energy consumption for residential buildings in Texas. Results showed that compared to a suburban area, the cooling load increased by approximately 6%, and the heating load decreased by 16%. The study attributed this phenomenon to an increase of cooling degree hours and a decrease of heating degree hours. However, Rong also noted that on a global scale, total energy consumption of residential buildings increased only 1% in a cooling dominated climate. A second study (Sun & Augenbroe, 2014) used a DOE reference commercial building type to demonstrate more specifically the impact of UHI on cooling and heating degree days. For Texas cities, such as Houston and El Paso, when buildings located in large city centers were compared to those in suburban areas, the analysis showed an increase in cooling degree days by ~1500 degree days and a decrease in heating degree days by only ~100 degree days. This

change in degree days directly translates into an overall increase in cooling load and a slight decrease in heating load.

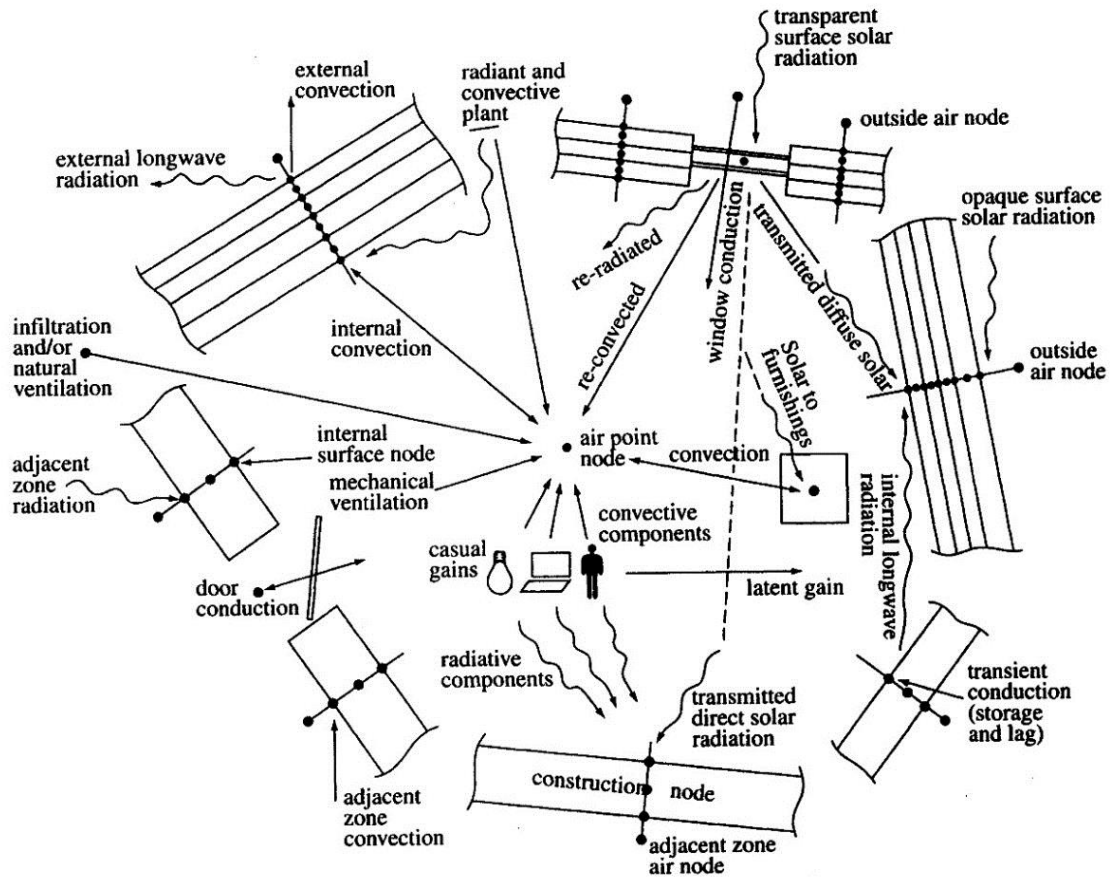
2. In heating-dominated climates, buildings in urban areas experience a variable reduction in the heating energy consumption owing to the UHI effect. A study by Kolokotroni et al. (2012) in London, UK, evaluated the impact of UHI on the heating and cooling load for an office building located in the city center. The study observed a decrease in heating load and an increase in cooling load for a building located in the city center versus a suburban area. Furthermore, the heating load was predicted to decrease between 35% and 45%, and the cooling load to increase between 23% and 30% by 2050. This increase and decrease in the building loads was attributed to the increasing air temperatures caused by UHIs in the city centers.

Within the US, Rong (2006) also documented the impact of UHI on a residential building in New York City. The study found an increase of nearly 220% per year in cooling energy consumption but only a 7% decrease per year in the heating energy consumption. This increase and decrease in cooling and heating energy consumption was attributed to an increasing UHI effect in the urban areas as compared to the rural areas. Additionally, the total energy consumption of a household in the state of New York decreased between 3% and 7%, again owing to the UHI effect. As documented by Santamouris (2014), similar UHI studies in heating-dominated climates in the US as those of Boston, MA, and Washington, DC, show similar trends.

Based on the above studies, the following can be concluded:

1. Increases in urban density cause UHIs, which modify the microclimate and which are characterized by higher ambient air temperatures and changes in wind speed and wind direction, as compared to suburban areas. Such changes in the microclimate exacerbate buildings' heating and cooling energy consumption.
2. In cooling-dominated climates, the increase in cooling energy consumption because of the UHI effect is much higher than the corresponding decrease in heating energy consumption. Conversely, in heating dominated climates, a decrease in heating energy consumption is noted with only a slight increase in cooling energy consumption. These increases and decreases in cooling and heating energy consumption are attributed to higher ambient air temperatures.

Such increases and decreases are also a function of design and operational characteristics, including the heating and cooling set point temperature, thermal zoning, zone ventilation rate, ventilation type, building insulation, and building infiltration rate. As outdoor ambient temperatures exceed the zone set point for most of the cooling period, the convective and radiative properties of the building envelope cause an increase in cooling energy consumption. In addition, as the zone ventilation rates increase, more energy is required to cool the outside air and meet the zone set point temperature. During the heating period, ambient air temperatures in urban areas are higher, resulting in the reduction of heating energy consumption.



**Figure 2. Building energy flow paths (Clarke, 2001)**

To improve building energy consumption predictions during the design stage, the findings discussed above reinforce the need to quantify the thermodynamic interactions between the natural and built environments (Figure 2).

Current urban planning and building design follow a somewhat linear process. Planning and design usually begin with a layout of the street grid, land use patterns, and building forms without accounting for resultant changes to the surrounding microclimate. Architects and system engineers then work on an individual building's system with limited knowledge concerning the implications of the urban microclimate on the building's energy consumption. Energy simulation engineers then predict the building's energy consumption based on weather data recorded at a remote site, typically located near the closest airport, or else typical meteorological year (TMY3) data. TMY3s are data



sets that contain hourly values of solar radiation and meteorological elements for a 1-year period (NREL, 2017). Depending on data availability, the base periods for the TMY3 algorithm span 1976–2005 and 1991-2005 (Wilcox & Marion, 2008). Thus, because TMY3s do not capture current microclimate conditions, they cannot be used to improve building energy consumption predictions.

Besides a paucity of local site weather data, designers and energy engineers lack the methods, tools, and expert knowledge to account for the effect of the microclimate when predicting building energy consumption. Many current urban microclimate assessment tools have been developed by climatologists; thus, they focus more on atmospheric physics than on such urban design variables as vegetation, building form, materials, outdoor air temperature, or wind patterns. Therefore, a more sophisticated approach is needed for quantifying the thermodynamic interactions between the urban microclimate and building systems. Section 1.2.2 provides a detailed review of the existing tools and coupling methods for predicting and quantifying the effects of urban microclimate on building energy consumption.

### **1.2.2. Existing methods and tools**

Building energy simulation is widely used for the following: (1) predicting the operational energy use and its corresponding greenhouse gas emissions (2) predicting energy reductions that can be achieved through appropriate urban planning and architectural design by employing energy efficient design strategies over a given baseline. For both cases, it is very important to simulate energy predictions, keeping in mind the thermodynamic effects of urban microclimate on building energy consumption once the building is built (Sun and Augenbroe, 2014).

### 1.2.2.1. Existing urban microclimate models and tools

Several models and tools can quantify UHI effects on urban microclimate on various scales. First, the urban mesoscale model is used at the city level (i.e., an area that is larger than a few hundred square meters). Second, the urban microscale model is employed with smaller neighborhoods

The first category of atmospheric models is the urban mesoscale model, in which the buildings are represented as urban form and which does not provide detailed modeling of the building geometry. The urban fabric consists of such physical parameters as landscapes, city furniture and vegetation, and the atmosphere above the urban area. The existing urban mesoscale model in urban climatology that is widely used for weather prediction is the Town Energy Balance (TEB) model (Masson, 2000).

The TEB model (Schoetter et al., 2015) uses as parameters the town-atmosphere dynamic and thermodynamic interactions. The city is represented as buildings that have the same height and width within the model mesh, the roof level being at the surface level of the atmospheric model. The buildings are modelled along identical roads, the lengths of which are greater than the widths. The other parameters that make up the city characteristics relate to roof, road, and building façade characteristics: albedo, emissivity, thickness, thermal conductivity and heat capacity. An average surface temperature is assumed for each of the three elements, roofs, roads and building facades.

Although the TEB model is an advancement from previous mesoscale models, it has limitations for predicting a single building's energy consumption. Masson (2000) identified the limitations of the TEB model as follows:

1. A grid mesh size larger than a few hundred meters (city scale) is required to employ the TEB model. Therefore, city-scale climate prediction results cannot be

coupled with a microscale building energy model to improve the building energy consumption predictions.

2. The TEB model offers a two-dimensional approximation of the 3D urban landscape. Although on a city scale the TEB model can predict atmospheric conditions accurately, because of the geometry approximation, larger domain size, and simplified thermal model, this model cannot be used to predict thermodynamic interactions on a building-by-building scale.
3. The vegetation model is a simplified model and does not take into account foliage temperature, complex exchange processes (transpiration and thermal shielding) and 3D vegetation modeling.

The second category of atmospheric models is the urban microclimate models. These models explicitly represent building geometry in varying degrees of detail. Examples of the existing tools used to calculate heat balance conditions are 3D-CAD and CitySim

The 3D-CAD tool uses a geographic information system (GIS) to model the buildings, ground surfaces, and vegetation (Asawa et al., 2008) for predicting the surface temperature distribution of buildings and outdoor spaces. The 3D-CAD model is transformed into a 3D-mesh model for heat balance calculations, which consider direct and reflected solar radiations, sky solar radiation, long-wave radiation, and convective heat transfer flux. The algorithm also accounts for weather conditions (relative humidity, air temperature, cloud cover and wind velocity). Although the 3D-CAD tool considers the convective and radiative effects between natural and built environments, the tool is designed primarily to estimate the surface and mean radiant temperatures of outdoor spaces. As noted by the author, the tool is used primarily as a thermal design and UHI prediction tool; hence, it does not incorporate the algorithms required for building energy

consumption predictions. Therefore, the tool currently cannot simulate a building energy model to estimate building energy consumption.

CitySim (Robinson et al., 2009)—built on its predecessor, SUNTool—uses a Java-based GUI to simulate and optimize building-related flows. The modeling of the 3D building is simplified to the building form as opposed to floor- and zone-level details. The calculation models for radiation and convection are simplified. The HVAC model is based on the psychrometry of humid air, which is considered an ideal mixture of air and vapor. As noted by Darren (2011), CitySim does not support detailed mechanical system design and control. Owing to the limitations of the thermal and the mechanical system models, CitySIM is not recommended for detailed building energy modeling. Berthou et al. (2015) and Page et al. (2013) also noted that CitySIM is an urban planning tool for street to district level modeling and calculation of renewable energy generation versus detailed building-by-building energy modeling.

#### **1.2.2.2. Existing building energy simulation tools**

Several energy simulation tools have been documented by Crawley et al. (2008) and Lam (2012). These energy simulation tools include BLAST, BSim, DeST, DOE.2 1E, Ecotect, Energy Express, Energy-10, DesignBuilder, eQUEST and EnergyPlus. Ideally, designers expect to be able to use the same tool for early stage design and for advancing their model as the design develops through the construction, commissioning, and monitoring stages. Currently, based on research, EnergyPlus is considered the most robust and comprehensive simulation tool that can address detailed energy modeling and model calibration based on measured data and cost estimation. However, it has significant limitations with respect to quantifying the thermodynamic effects on building energy consumption, mainly because EnergyPlus can simulate only a single building for which

the surrounding elements are assumed as shading elements. Therefore, during the simulation the energy model does not consider the various thermodynamic interactions between buildings, vegetation, and outside air. To quantify the effects of these thermodynamic interactions on building energy consumption, it is important to couple EnergyPlus with a microclimate simulation tool.

### **1.2.2.3. Existing coupling methods to quantify urban microclimate effects on building energy consumption**

Several studies have been conducted in coupling the effects of the urban microclimate on building energy consumption to various degrees of resolution.

At the mesoscale, Bueno et al. (2011) demonstrated a coupling scheme using TEB and EnergyPlus. Although EnergyPlus models can be very detailed, several limitations exist when coupling EnergyPlus with TEB. As discussed previously, the TEB model offers only a two-dimensional approximation of the urban canyon to represent urban 3D building geometry. In terms of radiation effects and surface temperature, TEB assumes average values for shortwave and longwave radiation on roofs, roads, and walls. These radiation effects and surface temperature calculations are performed on a district scale that measures up to a few hundred meters, not on individual façade or single building scale. The building energy model integrated in TEB is a one-node, single zone model. Therefore, the energy model does not represent actual building construction in terms of various material layers and properties or individual thermal zones. Therefore, as noted by Schoetter et al. (2015), because the TEB model is not designed for simulations at the scale of one building to represent actual building design but rather a representative building model, it cannot improve building energy consumption predictions.

Peng and Elwan (2012) demonstrated a reduced-order coupling, using ENVI-met for microclimate simulations and Ecotect for energy simulations, in generating urban site-specific weather files. Although the study accounted for the site-specific microclimate, the thermal model in Ecotect is a simplified CIBSE admittance method (Autodesk, 2016) for calculating the heating and cooling loads. In addition, Ecotect does not allow the definition of HVAC systems, a vital component in assessing building energy consumption and system efficiency. It should also be noted that Ecotect is now obsolete, so it could not be used to advance this research.

Similarly, a second study conducted by Oxizidis et al. (2008) generated site-specific weather files that are used for EnergyPlus simulation. The study used the MM5 model (UCAR, 2016) to generate site-specific weather data for 12 typical days representing each month of the year. First, this is a reduced order coupling because the method does not account for the effects of urban microclimate on such individual factors as convective and radiative heat flux and infiltration. Second, MM5 is a mesoscale climate model that does not represent the urban microclimate for single building energy simulation. Therefore, this method cannot be used to improve building energy consumption predictions on a microscale (single building).

More recently, studies conducted by Malys et al. (2015) and Bouyer et al. (2011) coupled SOLENE thermo-radiative models with CFD. The convective heat transfer coefficient was calculated using air temperature and mass rate of moisture. The thermal model was based a nodal network model, where each zone is assumed at a homogenous air temperature range. This means that each floor of the building was considered as one zone with the same indoor air temperature set-point. This single zone model does not accurately represent a building design with multiple thermal zones. In addition, long-

wave radiation and infiltration, which affect building energy consumption, are not accounted for. Although the study used the effect of convective heat transfer coefficient for coupling, the method has not been evaluated with measured data.

In contrast to the previous methods, Yang et al. (2012) demonstrated a one-way coupling between two sophisticated tools: the microclimate simulation tool ENVI-met v4.0 and the building energy simulation tool EnergyPlus v6. The method adopted for coupling overrides the convective heat transfer coefficient at every simulation time-step to calculate the zone energy balance through the energy balance for building outer surfaces. Owing to limitations in Energy Plus v6.0, the convective heat flux and long-wave radiation calculations did not consider the outside surface temperatures. This coupling model also excluded the implementation of infiltration in EnergyPlus, which has a big impact on building cooling energy consumption. In addition, this coupling model was built for a small hypothetical, test-case building in China. Hence, it does not represent a real-world building energy model with as-built design and construction details. Additionally, because of the hypothetical test case, the performance of the coupling method was not evaluated with measured building energy consumption.

Summarizing all the above-mentioned methods and tools for coupling thermodynamic interactions with a building energy model, it can be concluded that the study by Yang et al. (2012) may be the most robust method. This is because the method uses two simulation tools, ENVI-met and EnergyPlus, which are capable of modeling and predicting microclimate and building energy with a high degree of accuracy and detail. However, this method still lacks the full implementation of all the variables that affect the accurate prediction of building energy consumption. Therefore, this thesis proposes to extend the coupling method demonstrated by Yang et al. (2012).

### 1.2.3. Review of quantitative methods for evaluating microclimate model performance

The next step after developing the coupling platform is to test the accuracy of the microclimate simulated results with measurement data. Therefore, this section reviews variables and statistical metrics used by previous studies for a quantitative evaluation of the ENVI-met model performance.

Studies by Yang et al. (2013) and Wang et al. (2016) evaluated the performance of the ENVI-met model by comparing air temperature, relative humidity, surface temperature, and mean radiant temperature with measurement data. Yang et al. (2013) used root mean square error (RMSE), square of correlation coefficients ( $R^2$ ), and index of agreement (d). This study showed that  $R^2$  for all comparison variables (i.e., air temperature, relative humidity, and surface temperature) ranged between 0.52 and 0.97. The study by Wang et al. (2016) used  $R^2$  to compare the simulated and measured air temperature. The comparison showed that  $R^2$  ranged between 0.60 and 0.83 for air temperature in the winter and summer months.

Huttner (2012) evaluated ENVI-met model performance during its development from v3.0 to v4.0. The model had significant improvements in terms of modeling detailed building façade (i.e., 3-node to 7-node) and initializing the model boundary conditions (i.e., forcing air temperature and relative humidity). The statistical metric used to evaluate the performance of the ENVI-met v4.0 model is maximum deviation. The variables used to compare measured and simulated data were mean radiant temperature, air temperature, relative humidity, and wind speed.



Based on the above-mentioned studies, this thesis uses RMSE, correlation coefficient (R), and thermographic images as performance metrics to evaluate the ENVI-met microclimate model results. The variables used for this analysis are simulated air temperature, relative humidity, and building façade temperature.

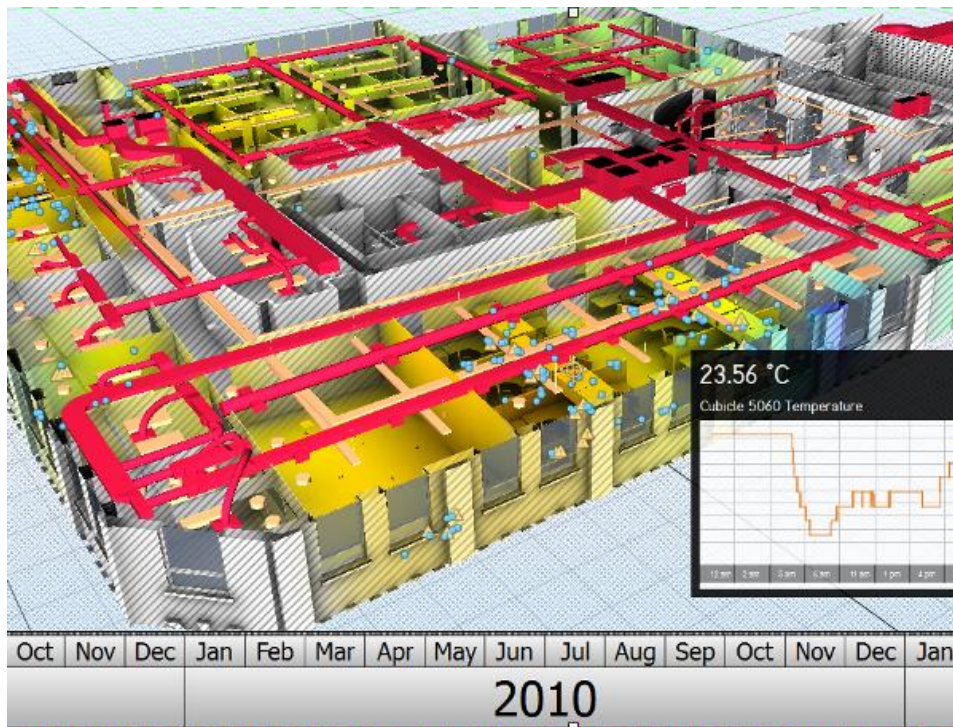
#### **1.2.4. Communication and visualization methods for design decision support**

Once the coupling platform is implemented and its performance evaluated, it is essential to map this high-fidelity simulated energy data spatially and temporally. This information is particularly important for urban planners and building designers in terms of optimizing energy consumption through sustainable design strategies. However, communication of high-fidelity urban scale simulated data can be cumbersome and error prone. Therefore, it is important to understand the availability of tools and methods for developing a design-decision-support method for urban energy information modeling.

First, the visualization applications available in the industry—Project Dasher (Autodesk Inc., 2017) and SimulationHub (CCTech, 2017) —were reviewed. Project Dasher is an ongoing research project from Autodesk (Figure 3).

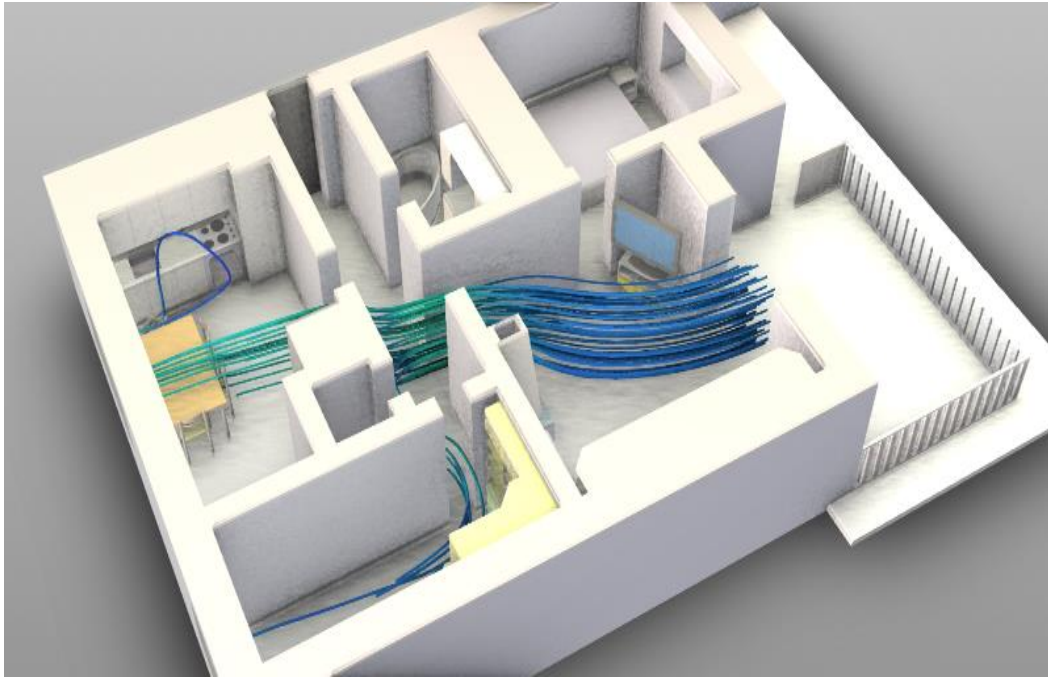
This is a BIM-based application that provides building owners with real-time building performance throughout the building life-cycle. The application uses building information modeling that acts as a visualization hub wherein collected data from various sources is aggregated and presented in 3D. This process helps to infer more complex causal relationships that pertain to building performance and the overall building operational requirements. Although the platform enables 3D visualization of real-time data, visualization of simulated data is not possible. It would be ideal if Project Dasher

could provide visualization of simulated data during design and construction, followed by real-time measured data during the operational phase.



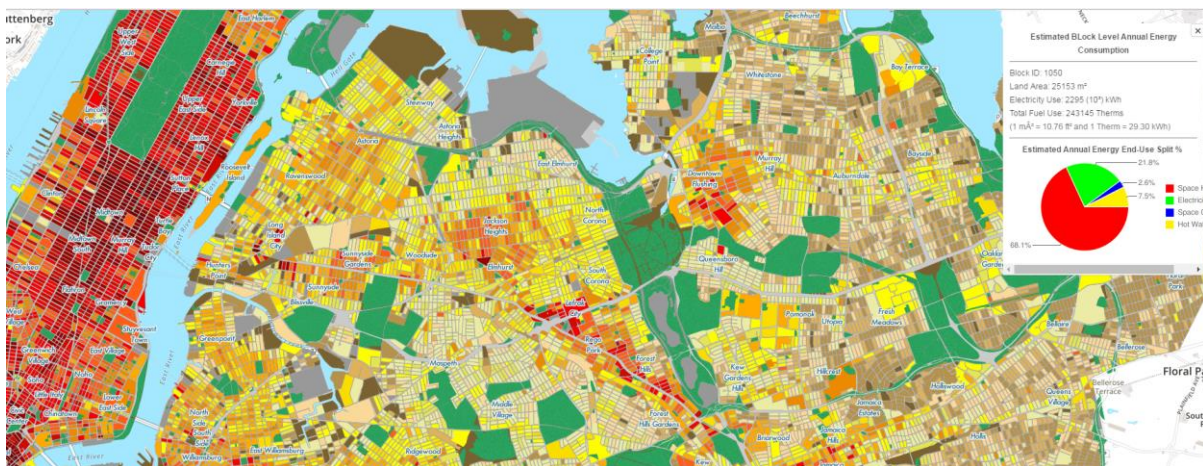
**Figure 3. 3D visualization of real-time measured data using Project Dasher (Autodesk, Inc., 2017)**

A second application, known as SimulationHub (Figure 4), is a cloud-based 3D CFD flow simulation app for designers that can be used across multiple platforms from mobile, tablet, and desktop devices (Center for Computational Technologies Private Limited, 2017). The primary use of this tool is for CFD flow simulations, not only in buildings but also in mechanical devices. However, this tool is able to provide visualization only for the simulated data within the tool and not simulated data from external tools.



**Figure 4. 3D CFD flow visualization in SimulationHub  
(CCTech, 2017)**

Second, in reviewing visualization platforms developed in the research field, Howard et al. (2012) demonstrated the visualization of New York City energy distribution using a 2D energy map (Figure 5). OpenStreetMap was the platform used to map the energy data. Annual energy end-use consumption was calculated using multiple linear regression to obtain electricity and total fuel intensities. However, this energy data visualization is purely on a 2D block/parcel level and does not provide 3D simulated data integration.



**Figure 5. 2D energy map of block level energy consumption for New York**

Padsala and Coors (2015) detailed SimStadt, a conceptual web-based, 3D city information model, using CityGML, a universally accepted, open, XML-based data model format for storing, representing, and sharing 3D urban models (Figure 6). The CityGML file was converted into an ArcGIS-compatible multipatch shapefile format for visualization.



Figure 6. 3D City information model developed with ArcGIS Pro

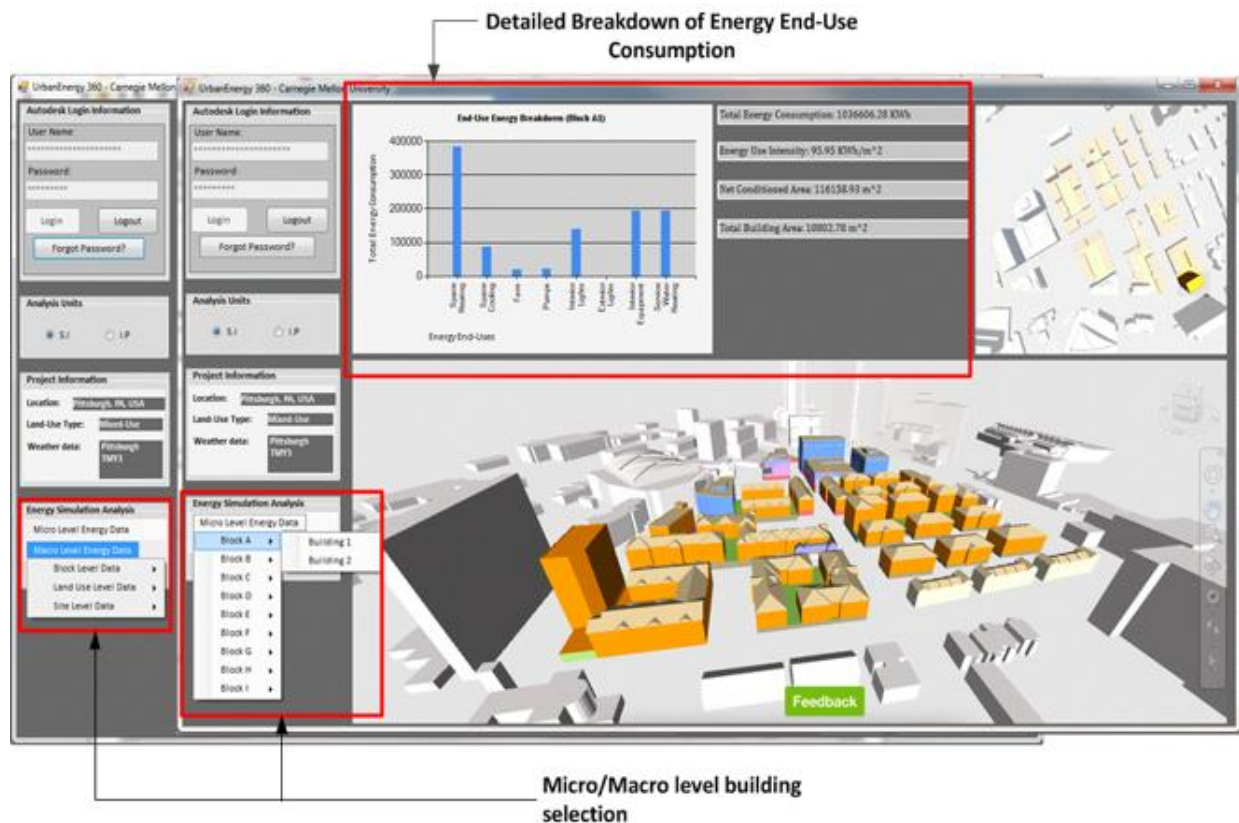


Figure 7. Autodesk BIM 360 Glue 3D visualization

Though ArcGIS was used in this study, the data visualized was only on a building scale as opposed to site level, block level, or floor level. The platform did not provide a scale-based visualization for building energy end-use data. In addition, the visualization was on a desktop version of ArcGIS and not a sharable web-based visualization platform.

More recently, Ramesh et al. (2013) demonstrated a conceptual visualization platform for communicating high-fidelity simulated building energy data using ArcGIS 10.0. That study showed data integration on a building scale; however, this is visualized on a desktop version of ArcGIS. The study went a step further by building a desktop application for visualizing block level, building level, land use level, and site level simulated energy data (Figure 7). Autodesk's BIM 360 Glue viewer was used for visualizing the simulated energy data.

However, again this study did not provide floor level and detailed land use level data. Another limitation is that this application is an executable file and not web-based. Therefore, it is impossible to share the visualization information to project stakeholders without the executable file installed.

From the literature review, it can be concluded that there is no web-based design decision support platform to visualize 3D high-fidelity simulated energy data that can help designers, urban planners, and other project stakeholders. Hence, as a secondary contribution, this thesis proposes to develop a web-based visualization platform using ESRI's ArcGIS Pro, Web Scene, and Story Map applications.

### 1.3. Summary of literature review and knowledge gap

Table 1 shows several gaps that exist in the urban microclimate modeling and coupling the thermodynamic interactions with a building energy model to improve building energy consumption predictions.

1. Coupling methods on the mesoscale and microscale are reviewed. The TEB model is more suited for a city scale microclimate modeling because the building model is a representative model and does not represent actual building design. In addition, thermal zoning, heat transfer calculations, and vegetation models are simplified. Therefore, it is recommended that the TEB model not be used to improve single building scale energy predictions.
2. Among the microscale coupling methods discussed, ENVI-met and EnergyPlus coupling Yang et al. (2012) is considered as a detailed approach to quantify the effects of urban microclimate to improve building energy consumption predictions. However, limitations exist with this method in terms of quantifying the effects of outside air temperature, wind speed, longwave radiation and infiltration completely. Due to EnergyPlus limitations, Yang's model did not account for building surface level outside air temperature and wind speed. These two variables significantly impact the calculation of radiation linear heat transfer coefficient and infiltration.
3. The coupling method by Yang, (2012) was implemented for a 24-hour period to estimate the cooling energy consumption. This is a very short time frame to evaluate the performance of the method to improve building energy consumption. Therefore, the method must be extended to various seasons and a longer duration to effectually understand the effects of the urban microclimate on building energy

consumption. Understanding the effects of the urban microclimate in the various seasons is important to estimate the variation in heating and cooling energy consumption.

4. In addition, the coupling method was implemented on hypothetical building with perimeter and core thermal zoning. Hence the performance of the method has not been evaluated with measured data. The evaluation of the method with measured data is specifically important should the method be extended to designers and energy analysts when predicting building energy consumption.
5. Methods and tools to communicate and visualize simulated energy data were reviewed. Industry tools and previous research studies have demonstrated the capabilities of desktop application for 2D and 3D data visualization. However, there is a lack of web-based 3D design decision support method to communicate high fidelity simulated data.

Therefore, this thesis addresses the gaps in a sequential manner: (1) To automate the urban microclimate modeling (2) To couple the effects of microclimate on building energy consumption using a real-world case-study and its implementation on a design case (3) To visualize the simulated energy data using a Web Scene platform.

**Table 1. Summary of literature review and knowledge gap**

	Urban scale modeling		Thermodynamic Coupling					Model performance		DDS
	Mesoscale	Microscale	Simplified		Detailed			Microclimate Variables	Building Energy consumption	
			Reduced-order	Weather file	Shortwave radiation	Longwave radiation	Convective heat flux			
Masson, 2000	●									
Schoetter et al., 2015	●									
Asawa et al., 2008		●	●							
Robinson et al. 2009		●	●							
Bruse, 2016		●	●					●		
Bueno et al., 2011	●		●						●	
Peng & Elwan, 2012		●		●						
Oxizidis et al., 2008	●			●						
Malys et al. 2015		●	●	●	◐			◐		
Bouyer et al. 2011					●			●		
Yang et al., 2012		●		●	●	◐		◐		
Ramesh & Lam, 2015		●		●	●			●		
Autodesk Inc, 2017										○
CCTech, 2017										○
Ramesh et al., 2013										◐
Coors, 2015										◐
Ramesh, 2017		●		●	●	●	●	●	●	●



## 1.4. Hypotheses

Based on the knowledge gaps, the hypothesis of this thesis is:

- A coupled urban microclimate and building energy model can improve the prediction of building heating and cooling energy consumption.
- The microclimate model must be correctly initialized to obtain results that are comparable to measured data.

## 1.5. Objectives

The proposed research on developing a coupling and visualization method to quantify the thermodynamic interactions between the natural environment and the built environment aims to:

1. Conduct initialization analyses to achieve the ENVI-met microclimate simulation results that are comparable to measured data.
2. Develop a method for coupling whole-building energy simulation program (EnergyPlus) with urban scale prognostic climate simulation program (ENVI-met).
3. Evaluate the performance of the coupling method by comparing the simulated and measured building heating and cooling energy consumption.
4. Demonstrate how the coupling platform can be extended to a design case to improve building energy consumption predictions.
5. Develop a design decision support method to communicate and visualize the high-fidelity simulated energy consumption to assist designers, urban planners, mechanical engineers and other project stakeholders during the design phase.

## 1.6. Dissertation chapter overview

The development of the above-mentioned thesis objectives and hypothesis testing results will be explained in detail in the following chapters.

**Chapter 2**, *Thesis method* details the method used for every task proposed to achieve the coupling platform and implementation of the coupling platform on a design case. This section also provides a summary of the tools used to achieve the thesis objectives.

**Chapter 3**, *Urban microclimate model: Setup, simulation and comparison with measured data*, explains the overall concept of accurate urban microclimate modeling using the Center for Sustainable Landscapes (CSL) case-study in three parts. The first part, describes process of automating the ENVI-met 3D model construction using ArcGIS 10.1 for CSL. The second part demonstrates experimental setup in CSL and statistical analysis of the simulated and measured air temperature, relative humidity and façade temperature. The third part details the process ENVI-met model initialization and its importance to achieve microclimate simulation results that are comparable to measured data.

**Chapter 4**, *Implementation of coupling method to improve building energy consumption predictions*, explains the development of the coupling platform. The first part describes the method to extract data from the ENVI-met microclimate model simulation. The extraction is required to accurately map the case-study building geometry between both simulation tools. The second part describes the coupling process for microclimate factors convection heat transfer coefficient, long-wave radiation, and infiltration. After the coupling process, comparative analysis of building energy consumption is discussed for six cases (summer, winter, swing seasons).

**Chapter 5**, *Design case implementation of coupling method to improve building energy consumption predictions*, describes the implementation of the coupling method on the Lower Hill District Redevelopment, Pittsburgh, PA. After the simulated microclimate data was extracted, the coupling method was implemented on a mixed-use building for the design case. Similar to the CSL case, comparative energy consumption analysis was conducted for the six climate conditions. After the analysis, the simulated energy data was mapped and visualized using ArcGIS Pro, Web Scene Viewer and Story Maps.

**Chapter 6**, *Conclusion*, summarizes the research findings, and hypotheses testing results. Secondary contributions and industry applicability of the coupling method are also reported. Finally, potential future work and limitations are discussed in the last part of the chapter.

## **Chapter 2: Thesis Method**

### **2.1. Overview**

As established in Chapter 1, three significant gaps exist in quantifying the effects of the urban microclimate on building energy consumption, (1) automating the urban microclimate model generation, (2) coupling the effects of microclimate variables on building energy consumption using a real-world case study, and (3) visualizing this simulated building energy data.

Chapter 2 describes the methods used to achieve the thesis objectives and hypotheses. Section 2.2 provides details on the tools used in this thesis. To validate the proposed hypotheses, Section 2.3 provides a detailed method: (1) To automate the urban microclimate model generation and simulation process (2) To couple this microclimate simulated effects with building energy simulation using a real-world case study located in Pittsburgh, PA, USA (3) To develop the visualization method for design decision support.

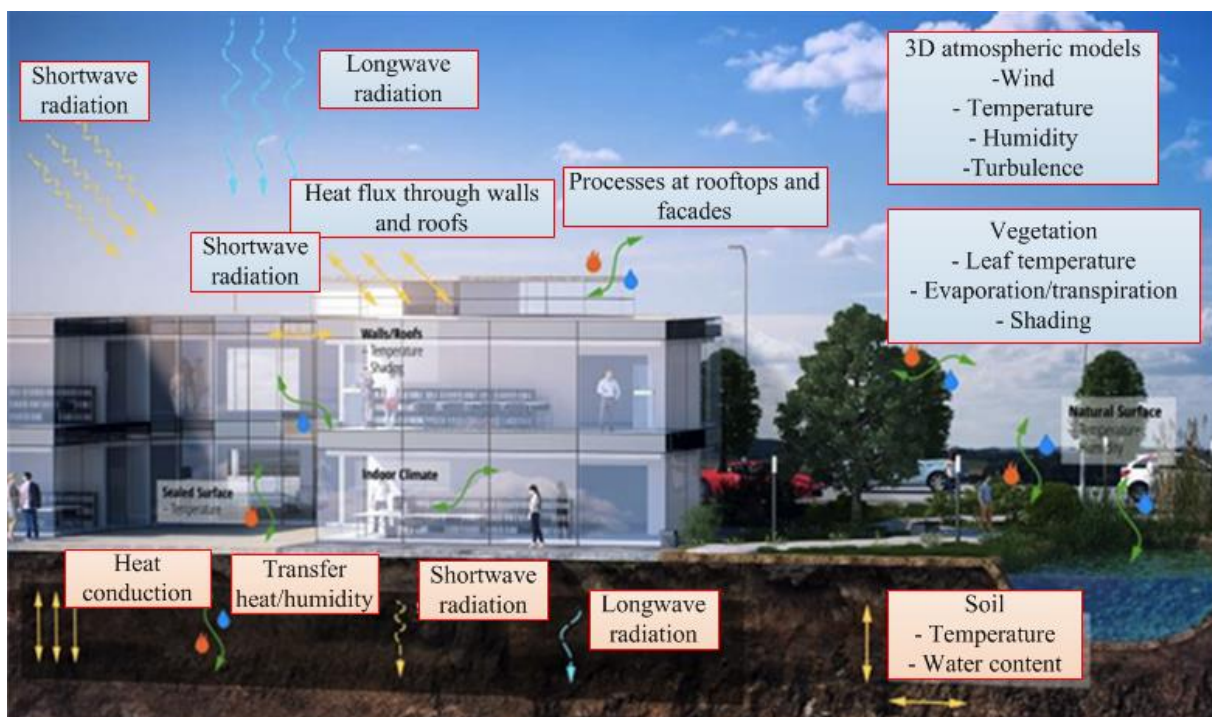
### **2.2. Summary of tools used in the thesis study**

The thesis uses three tools to achieve the above stated objectives and hypotheses; ENVI-met v4.0 Professional is used for simulating the microclimate, EnergyPlus v8.6 is used to perform the building energy simulation and Building Controls Virtual Test Bed (BCVTB) is used as the middleware coupling platform to exchange simulated data between ENVI-met and EnergyPlus.

### 2.2.1. ENVI-met v4.0 (Microclimate simulation)

ENVI-met is a prognostic three-dimensional climate model designed to simulate the surface-plant-air interactions in urban environment. ENVI-met is designed for microclimate simulations to analyze small-scale interactions between individual buildings, surfaces and vegetation (Figure 8). ENVI-met can simulate microscale models with a horizontal resolution from 0.5 m – 10 m with a time step of 1-5 seconds (ENVI-met, 2017)

In the current version of ENVI-met, it is possible to force the air temperature and relative humidity for the one-dimensional model which serve as lateral boundary conditions. This not only helps in increasing the stability of the 3D model, but also helps in achieving simulation results that are comparable to measured data.



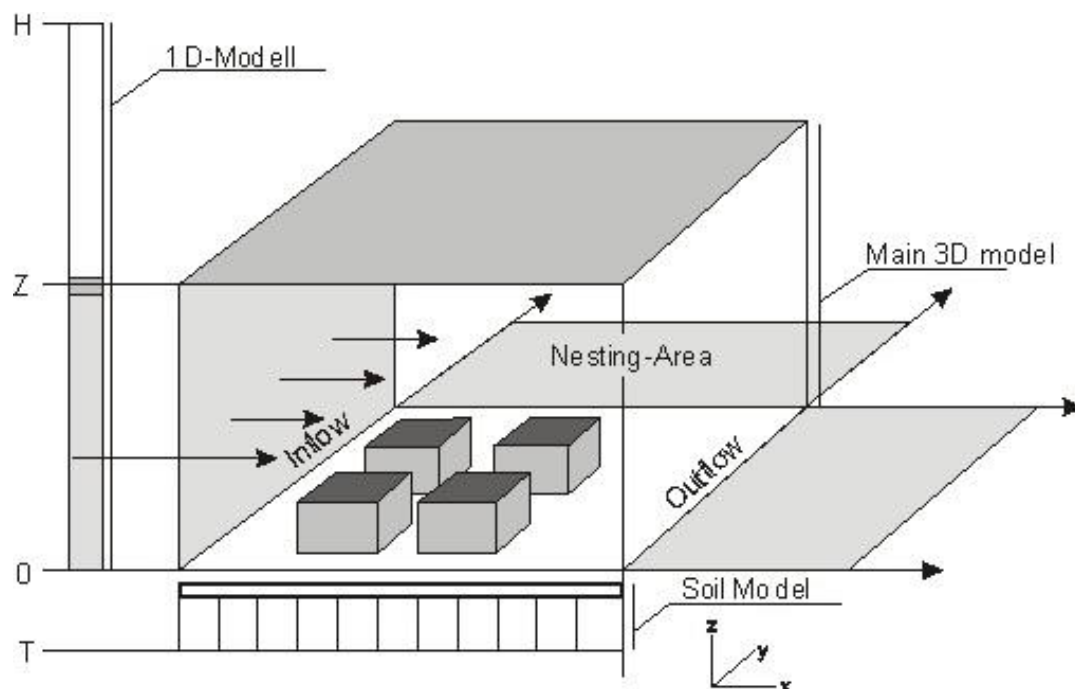
**Figure 8. Thermodynamic interactions between the built and the natural environment** (adapted from ENVI-MET, 2017)

The ENVI-met model consists of several sub-models (Figure 9) that interact with each other:

- 1-D boundary model
- 3-D atmospheric model
- 3-D/1-D soil model

The one-dimensional boundary model is used for the model initialization and as boundary conditions of the three-dimensional atmospheric model. The 1-D model is calculated from ground level ( $z=0$ ) to  $H = 2500\text{m}$  above ground level.

The main prognostic variables calculated by ENVI-met are: (1) Wind speed and wind direction (2) Air, soil and façade temperature (3) Air and soil humidity (4) Turbulence and (5) Radiative fluxes. Various sub-models that are described below are coupled with each other to calculate the above variables.



**Figure 9. ENVI-met sub-models (Bruse, 2004)**

The sub-models are divided into:

### 1. Atmospheric model

The atmospheric model contains a full 3D computational fluid dynamics (CFD) model which solves the Reynolds-averaged non-hydrostatic Navier-Stokes equation for each grid in space and for every time step.

The air temperature and specific humidity of the air are determined by different sources and sinks of sensible heat and vapor inside the model domain. The ground surface and vegetation act as a source or sink for both air temperature and humidity in the atmospheric model. Building façades and roofs mainly act as surfaces interchanging heat with the atmosphere, but can also act as humidity sources if the façade or rooftop has vegetation.

Turbulence is calculated using the E-epsilon 1.5 order closure or k-epsilon model.

Radiative flux is calculated by shading elements, reflections by different surfaces and building materials and the effect of vegetation.

### 2. Soil model

The surface temperature and the distribution of soil temperature is calculated for soils up to a depth of -4m.

Simulating the water balance of a surface and the soil is crucial in urban microclimatology. While humid soils can act as cooling devices, dry soils are often hotter than asphalt.

ENVI-met solves the soil hydraulic state of the soil based on Darcy's law considering evaporation, water exchange inside the soil and water uptake by the plant roots.

Water bodies are represented as a special soil type. The calculated processes inside the water include the transmission and absorption of shortwave radiation inside the water.

### 3. Vegetation model

ENVI-met is able to model not only simple plants such as grass, but also complex 3D vegetation geometries like large trees. All plants are modeled as individual species with an integrated water balance control model and heat and water stress model.

Vegetation interacts in various ways with the environment, such as heat and vapor exchange between plant leaves and the atmosphere. A complex raytracing algorithm is used to analyze the plant impacts of solar radiation and its impacts on longwave radiation exchange.

### 4. Built environment and building system

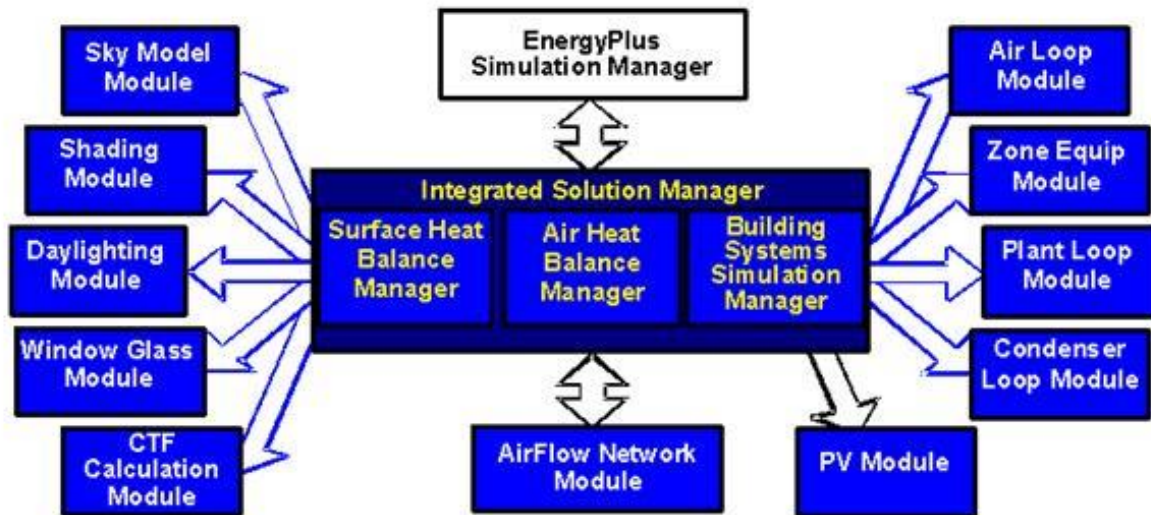
Modeling of the façade and roof can consist of up to three layers of materials.

ENVI-met consists of a 7-node wall temperature calculation model to simulate the wall temperature between the envelope layers. The simulated wall temperature data can be achieved for every grid cell.

## **2.2.2. EnergyPlus v8.5 (Building energy simulation)**

EnergyPlus is a whole building energy simulation program that engineers, architects, and researchers use to model both energy consumption – for heating, cooling, ventilation, lighting, and plug and process loads – and water use in buildings. Its development is funded by the U.S. Department of Energy Building Technologies Office.





**Figure 10. EnergyPlus – Internal modeling elements (DOE)**

The main features of EnergyPlus (Figure 10) include (DOE):

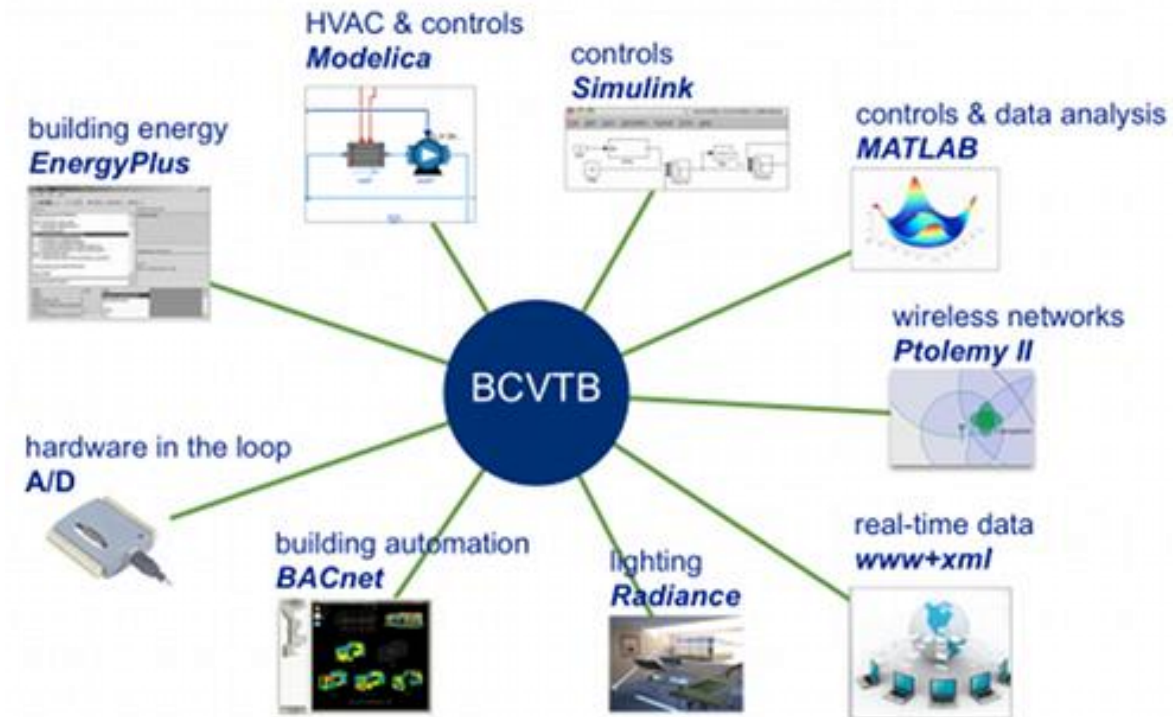
1. Integrated and simultaneous solution to achieve building response that is tightly coupled with the primary and secondary systems.
2. Heat balance calculation for assessing the building thermal loads. This calculation is conducted simultaneously for radiation and convection effects at both interior and exterior building surfaces during each time step.
3. Transient heat conduction through building elements such as walls, windows, roofs, floors using conduction heat transfer algorithms.
4. Combined heat and moisture transfer models that account for moisture absorption and desorption by integrating into conduction transfer model or through an effective penetration depth model (EMPD).
5. Anisotropic sky model for improved calculation of diffuse solar radiation.
6. Energy management systems that help in coupling data from external programs with EnergyPlus.

Therefore, given the robustness of the tool to calculate the various heat transfer interactions, this thesis uses EnergyPlus to couple the ENVI-met simulated microclimate data.

### **2.2.3. Building Controls Virtual Test Bed (BCVTB)**

BCVTB is a modular, extensible and open-source software environment developed by U.S Lawrence Berkeley National Lab (LBNL). This platform allows users to couple different simulation programs for co-simulation of building systems. In addition to interfacing with various simulation programs, BCVTB also supports real-time simulation through coupling simulators with hardware in the Building Automation system.

BCVTB is based on an open-source Ptolemy II software environment which serves as a middleware between arbitrary number of simulation programs (Figure 11). Ptolemy II software has a graphical user interface for coupling simulation tools and control interfaces. A fixed synchronization of time step is assumed for the data exchange between the coupled simulation programs. Therefore, BCVTB offers a quasi-dynamic coupling platform. In this study, BCVTB is used to couple the simulated ENVI-met microclimate results with EnergyPlus.



**Figure 11. The BCVTB co-simulation platform**

### 2.3. Method Description

The thesis method is divided into three distinct approaches (Figure 12). Section 2.4.1 describes the method employed to automate the generation and simulation of the urban microclimate. The section also discusses the process used to conduct a detailed comparison of the simulated and measured urban microclimate variables such as air temperature and relative humidity. Section 2.4.2 details the implementation of the coupling platform between ENVI-met v4.0 and EnergyPlus v8.6 using Building Controls Virtual Test Bed (BCVTB). The coupling platform is described in terms of (1) Convection and radiation heat fluxes as surface boundary conditions and (2) Heat and moisture transfer through infiltration. Section 2.4.3 details the process used to visualize the simulated data using the ArcGIS platform.

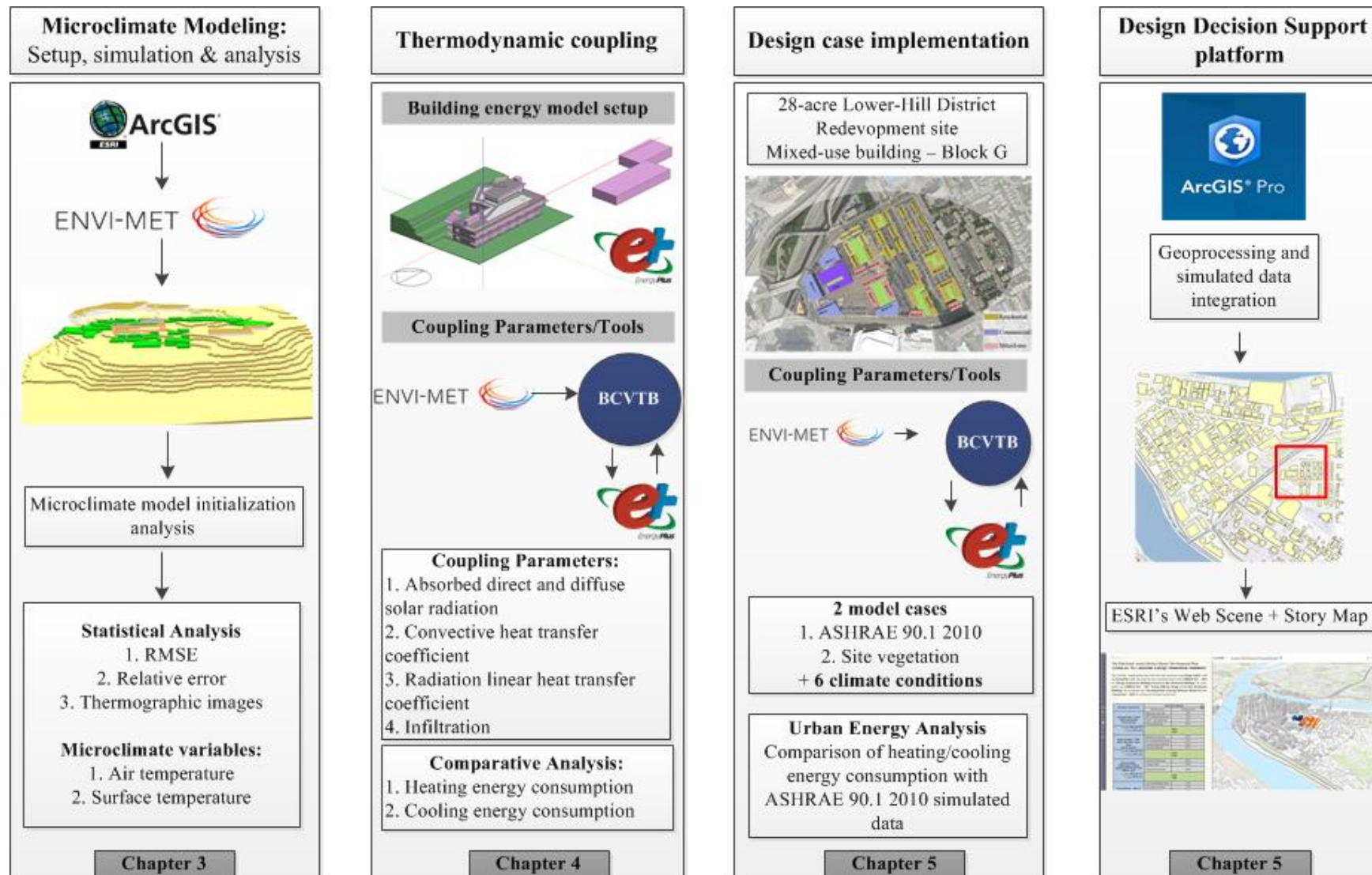


Figure 12. Overview of thesis method

### 2.3.1. Automation and modeling of ENVI-met area input model

The current process for developing an urban scale 3D model of the study domain in ENVI-met requires manual tracing on a raster image to model buildings, vegetation and the site topography. This task is labor and time intensive which increases in complexity as the model resolution and the domain area increases. Therefore, this section details a method to automate the ENVI-met model generation process using LIDAR data and 3D analyst functions in ArcGIS (Figure 13).

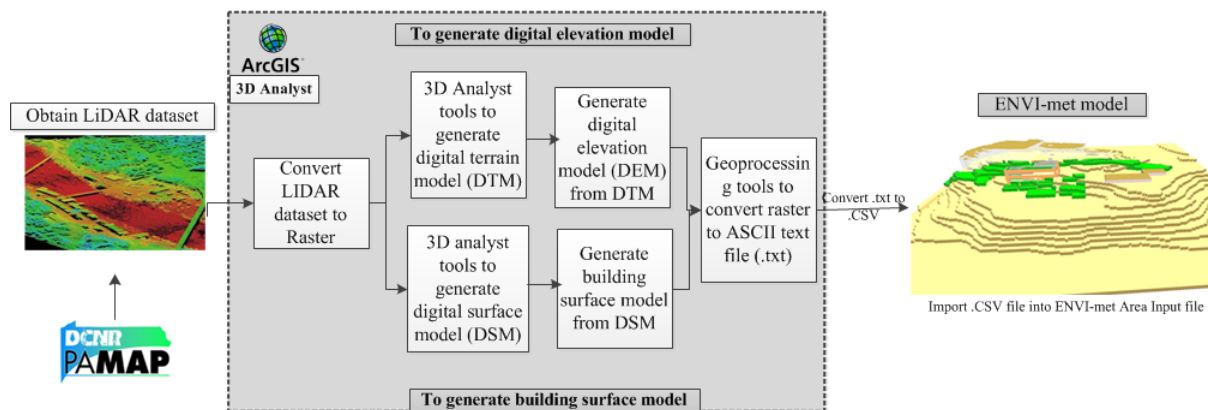


Figure 13. Workflow for automating ENVI-met model generation

LiDAR (Light Detection And Ranging) laser scanners collect geographic point cloud data that is used to create 2D surfaces and 3D features. Geographic LiDAR data is commonly available as LAS (LiDAR Aerial Survey) files. The processed data from the laser scanners into LAS files have points that represent bare earth, vegetation, buildings, terrain, etc.

For this research, the LAS dataset for the case-study domain is obtained from the Pennsylvania Department of Conservation and Natural resources (PA DCNR). The next step is to generate two surface models, a Digital Surface Model (DSM) and a Digital Terrain Model (DTM) using geoprocessing tools in ArcGIS Pro. The two surface models

are used to create a normalized, nDSM surface, which is the difference between the DSM and DTM surface models. Random points are then generated using a 2D layer of building footprints and the normalized surface model is applied to these points which will generate a height Z value for each random point. The highest point that is generated is the building height. The 3D analyst procedure is repeated to the DTM surface model to generate the domain topography.

After the DTM and nDSM are created, these raster images are converted into ASCII files which converted into a .csv format that is directly used as Area Input File in ENVI-met to generate the topography and the buildings.

### **2.3.2. ENVI-met microclimate model initialization**

After the generation of the ENVI-met area input model, a study is conducted to determine the accurate procedure to initialize the microclimate model. This analysis is required to help achieve results that comparable to measured data. Based on the literature review, past studies have investigated climate conditions which have a regular pattern as opposed to thesis case-study location, Pittsburgh, PA, USA. Pittsburgh, is known to have a wide range between the maximum and minimum conditions that can occur within a 72-hour period. This variation in climate conditions is especially true during the winter and swing seasons, given that Pittsburgh is a heating dominated climate.

In addition, previous research on ENVI-met microclimate simulation focus on predicting only a few hours or at a maximum a 24-hour period. However, the objective of this initialization study is to be able to extend ENVI-met to predict the microclimate for a 72-hour period. A rule-based method can be derived from this initialization study. The rule-

based method can determine the number of microclimate simulations that would be required to predict the microclimate on an annual basis.

The accurate initialization of the microclimate model is dependent on the 24-hour forcing of boundary conditions (air temperature and relative humidity) in the configuration file. For example, to predict a 24-hour period, the model is initialized by forcing boundary conditions that represent the desired timeframe. However, since this initialization is based on a 24-hour period in ENVI-met, to extend the microclimate prediction to a 48- or 72-hour period, a method is required to determine this 24-hour forcing input (air temperature and relative humidity).

In this thesis, the microclimate simulation is extended to predict a 72-hour period. Therefore, the method used in this thesis to determine forcing inputs is to derive an average of the 72-hour period as model boundary conditions. However, weather patterns are not consistent (daily minimum and maximum), especially during the winter and swing periods. Therefore, forcing using a 72-hour average air temperature and relative humidity may not provide microclimate predictions that are comparable to measured data. Therefore, as a first step, all cases are simulated using a 3-day average air temperature and relative humidity as the forcing inputs. A statistical comparison using relative error and RMSE are used to understand the variation between the simulated and measured data. Cases that have a relative error that is greater than 25% are then re-simulated using 1-day initialization and re-compared with measured data air temperature and relative humidity. The details of the ENVI-met model initialization inputs for the case-study are described in detailed in Chapter 3.

### **2.3.3. Coupling of urban microclimate model with building energy model**

After the accurate simulation of the ENVI-met microclimate model, the simulated data is coupled with the building energy model using BCVTB and EnergyPlus. The coupling involves two steps: (1) Data mapping platform using BCVTB to extract and process the ENVI-met simulated data which is used in the EnergyPlus model and (2) Developing the coupling platform in EnergyPlus using BCVTB as the middleware. The following two sections provide details to achieve the above described steps.

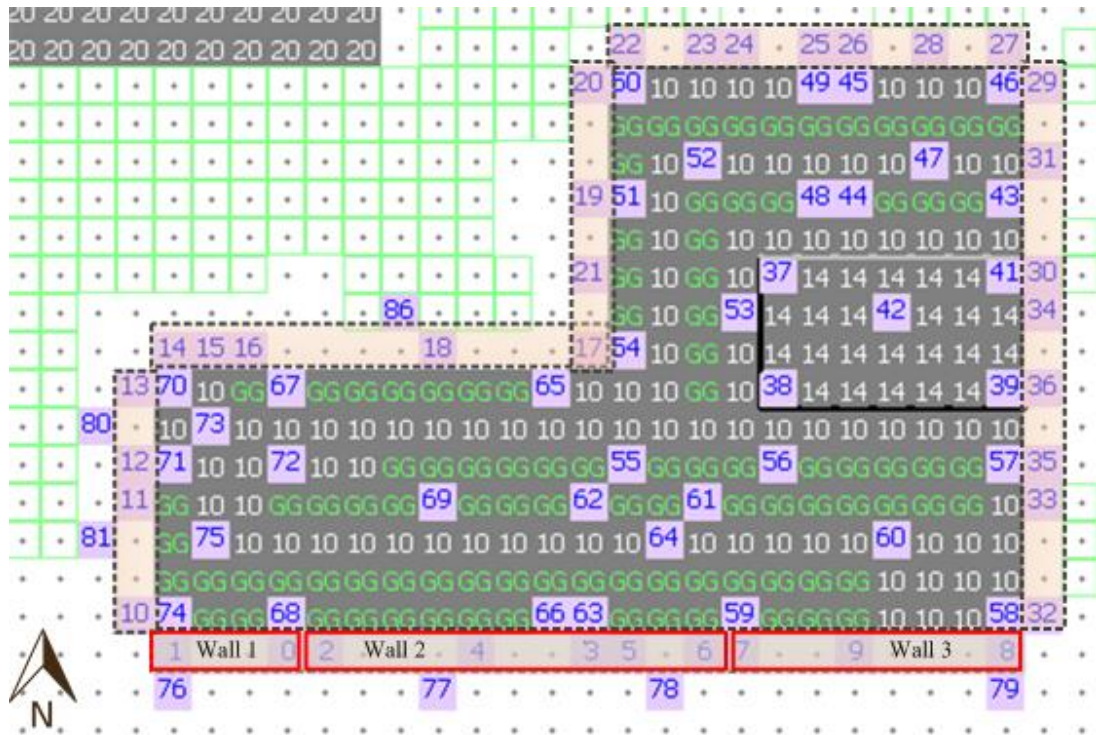
#### **2.3.3.1. Data mapping for data exchange**

An essential first step is to map the ENVI-met simulated data to a format that can be used for coupling with EnergyPlus. In ENVI-met, the 3D model geometry is based on structured grids while in EnergyPlus building envelope elements are considered single entities. In ENVI-met, each of these surfaces is divided into grids based on the model resolution, which is 2m in the thesis case-study. Simulation data is recorded using the receptor function in every grid (every 2m) along the height of the building. Therefore, to map the simulated microclimate data from ENVI-met to EnergyPlus, each surface is treated as individual unit (e.g. each wall, roof is a separate unit) in both tools. The receptor function in ENVI-met is used to record the meteorological data along the building surfaces as shown in Figure 14.

To determine the meteorological variables along every façade, every wall and roof entity is divided based on the thermal zoning of the EnergyPlus case-study model. Since the façade is divided into several sub-surfaces, the average value for the meteorological variables (air temperature, relative humidity and wind speed) is calculated from the



receptor output corresponding to each of the sub-surfaces. For example, from Figure 14, the south façade is divided into three sub-surfaces based on the EnergyPlus thermal zoning. Therefore, an average value is calculated for each of these sub-walls in BCVTB. This process is repeated for every façade and roof to derive the simulated air temperature and wind speed which is then used to couple with the EnergyPlus model.



**Figure 14. Layout of receptors for recording simulated data in ENVI-met**

### 2.3.3.2. Implementation of coupling platform

After the ENVI-met simulated data was processed into a format that can be used in the EnergyPlus simulations, the next step was to implement the coupling platform. In EnergyPlus, the internal load for a zone is calculated using the following energy balance equation:

$$Q_{internalloads} = Q_{internalheatgains} + Q_{convectiveheattransfer} + Q_{infiltration} + \Delta E_{air} \quad (1)$$

Where,

$Q_{internalloads}$  - Building heating/cooling loads

$Q_{internalheatgains}$  – Building internal heat gain from people, equipment's and lights

$Q_{convectiveheattransfer}$  – Convective heat transfer between zone interior surfaces

$Q_{infiltration}$  – Heat transfer due to infiltration with outdoor air

$\Delta E_{air}$  – Change of energy stored in the zone air

From equation (1), convective heat flux and heat flux due to infiltration is caused by the interaction of the building outside surface with the surrounding urban microclimate. Therefore, it is essential to account for the actual outside surface microclimate conditions to improve building internal load calculation. For this, the heat balance calculation of the outside face of a building is given by:

$$q_{asol} + q_{LWR} + q_{conv} - q_{ko} = 0 \quad (2)$$

Where,

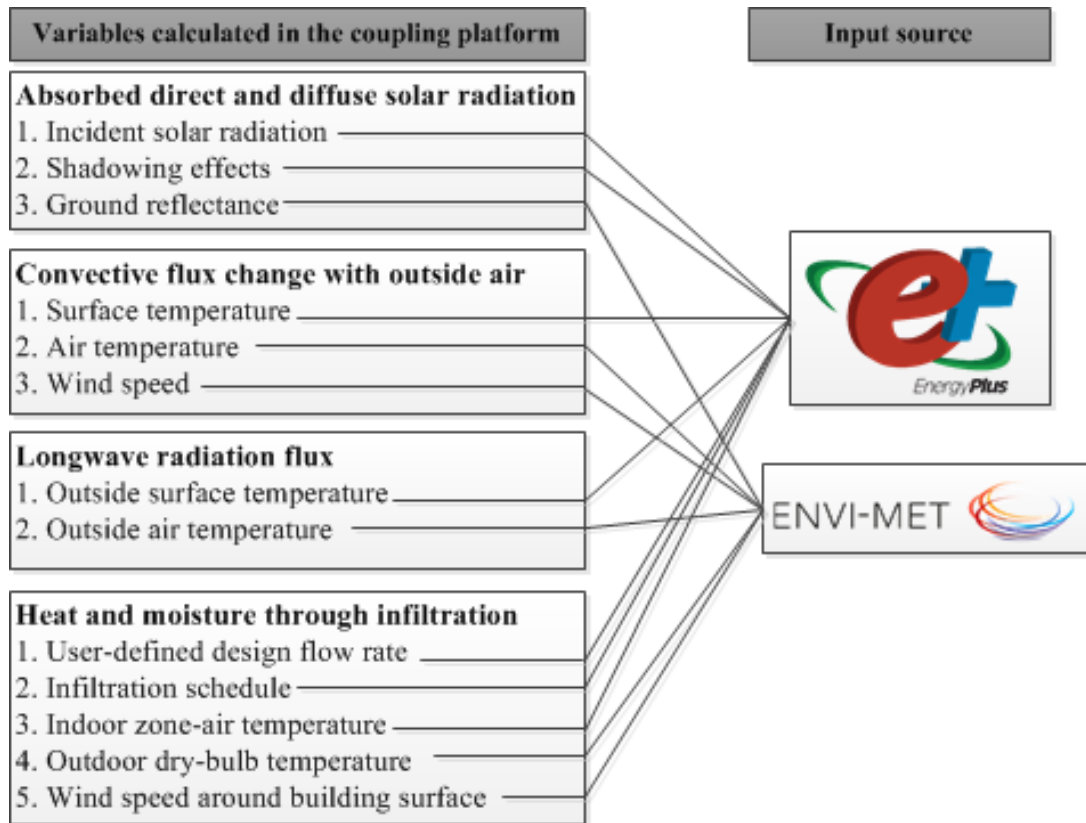
$q_{asol}$  - Absorbed direct and diffuse solar radiation heat flux

$q_{LWR}$  - Net longwave (thermal) radiation flux exchange with the air and surroundings

$q_{conv}$  - Convective flux change with outside air

$q_{ko}$  - Conduction heat flux (q/A) into the wall

From equations (1) and (2), the coupling is executed in three steps based on the variables (Figure 15). First, the EnergyPlus weather file and absorbed direct and diffuse solar radiation fluxes; second, the convective heat transfer coefficient and the radiation linear heat transfer coefficient using the Surface Boundary Conditions object; and third, infiltration using Energy Management System (EMS) actuators and zone infiltration object in EnergyPlus. Figure 15 provides a detailed list of all the variables and the input source for the coupling platform.



**Figure 15. Variables implemented and the input source in the coupling platform**

Figure 16 details the three steps required to implement the coupling variables as described in the following section.

### 2.3.3.2a. Absorbed direct and diffuse solar radiation flux

ENVI-met and EnergyPlus use Ray-tracing method for shadow calculations. However, there are differences in the physical models and the numerical schemes between both software.

The numerical and physical differences are:

1. In ENVI-met only one state is present in a grid cell at each model time step, i.e., sunlit or shaded; however, EnergyPlus calculates the incoming solar radiation

based on the sunlit area of the surface. Therefore, EnergyPlus provides a more realistic modeling approach for shadowing calculation.

2. ENVI-met uses isotropic diffuse solar radiation model. EnergyPlus takes into account the anisotropic radiance distribution of the sky. This means, ENVI-met diffuse solar radiation calculation is independent of building orientation while EnergyPlus calculation change with building orientation and is therefore more accurate.
3. For the calculation of solar reflection, ENVI-met assumes only diffuse reflection, but all three patterns of reflection (i.e. beam to beam, beam to diffuse and diffuse to diffuse) are accounted for by EnergyPlus.
4. In ENVI-met, the albedo of various ground surface (asphalt, pavement, vegetation, and water) is defined by users. However, a homogenous ground surface with a given albedo is assumed in EnergyPlus.
5. For shadowing effects from vegetation, ENVI-met considers vegetation as a turbid medium, and calculates the transmittance of vegetation as a function of the optical path of solar beam through leaves and leaf area index. However, EnergyPlus assumes vegetation as obstructions like other shadowing elements, with a constant or scheduled transmittance and at the same temperature as outside air temperature.

From the above described differences between the two software, EnergyPlus calculations for diffuse solar radiation, solar reflection and shadowing are more accurate when compared to ENVI-met. However, calculations for ground reflectance is simplified in EnergyPlus. Therefore, the ground reflectance inputs are derived from ENVI-met simulations as an input into EnergyPlus.

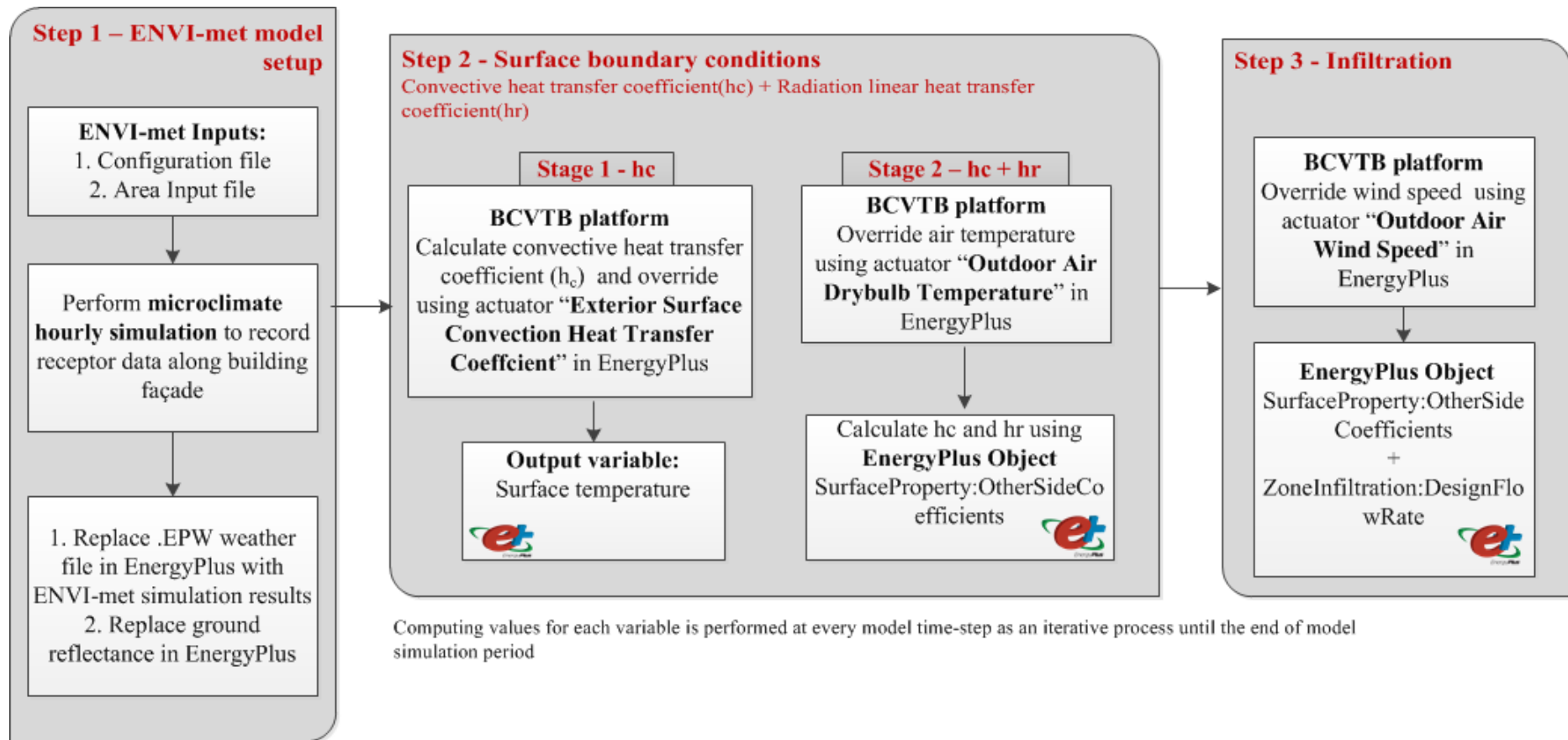


Figure 16. Method for coupling ENVI-met microclimate simulation data and EnergyPlus model

### 2.3.3.2b. Surface boundary conditions

After defining the absorbed shortwave direct and diffuse shortwave radiation in EnergyPlus, the next step is calculating the surface boundary conditions by coupling the ENVI-met simulated air temperature and wind speed and EnergyPlus calculated surface temperature. The variables that account for surface boundary conditions are convective heat transfer coefficient (CHTC) and the radiation linear heat transfer coefficient ( $h_r$ ). This is implemented in two stages.

#### *Stage 1 – Convective Heat Transfer Coefficient*

Heat transfer through surface convection is modeled in EnergyPlus using:

$$Q_c = h_{c\ ext} - A (T_{surf} - T_{air}) \quad (3)$$

Where,

$Q_c$  – Rate of exterior convective heat transfer

$h_{c\ ext}$  – Exterior convection coefficient

$A$  – Surface area

$T_{surf}$  – Surface temperature

$T_{air}$  – Outdoor air temperature

Convective heat transfer coefficient is determined by empirical correlations. There are several correlations and significant differences between these correlations (Defraeye, 2011). Many of these correlations available in EnergyPlus are based on wind speeds from the local weather station and only represent site level wind speeds. However, when using ENVI-met predicted wind speeds which introduces flow field around the building (CFD based on Reynold's-Navier Stokes), the existing EnergyPlus correlations are not valid to

calculate CHTC. This is because ENVI-met simulations predict wind speeds for every building surface based on grid cells. Therefore, to couple the wind speed for every building surface, a linear law based on ISO 6946 (6946) is proposed for calculating the CHTC:

$$h_{c \text{ ext}} = 4 + 4v \quad (4)$$

Where,

$h_c$  – Convective heat transfer coefficient

$v$  - wind speed front of the building surface

Therefore, CHTC is calculated for every surface of the case-study building using equation (4). This calculated CHTC is overwritten using the Energy Management System (EMS) feature in EnergyPlus.

The EMS feature in EnergyPlus provides a pathway to develop custom controls and modeling procedures for EnergyPlus models. A programming language called EnergyPlus Runtime Language (Erl) is used to describe the control algorithms. The ExternalInterface object allows coupling EnergyPlus to BCVTB at each zone time step. In this study, the object used in EnergyPlus is ExternalInterface:Actuator, where at each zone time step, the calculated CHTC value is received from BCVTB. The ExternalInterface:Actuator used to overwrite this CHTC value is “Exterior surface convection heat transfer coefficient”. Chapter 3 provides a detailed layout of the layout of the data communication between BCVTB and EnergyPlus to implement convective heat transfer coefficient.

### ***Stage 2 – Convective Heat Transfer Coefficient + Radiation linear heat transfer coefficient***

After the successful coupling of CHTC, the next step is to couple the radiation linear heat transfer coefficient (hr). When implementing hr using BCVTB, it was found that, the

External Interface data exchange between BCVTB and EnergyPlus has a limitation of 1024 values at any given time. This is mainly due to complex nature of the case-study model, which leads to numerous wall and roof surfaces as detailed in Chapter 3. Therefore, an alternative approach was adopted for the implementation of coupling  $h_c$  and  $h_r$  to overcome this limitation.

From EnergyPlus, the variables that affect the calculation for radiation linear heat transfer coefficient is:

$$h_{r,air} = \frac{\varepsilon\sigma F_{air} (T_{Surface}^4 - T_{air}^4)}{T_{surface} - T_{air}} \quad (5)$$

Where,

$h_{r,air}$  – Radiation linear heat transfer coefficient

$\varepsilon$  – long-wave emittance of the surface

$\sigma$  – Stefan-Boltzmann constant

$T_{surface}$  – outside surface temperature

$T_{air}$  – outside air temperature

The alternative approach uses the SurfaceProperty:OtherSideCoefficients object in EnergyPlus to calculate  $h_c$  and  $h_r$ . This was achieved by (1) coupling the ENVI-met simulated air temperature outside every building surface using the EMS actuator, “Outdoor Air Drybulb Temperature” in the ExternalInterface; (2) specifying Exterior Dry-Bulb Temperature Coefficient and Ground Surface Temperature Coefficient in the SurfaceProperty:OtherSideCoefficients object that sets the other side conditions for a surface. By setting the two coefficients, EnergyPlus calculates the Exterior Surface Temperature which is then to calculate  $h_c$  and  $h_r$  within EnergyPlus.



### 2.3.3.2c. Heat and moisture transfer through infiltration

After the successful implementation of the surface boundary conditions, the next variable implemented in the coupling platform is infiltration. Infiltration in buildings is caused due to opening and closing of doors and windows, cracks through windows and small amounts through building elements. It is calculated in EnergyPlus using equation (5).

$$Infiltration = I_{design} + F_{schedule}[A + B |T_{zone} - T_{odb}| + C(windspeed) + D(windspeed)^2] \quad (5)$$

Where,

$I_{design}$  – User-defined design flow rate

$F_{schedule}$  – Infiltration schedule

$A, B, C, D$  – coefficients (typically 1,0,0,0)

$T_{zone}$  – Indoor zone air temperature

$T_{odb}$  – Outdoor dry-bulb temperature

$windspeed$  – wind speed around building surface

From equation (5), we see that the meteorological conditions that impact infiltration are Exterior Dry Bulb Temperature and Wind Speed. From Section 2.3.3.b, Exterior Dry-Bulb Temperature is implemented using the EMS actuator “*Outdoor Air Drybulb Temperature*”. Therefore, to couple wind speed, the EMS actuator used is “*Outdoor Air Wind Speed*”. By coupling the wind speed for every building surface, the infiltration calculation in EnergyPlus is taken into account.

### 2.3.4. Visualizing simulated building energy data

After implementing the coupling platform, the next step was to map and visualize the high-fidelity simulated energy data on a web-based platform. This visualization platform is important to effectively communicate the predicted high-fidelity energy data to project

stakeholders in an organized manner. The thesis used ESRI's ArcGIS Pro, Web Scene and Story Map applications to develop the visualization platform for the Lower Hill District.

1. **Mapping CAD Data:** To build the 3D model of the Lower Hill District and its surroundings, the CAD plan is developed based on the design guidelines obtained from the design team. Then, the CAD drawings are mapped with the topography base map and elevation layers. The elevation and basemap layers in a scene provide context and reference to the other operational building layers.
2. **Defining coordinate system:** When creating 3D Scene, it is important to define the horizontal and vertical coordinate systems. Horizontal coordinate systems locate data across the surface of the data, and vertical coordinate systems locate the relative height of the data. The selection of the coordinate system can have significant impact on the performance and results generated by a geoprocessing tool. The 3D building and floor features use projected coordinate system 'NAD 1983 StatePlane Pennsylvania South FIPS 3702 Feet' and geographic coordinate system 'GCS North American 1983.'
3. **Converting features to 3D symbology:** Next, geoprocessing tools are used to digitize and extrude the 2D CAD map to generate z-enabled 3D multipatch features of the buildings. The 2D polygon features are extruded vertically to create building blocks.

A multipatch feature is a GIS object that stores a collection of patches to represent the boundary of a 3D object as a single row in a database. These patches store information such as texture, color, transparency and geometric information that represent the feature. The Z-values in the multipatch represent the shape and elevation of the feature. After the building multipatch features are created,

geoprocessing tools, extrude and split floors from the facility tool toolbox is executed to obtain floor level detail for every building.

Geoprocessing is a framework and a set of tools for processing geographic and related data. These tools enable managing GIS data in an automated way.

Geoprocessing tools have both inputs and outputs. The 3D multipatch features of the buildings and the floor heights are used as input parameters to generate floor level multipatch features.

4. **Organizing data:** Next, the simulated energy data is added as attributes to the multipatch building features. The attribute table helps to map and visualize the simulated data for every building. The fields toolset in the Data management toolbox contains a set of tools to add and make edits to the fields for every building feature. The fields used to visualize the simulated energy data are energy use intensity (EUI), energy consumption, net building area, net conditioned and unconditioned building area and building height.
5. **Publish to ArcGIS Online:** After mapping the simulated energy data for all the buildings, the multipatch features are converted into scene layer package. A package is a compressed file containing GIS data. A scene layer package contains a cache of multipatch building features that are published as a web scene layers to ArcGIS Online and Portal for ArcGIS with ArcGIS Data Store.
6. **Creating & sharing Web Scene and Story Map:** After publishing the building multipatch features to ArcGIS Online, a Web Scene is created using ArcGIS Scene Viewer. The web scene layer is embedded into a Story Map, that is deployed as a visualization platform. To share the web scene layer, it is essential to obtain an organizational account with ArcGIS Data Store privileges and an active 3D scene. In addition to embedding the Web Scene, Story Map is a powerful open source

platform to create maps, add text, images and video content that can be shared publicly for visualization.

This thesis aims to provide a seamless method to achieve the visualization platform. A synthesized description of the process is provided in Appendix B.

## **2.4. Summary**

To summarize, this chapter has described the thesis method to (1) automate the urban microclimate model generation and simulation process using ArcGIS Pro (2) couple this microclimate simulated effects with building energy simulation using a real-world case study located in Pittsburgh, PA, USA using ENVI-met, EnergyPlus and BCVTB as the coupling platform and (3) develop the visualization platform for design decision support.

The automation of the ENVI-met microclimate model is achieved using geoprocessing tools in ESRI's ArcGIS Pro. Next, initialization study of the ENVI-met microclimate model is conducted for 24 climate conditions of Pittsburgh, PA. From the initialization analysis, 6 cases (summer, winter, swing) are selected to implement the coupling method. After the simulated data is mapped to the format that is acceptable by EnergyPlus, the coupling method is implemented in two stages using BCVTB and EnergyPlus. Finally, the simulated energy consumption data is visualized using ArcGIS PRO, Web Scene Viewer and Story Map applications.

## **Chapter 3: Urban Microclimate Modeling: setup, simulation and model performance**

### **3.1. Overview**

As described in Chapter 2, to couple the microclimate effects on building energy consumption, it is important to understand how to accurately model and simulate the microclimate using ENVI-met. Chapter 3 describes the model setup, simulation and comparison of simulated and measured data using the CSL case study. Section 3.2 describes the case-study domain for the microclimate modeling and the coupling platform. Section 3.3 details the experimental setup to compare the simulated microclimate with measured data. Section 3.4 describes the automation and microclimate model setup for the case-study building. Section 3.5 provides a comparison and statistical analysis of the microclimate simulation results with the measured data in three steps: (1) analysis of air temperature and relative humidity with the CSL on-site weather station data, (2) analysis of simulated air temperature with measured experiment points, and (3) analysis of simulated and measured façade temperature. After the discussion of simulated and measured variables, Section 3.6 details the importance of accurate ENVI-met model initialization. In addition, this section describes a rule-based method to derive the number of simulations that is required to predict the microclimate on an annual basis.

### **3.2. Case-study for urban microclimate modeling**

The case-study selected for the urban microclimate modeling and coupling of the thermodynamic interactions is a zero-energy, LEED Platinum certified medium-size

office building – Phipps Center for Sustainable Landscapes (CSL) in Pittsburgh, Pennsylvania, USA as shown in Figure 17. The building is a 2,263m<sup>2</sup> education, research and administration facility. The case-study site is located in the city center; however, it is surrounded by vegetation and a lake. Therefore, the microclimate conditions are not strictly urban, but represent the urban conditions more closely when compared to rural conditions.



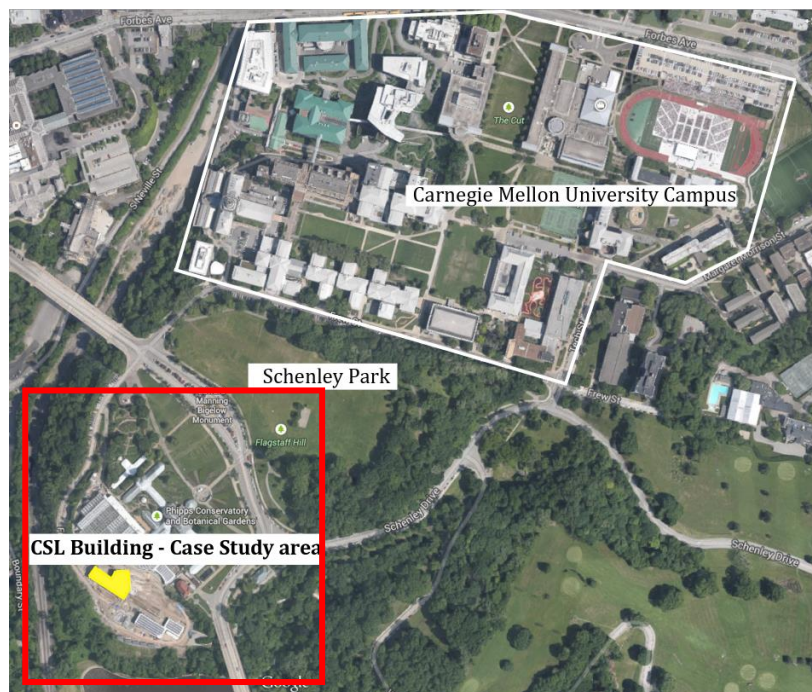
**Figure 17. As-built view of the Center for Sustainable Landscapes (Schrag, 2017)**

The CSL case-study was strategically selected keeping in mind three important criteria (Figure 18):

1. The area has various land uses such as office building, naturally ventilated botanical garden (Phipps Conservatory), vegetated areas (Schenley Park) and a lake, northeast of the CSL building. Therefore, the ENVI-met model considers the effects of vegetation, water bodies and the built environment on the microclimate.
2. The CSL building is adjacent to Carnegie Mellon University campus, which has a dense network of administrative, educational, resident halls and parking lots. This provides potential for expanding the study area to evaluate the influence of the

built environment on the urban microclimate and vice versa in terms of energy consumption.

3. The CSL building has an on-site weather station, which helps in comparison of simulated data with actual on-site data rather than a local weather station near the airport (suburban). Weather station located by the airport record data that depict suburban microclimate conditions and do not represent the city microclimate conditions. Therefore, comparison with on-site weather data is especially required to validate the accuracy of the ENVI-met microclimate model.

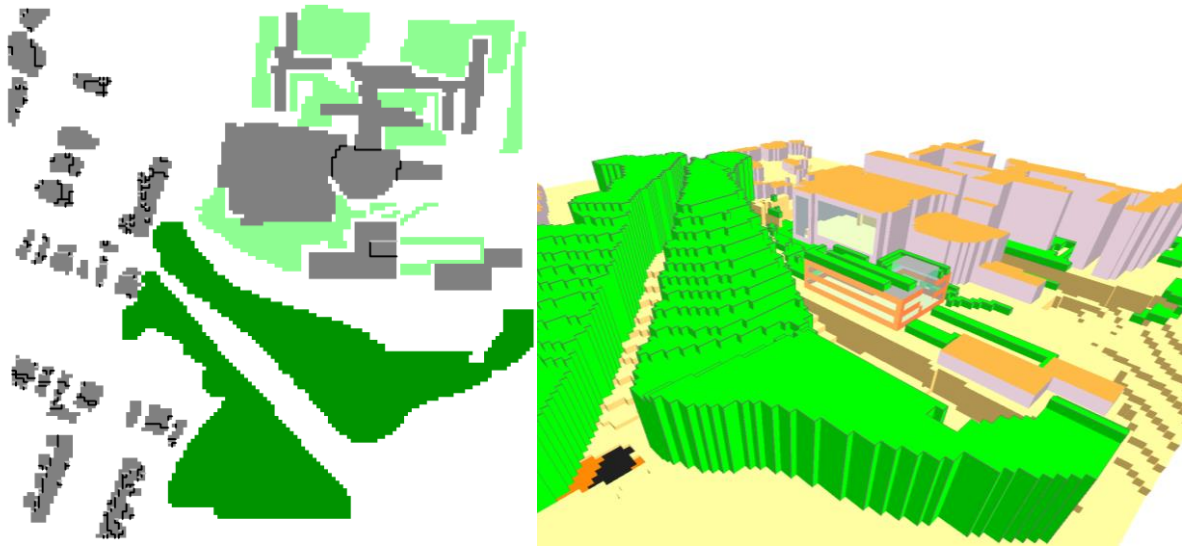


**Figure 18. Location of the CSL Building**

4. The CSL building also has a calibrated EnergyPlus whole building energy model. This helps accurately estimate and compare the heating/cooling energy consumption of the simulated and measured data using the BCVTB coupling framework.

(quoted from Ramesh and Lam, 2015)

Figure 19 shows the 2D and 3D microclimate model of the CSL building and its surroundings modeled in ENVI-met. The domain size of 150mx150m with a 2m model resolution was selected for the initialization and coupling study.



**Figure 19. ENVI-met microclimate model of the CSL building**

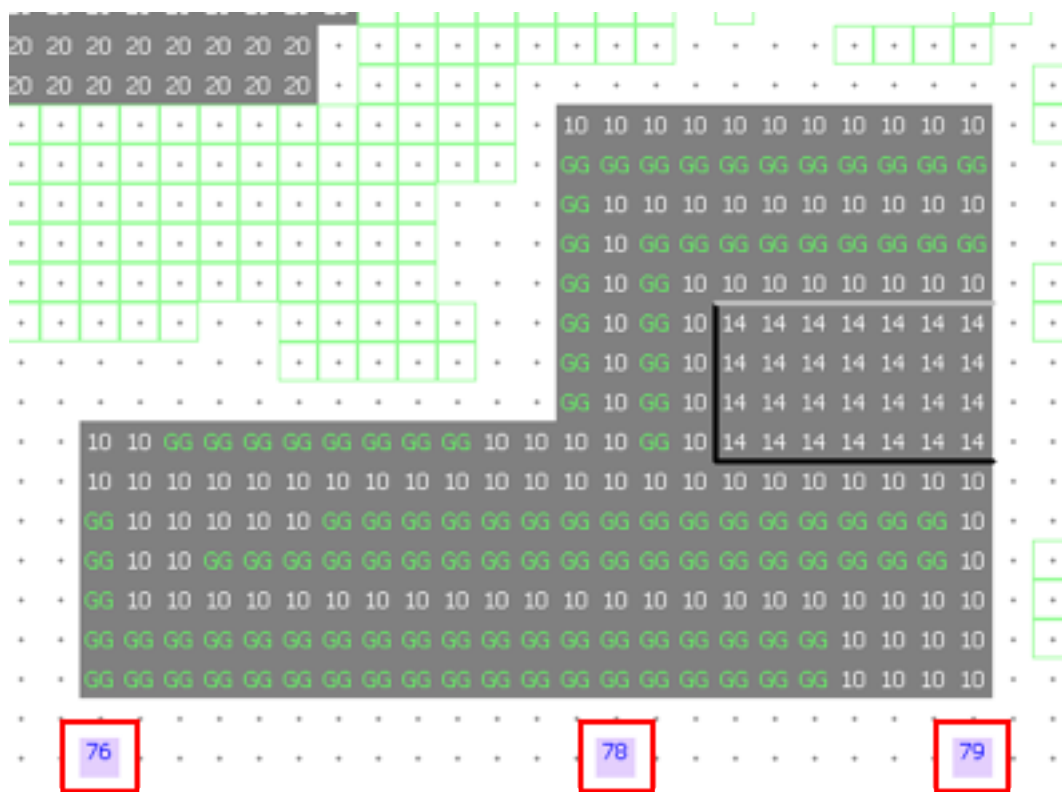
The domain size was strategically selected as 150mx150m to account for: (1) All the surrounding elements such as Phipps conservatory, other commercial and residential buildings, dense vegetation, the lake, and the site topography (2) Developing a high-resolution microclimate model and (3) Availability of computational power to complete simulations within a reasonable time period.

### **3.3. Experimental setup for simulated & measured data comparison**

To compare the accuracy of the simulated data, an experiment was conducted to measure the air and building façade temperatures. The air temperature was recorded at three points along the CSL south façade. The air temperature data was logged at a 10-min interval which was then averaged to compute the hourly air temperature. Figure 20 shows three measurement points (76, 78, 79) along the south façade. The sensors were setup at 2m



height above the ground. The south façade was selected because there were no entryway restrictions or blockage by adjacent buildings. The points were selected to be integrated with the existing infrastructure around the site vegetation. The comparison was conducted for a 3-day period each month between May – August 2016 (summer). The summer period was selected because the HOBO sensors deployed for this experiment was not recommended for use during the swing or winter conditions.



**Figure 20. ENVI-met model receptor points corresponding to the experiment setup**

Another variable that was used to compare the ENVI-met predicted data with the measured data was building façade temperature. Thermographic images were used to record spot measurements capturing the solar radiation effect on the building façade during the morning and the afternoon hours. The measurement was recorded on June 14 at 10am (north, east) and 2pm (south, west) respectively.

Figure 21 shows the equipment's that was used to measure air temperature and the façade temperature.

- **HOBO Air/Water/Soil temperature sensor (TMC6/TMC20 – HD):** The HOBO sensor was used to measure the air temperature. The temperature sensor has a measurement range of  $-40^{\circ}$  to  $100^{\circ}\text{C}$  in air with an accuracy of  $\pm 0.25^{\circ}\text{C}$ .
- **HOBO Data Logger (U12):** The HOBO data logger is connected to the air temperature sensor to record and store the hourly measured data.



**Figure 21. Equipments used to measure air and façade temperature**

- **The FLIR Thermal Imaging camera:** This camera was used to capture the building façade temperature. The simulated façade temperature is compared with measured thermographic images that are captured at a specific time on a specific day.



**Figure 22. CSL experiment setup along the south façade**

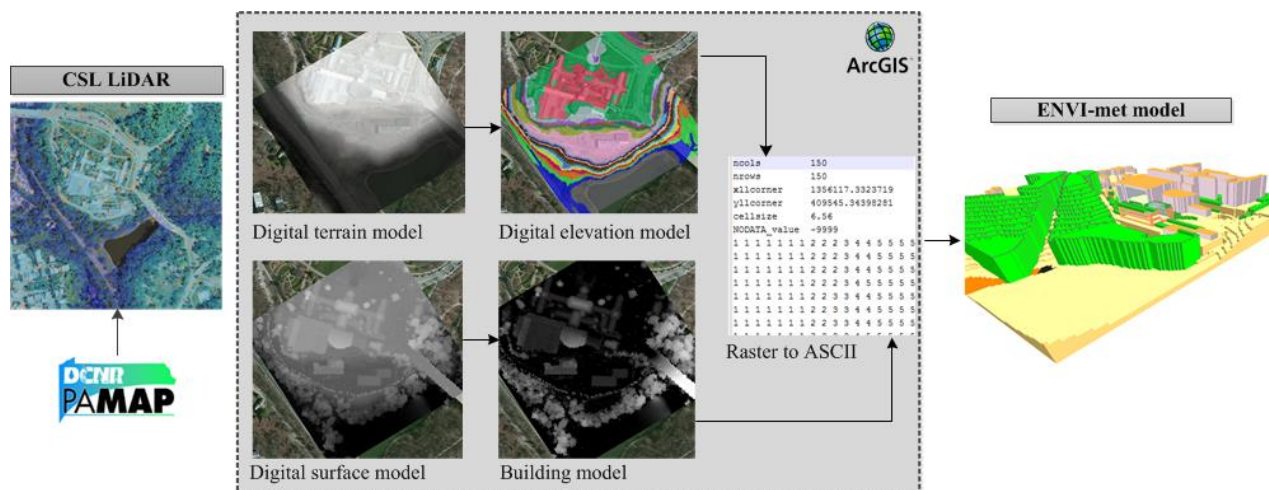
Corresponding to the experimental setup, the ENVI-met model was able to simulate hourly air temperature representing the experiment location points (76, 78, 79) using the receptor function as shown in Figure 20.

The ENVI-met simulated air temperature and relative humidity was also compared with the on-site weather station data (Point 39). It should also be noted that the weather station data has a very high degree of accuracy compared to the HOBO air temperature sensors.

### **3.4. Urban microclimate model generation and initialization**

This section describes the process of creating and initializing an ENVI-met model of the CSL case-study site as described in Chapter 2 Section 2.3.1. Figure 23 shows the detailed method of creating the ENVI-met model using ArcGIS Pro.

The first step to automate the ENVI-met model generation was obtaining LiDAR data of the CSL case-study site from the Pennsylvania Department of Conservation and Natural resources (PA DCNR). The next step was to generate the Digital Terrain Model (DTM) and Digital Surface Model (DSM) to derive the respective site elevation and building elevation using the 3D analyst function in ArcGIS.



**Figure 23. Automation of ENVI-met microclimate model for CSL**

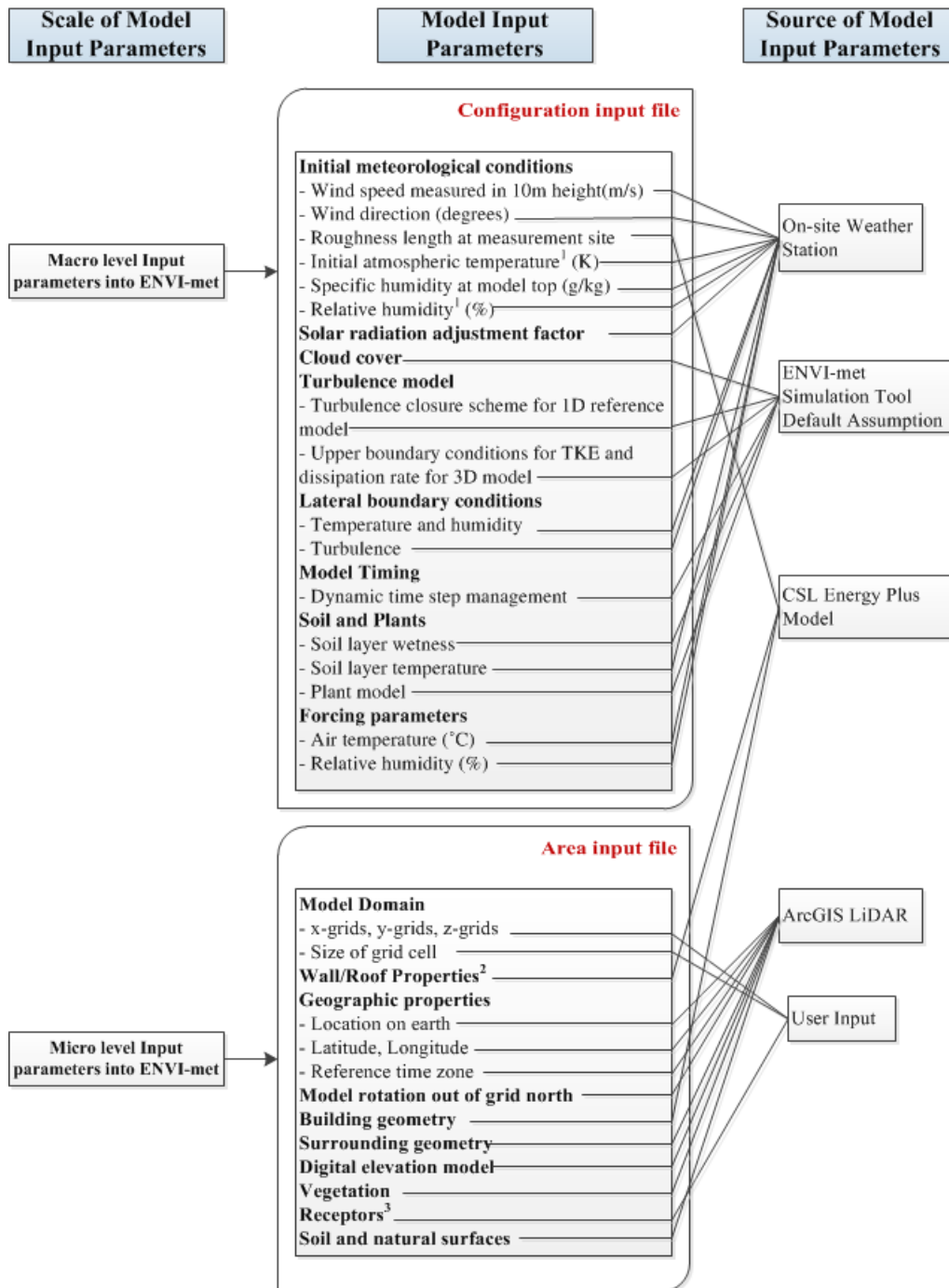
The Digital Elevation Model and the building model was then converted into ASCII .txt format which is directly used as input to the ENVI-met area input file to generate the CSL ENVI-met microclimate model.

After successfully generating the ENVI-met model of CSL using ArcGIS, the next step was to conduct the microclimate model initialization study as described in Chapter 2 section 2.3.2. As discussed in Chapter 2, Section 2.3.2, in order to compare the results of the ENVI-met simulation with weather station measured data, it is necessary to “force” the inflow boundary conditions of the model. The current version of ENVI-met allows the forcing of air temperature and relative humidity for a 24-hour period. This forcing function is extremely important to initialize the microclimate model accurately. The forced 24-hour air temperature and RH serve as model inflow boundary conditions for the entire simulation period.

For this thesis, two climate periods have been simulated for every month in order to represent the annual microclimate conditions. The two periods are selected based on the cloud cover to represent sunny and cloudy atmospheric conditions. Therefore, a total of

24 climate conditions are simulated to represent the annual microclimate of the CSL case-study site. Each of the 24 cases are simulated for a 3-day (72 hour) period.

Figure 24 provides details on the ENVI-met model input parameters and the input source that are required to initialize and run the microclimate simulation.



**Figure 24. Flowchat indicating ENVI-met simulation input parameters and source (Ramesh and Lam 2015)**

1. **Forcing meteorology inputs:** By forcing air temperature and relative humidity for a 24-hour period, the tool allows the user to manually define the diurnal variations at the inflow boundary conditions.
2. **Wall/Roof properties:** Specify wall and roof properties based on the construction layers and properties of the individual construction layers. ENVI-met v4.0 is capable of modelling construction materials for up to three layers from the outside to the inside of the wall/roof.
3. **Receptors:** Selected points inside the model, which provide results on the state of the atmosphere, the surface and the soil at each of these selected points.

From the figure, it can be seen that the model input can be described as macro level inputs and micro level inputs. At the macro level, the inputs correspond to the meteorological variables that impact the domain microclimate. These macro level input variables include air temperature, relative humidity, wind conditions and soil temperature and wetness. The macro level meteorological inputs are derived from the CSL on-site weather station and uses the ENVI-met default algorithms. At the micro level, the model inputs correspond to the CSL site area input file. The area inputs mainly describe the model resolution, global reference for sun angle estimation during simulation, and the CSL domain features such as built environment geometry, vegetation and ground surfaces.

**Table 2. ENVI-met model configuration and area file input parameters  
(e.g. for June 2-4)**

Model input parameter	Input
<b>3-D Model Settings</b>	
Domain size	150m x 150x 30m
Grid size	2m x 2m x 2m
Location	40.44° N, -79.98° W
Reference time zone	UTC -5:00
<b>Meteorology: Basic Settings</b>	
Wind speed measured in 10m height	0.97 m/s
Wind direction	27.47 degree
Roughness length at measurement site	0.1
Initial temperature of atmosphere	Calculated by ENVI-met when forcing is used
Specific humidity at model top	11.4 g/kg
<b>Meteorology: Simple Forcing</b>	
Temperature (°C)	Measured air temperature for 24-hour period
Relative humidity (%)	Measured RH for 24-hour period
<b>Soil and plants</b>	
Upper, middle and deep soil layer	Soil wetness: 50%; Initial Temperature:297K

The complexity of the area input file also determines the computational resources required to complete a 72-hour simulation. For example, for a domain size of 150m X 150m and 2m model resolution, the computational time is approximately 7-10 days which reduces when the model resolution is reduced to 3m or 5m. However, reducing the model resolution also compromises the accuracy of the simulated ta and hence this thesis uses a model resolution of 2m.

Table 2 shows an example of the meteorological and area file inputs for the simulation period June 2 – 4, 2016 that were required to initialize and simulate the ENVI-met model.

### **3.5. Comparison of simulated data to measured data**

This section provides a detailed statistical discussion of how the simulated data compares to measured data. As previously discussed, 24 cases were simulated to represent the annual climate conditions of Pittsburgh, PA. This analysis of simulated data and measured data was conducted in three steps. First, the simulated air temperature and relative humidity was compared with the measured on-site weather station data (Section 3.5.1). The location of the on-site weather station was recorded as Point 39 using the receptor function in the ENVI-met model. Second, the simulated air temperature is compared to the measured air temperature recorded by the experimental setup (Section 3.3) along the south and west façade (Section 3.5.2). The points used for comparison are Point (76, 78, 79) on the south façade and Point (80, 81) on the west façade as highlighted Figure 18. Third, the simulated façade temperature is compared to measured thermographic images for June 14 at 10am and 2pm (Section 3.5.3). The metrics used for comparison for the first and second steps are root mean square error (RMSE) and correlation coefficient (R). This third step also uses spot measurements from the thermographic images to gain a more accurate representation of the façade temperature.



### 3.5.1. Analysis of air temperature and relative humidity

As described above, the first step was to conduct a statistical analysis of the simulated and measured air temperature and relative humidity. The measured data was obtained from the on-site CSL weather station which is indicated as Point 39 (Figure 20). Table 3 tabulates the statistical comparison (RMSE and R) for air temperature and relative humidity for the 24 cases.

**Table 3. Statistical comparison of simulated and weather station measured air temperature and relative humidity**

Simulation Period (2016)	Weather Station (Point 39)			
	RMSE		R	
	Air temperature (°C)	Relative humidity (%)	Air temperature (°C)	Relative humidity (%)
January 5 - 7	5.05	12.62	0.61	0.84
January 20 - 22	1.54	4.76	0.89	0.93
February 15- 17	1.98	11.46	0.45	0.12
February 20- 22 (3-day average)	4.73	10.07	0.55	0.79
February 20- 22 (1-day)	1.56	6.61	0.97	0.91
March 8 - 10	3.55	17.58	0.65	0.40
March 22 - 24	5.75	15.8	0.91	0.91
April 13 - 15 (3-day average)	4.05	7.10	0.82	0.93
April 13 - 15 (1-day)	2.13	4.83	0.97	0.96
May 9 -11	2.91	14.16	0.71	0.61
May 23 - 25	3.01	13.06	0.91	0.90
June 12-14	3.34	8.57	0.67	0.84
June 2 - 4	1.91	9.99	0.92	0.77
July 19 - 21	2.76	13.26	0.85	0.66
July 2 - 4	1.58	14.22	0.93	0.63
August 22-24	5.41	8.30	0.91	0.95
August 15 - 17	1.91	9.99	0.78	0.68
September 20 - 22	2.08	8.77	0.97	0.96

September 28 - 30	2.59	15.40	0.71	0.47
October 4 - 6	2.03	7.65	0.94	0.95
October 7 - 9	1.53	10.59	0.94	0.78
November 12 - 14	2.05	7.90	0.98	0.96
November 18 - 20	6.93	11.47	0.30	0.51
December 1 - 3	1.04	11.35	0.50	0.46
December 19 - 21	3.23	7.14	0.57	0.71

The comparison of the simulated and measured data of the 24 cases is discussed below in terms of RMSE and correlation coefficient (R) for the summer, winter and swing seasons.

The simulations were conducted for 2016. The analyses are divided based on the following seasons: November – early March is considered winter, late May – August is summer, late March – early May and September - October are considered swing seasons.

From the statistical analysis in Table 3, the following observations can be made:

1. Results show for the winter months (November – February), when the measured air temperature pattern is not regular in terms of the daily minimum and maximum, the model should be initialized with 1-day data and simulated for every 24-hour period. By initializing the model with a 3-day average data, the RMSE for air temperature and relative humidity is higher than the summer months. This is especially true for November and December 2016 when the daily difference between the minimum and maximum air temperature is greater than 15°C for Pittsburgh. Hence, the ENVI-met model is unable to simulate with accuracy, this broad range which is again validated by the correlation coefficient R. For example, looking at the statistical analysis for February 20 – 22, it is seen that when the ENVI-met model is initialized using the 3-day average data, the RMSE for air temperature and relative humidity is higher (4.73°C and 10.07%) as compared to when the model is initialized with 1-day data. This variation is also evident when

comparing the correlation coefficient for air temperature and relative humidity (0.55 and 0.79) which is much lower than when the model is initialized with 1-day data (0.97 and 0.91). Therefore, results show for the winter months, when the measured air temperature pattern is not regular in terms of the daily minimum and maximum, the model should be initialized with 1-day data and simulated for every 24-hour period.

2. Results show for the summer months (May – August), the model is able to predict the air temperature and relative humidity with a high degree of accuracy using a 3-day average initialization. When the model is initialized with 3-day average data, the RMSE for air temperature and relative humidity is between 4°C - 5°C and 8% - 13% respectively. It should also be noted that since the difference between the maximum and minimum air temperature is less than 10°C, the simulation period has a relatively regular pattern. This is also evident from comparing the correlation coefficient, which in most cases are higher than 0.85 for air temperature. Therefore, the ENVI-met model can predict the air temperature and relative humidity with a high degree of accuracy using a 3-day average initialization during the summer months.
3. Results show for the swing months (late March – early May and September - October), the accuracy of the simulated data depends on the pattern of the air temperature and relative humidity used to initialize the model. For example, results for April 13 – 15 show that using a 3-day average has a higher RMSE and lower correlation coefficient than initializing the model with 1-day data. This variation is because the daily minimum and maximum air temperatures vary during the simulation period. However, for October 4 – 6, results show that by initializing the model with 3-day average data, the model can predict the air temperature and

relative humidity with a high degree of accuracy in terms of RMSE and correlation coefficient. Therefore, it can be concluded that for the swing months the ENVI-met model initialization depends on the pattern of measured data in terms of variations in the minimum and maximum air temperature.

### 3.5.2. Statistical analysis of simulated with experiment measured air temperature

As a second step to evaluate the accuracy of the ENVI-met model prediction, the simulated air temperature is compared with the measured data from the experiment points (76, 78, 79).

**Table 4. Statistical comparison of simulated and experiment measured air temperature**

Simulation Period (2016)	Point 76		Point 78		Point 79	
	Air temperature (°C)					
	RMSE (°C)	R	RMSE (°C)	R	RMSE (°C)	R
May 23 - 25	3.93	0.92	3.59	0.92	3.64	0.92
June 2 - 4	2.17	0.87	2.20	0.88	2.39	0.86
June 17 - 19	3.45	0.90	2.98	0.90	3.51	0.87
July 2 - 4	1.76	0.93	1.73	0.93	1.84	0.93
July 19 - 21	3.55	0.91	3.21	0.85	3.11	0.91
August 15 - 17	2.19	0.68	1.42	0.63	2.23	0.68
August 22-24	7.53	0.67	2.53	0.90	3.13	0.92

Similar to the previous discussion, results show for the summer months the ENVI-met model is able to predict the air temperature for all the experiment points with a high degree of accuracy. From Table 4, August 15 – 17, it is seen that though the RMSE for the three points are low, the correlation coefficient is also low. This is due to the sudden increase in air temperature on day 2 of the simulation period which is discussed in detail

in Section 3.6. Also, for August 22 – 24, it is seen that Point 76 has a high RMSE (7.53°C) and a low R coefficient (0.67). It was observed that the HOBO sensor at this point started failing and the recorded data at this point did not accurately represent the air temperature.

### 3.6. Analysis of ENVI-met model initialization

Based on initial analysis of the 24 simulation cases detailed in Table 3, six cases were selected to study the simulation results of the 3-day average and the 1-day forcing to initialize the model inflow boundary conditions. These six cases are analyzed more deeply to assess the importance of accurate ENVI-met model initialization. The six cases are representative of winter (January and February), summer (June and August) and swing (April and October) climate conditions in Pittsburgh, PA.

Figure 25 shows the comparison of simulated and measured air temperature and relative humidity for January 20 – 22, characterized as a winter condition in Pittsburgh, PA.

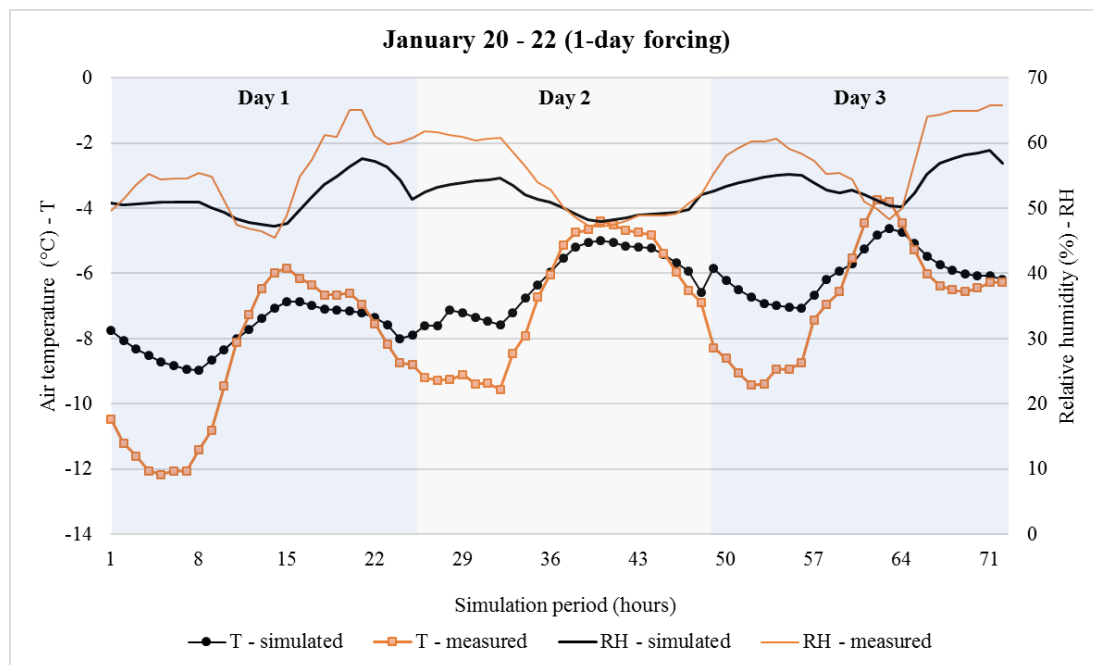
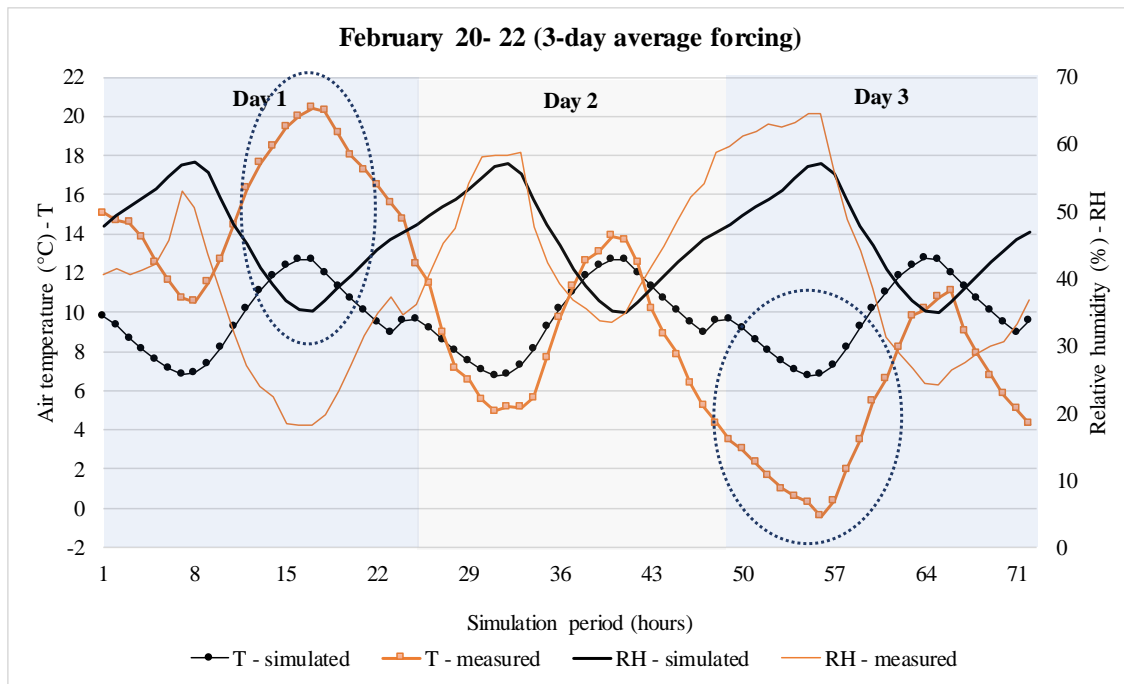


Figure 25. Comparison of simulated and measured data for January 20 - 22

The measured forcing input (air temperature and relative humidity) does not have a regular pattern. Therefore, the ENVI-met model is initialized by a 1-day measured air temperature and relative humidity. This initialization process was repeated using the measured data for day 2 and day 3. The following observations can be made from the simulation results:

1. Although there is a temperature difference of  $\sim 3^{\circ}\text{C}$  at the start of the simulation, the model is able predict the 3-day pattern to a fair degree of accuracy. The RMSE for air temperature is  $1.54^{\circ}\text{C}$  for the simulation period (Table 3). The correlation between the measured and simulated air temperature is 0.89 which means there is a high degree of correlation between the predicted and measured air temperature. Therefore, results show that although the difference between predicted and measured minimum temperature is approximately  $2^{\circ}\text{C}$ , the model is still able to predict the other hours with a high degree of accuracy.
2. Comparing the simulated and measured relative humidity (RH), results suggest that the model is able to predict the pattern to a high degree of accuracy with a correlation of 0.93 and an RMSE of 4.76%.



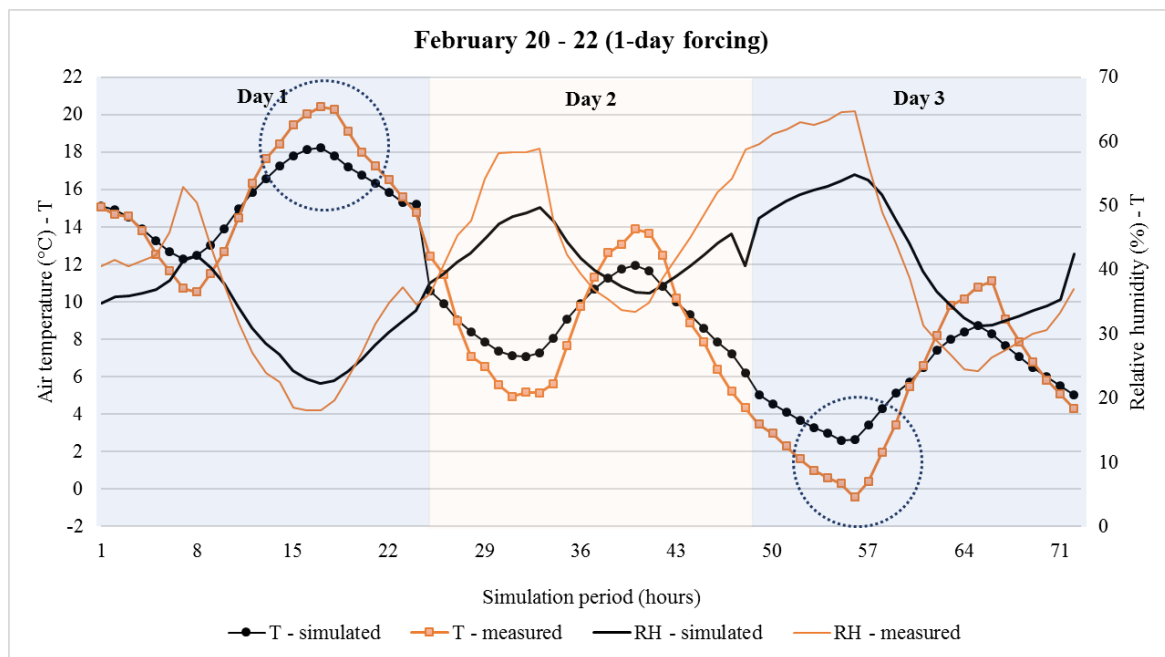
**Figure 26. Comparison of simulated and measured data for February 20 – 22**

Figure 26 and Figure 27 shows a comparison of simulated and measured air temperature and relative humidity for February 20 – 22 using 3-day average and 1-day forcing for model initialization. The following observations and conclusions can be made:

1. Figure 26, which uses 3-day average as the forcing conditions, indicates that maximum and minimum air temperature varies to a great extent between day 1 and day 2 & 3. The measured maximum on day 1 is 20.4°C, whereas the maximum on day 2 & 3 are 13.8°C and 10.7°C respectively. The same pattern occurs for relative humidity, where day 1 is lower (maximum of 52.9%) when compared to day 2 & 3 (maximum of 64.6%). The correlation between simulated and measured air temperature is 0.55 and relative humidity is 0.78, which is low due to the 3-day average model initialization. Therefore, initializing the model with the 3-day averaged air temperature and relative humidity does not accurately represent the

measured data. Hence the model is unable to accurately predict the 3 days that is comparable to measured data.

- Figure 27 shows that by simulating the same model with forcing 1-day air temperature and relative humidity, the model prediction is comparable to the measured data with a RMSE of 1.56°C for air temperature and 6.61% for relative humidity. The correlation between simulated and measured air temperature is 0.97 and relative humidity is 0.91. Therefore, when the initialization pattern in terms of minimum and maximum air temperature is not consistent for the simulation period, results show the ENVI-met model should be initialized for every 24 hours of the simulation period using the forcing function in ENVI-met.



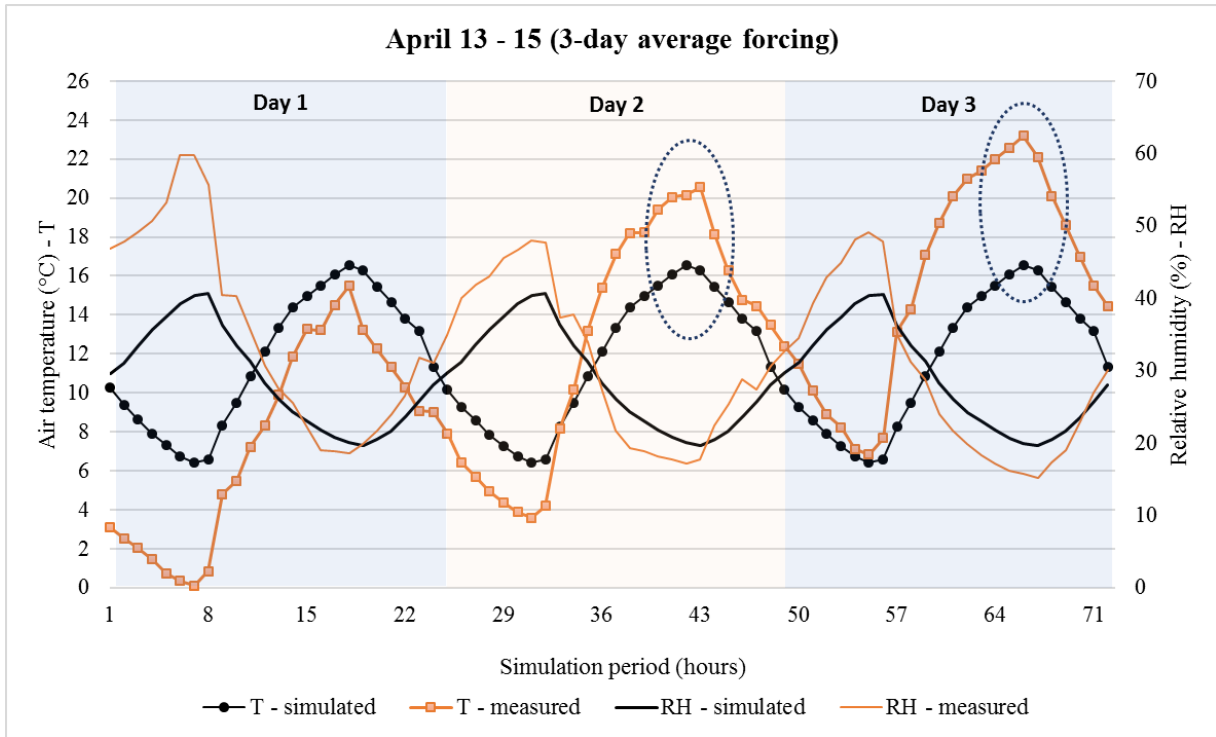
**Figure 27. Comparison of simulated and measured data for February 20 – 22**

Figure 28 and Figure 29 shows a comparison of simulated and measured air temperature and relative humidity for April 13 - 15 using 3 – day average and 1 - day forcing for

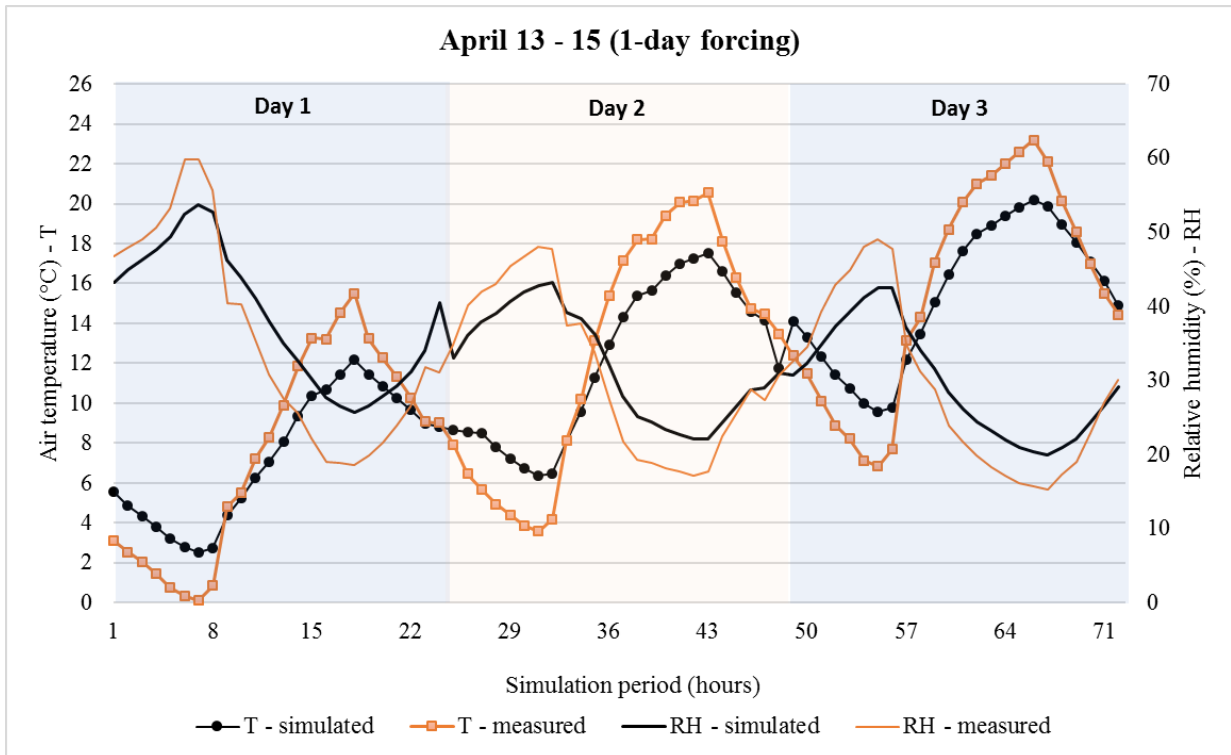


model initialization. This period is considered as swing season in Pittsburgh, PA. The following observations and conclusions can be made:

1. Figure 28, which uses a 3-day average initialization does not accurately represent the measured air temperature and relative humidity. The maximum air temperature varies between day 1, 2 and 3 with a difference of 2°C - 4°C. This is also evident during the start of the simulation where the difference between measured and simulated air temperature is approximately 6°C. Therefore, when using the 3-day average for initialization, the model is unable to predict the air temperature and relative humidity with accuracy.
2. Figure 29, shows that using 1-day initialization, the model is able to predict the air temperature and relative humidity that is comparable to the measured data from the start of the simulation. The RMSE is 2.13°C and 4.8% for air temperature and relative humidity respectively. Therefore, as highlighted in the previous discussion, when the initialization pattern in terms of minimum and maximum air temperature is not consistent for the simulation period, results show the ENVI-met model should be initialized for every 24 hours of the simulation period.



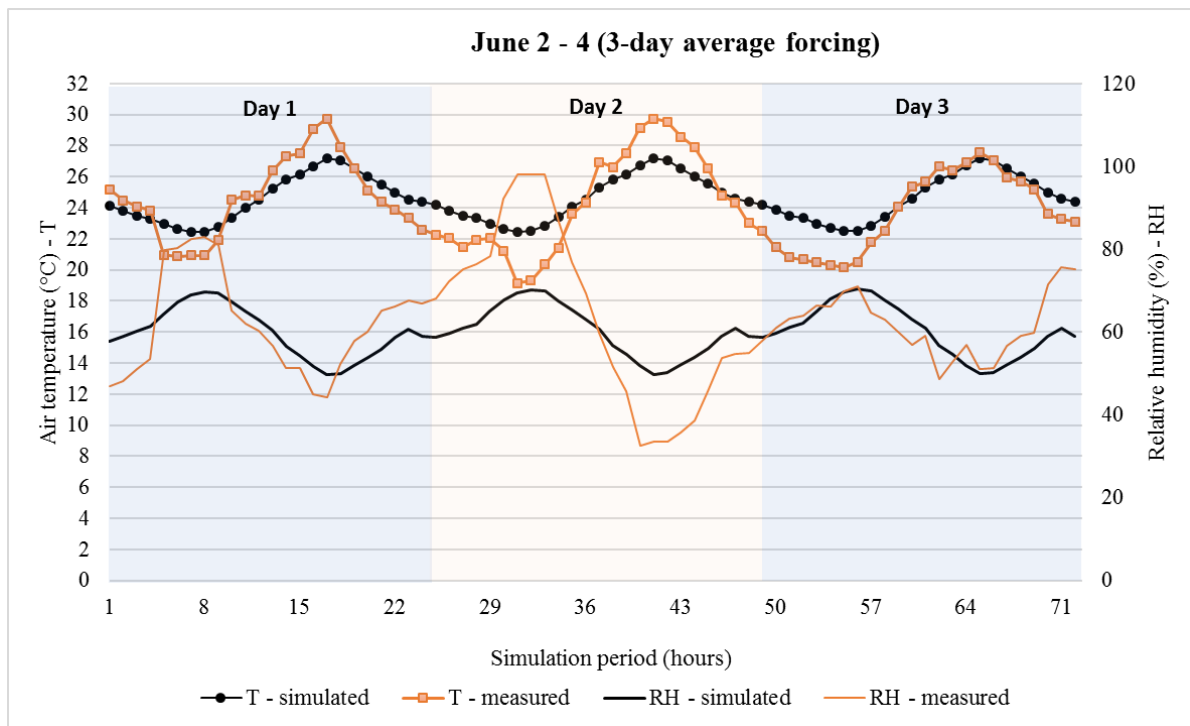
**Figure 28. Comparison of simulated and measured data for April 13 - 15**



**Figure 29. Comparison of simulated and measured data for April 13 - 15**

Figure 30 shows the comparison of simulated and measured air temperature using 3-day average initialization for June 2 – 4. The following observations can be made:

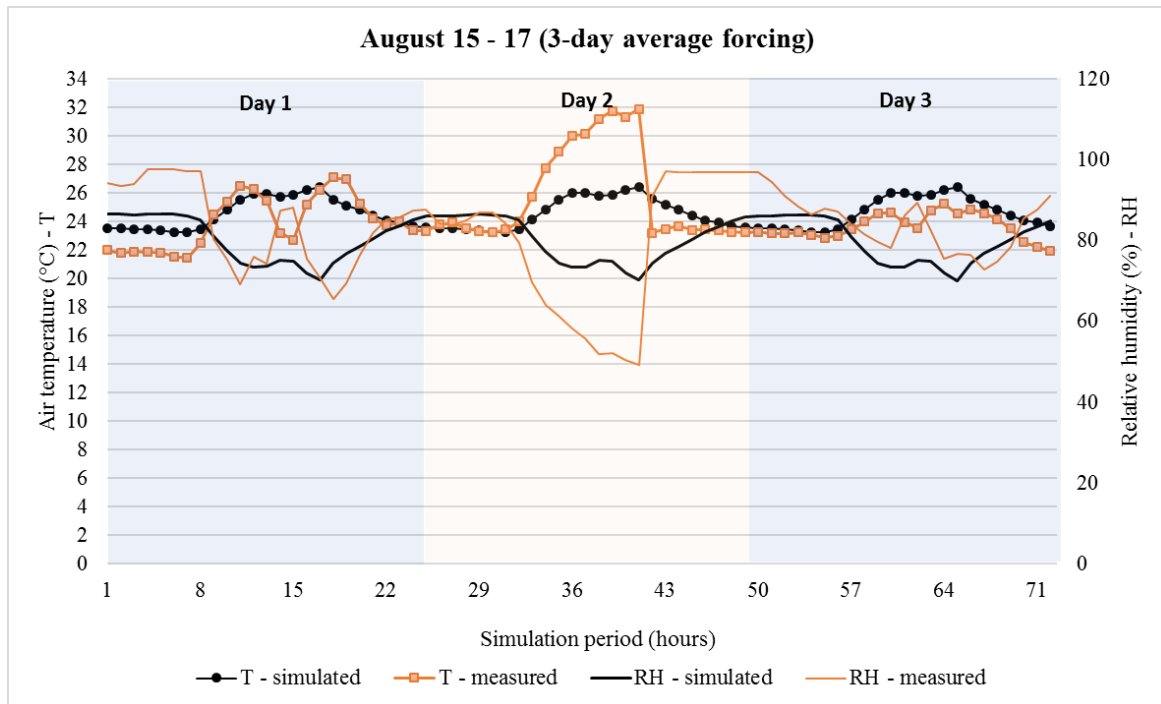
1. It can be seen that the measured air temperature has a regular pattern in terms of the maximum and minimum which varies between 28°C - 30°C for the simulation period. Therefore, by initializing the model with a 3-day average, the model is able to predict the air temperature with RMSE 1.91°C and relative humidity of 9.99%. The correlation for air temperature is 0.92 which shows a high degree of agreement with the measured data. The correlation for relative humidity is 0.77, which is mainly attributed to Day 2 when the pattern is not similar to day 1 and day 3.



**Figure 30. Comparison of simulated and measured data for June 2 - 4**

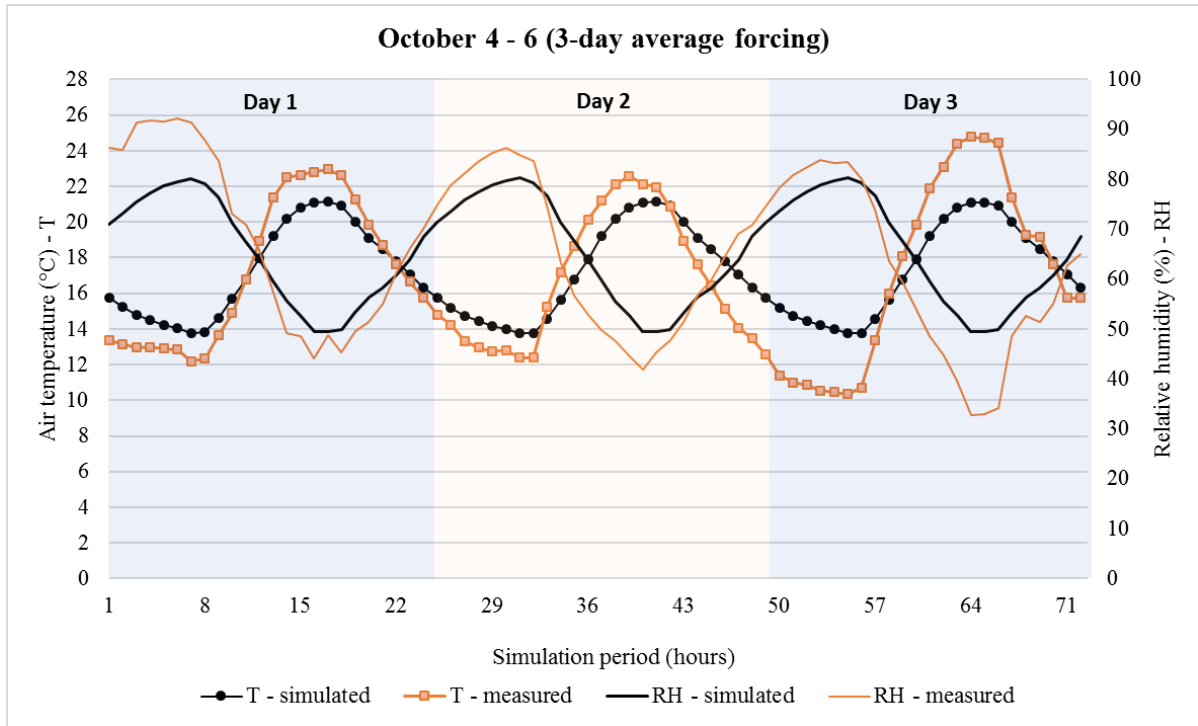
Figure 31 shows the comparison of simulated and measured air temperature and relative humidity using 3-day average initialization for August 15 - 17.

It is observed that the measured air temperature and relative humidity have a steady pattern throughout the 3-day simulation period. The daily variation between the maximum and minimum air temperature and relative humidity is approximately 6°C, which is low when compared to winter and swing seasons where the variation is between 10°C - 15°C .



**Figure 31. Comparison of simulated and measured data for August 15 -17**

Due to this regular air temperature pattern in the summer months, the RMSE and correlation coefficient for air temperature and relative humidity are 1.91°C and 9.99% and 0.78 and 0.68 respectively. The correlation coefficient for this summer case is lower than the other cases because of the sudden increase and decrease in air temperature and relative humidity that is observed on day 2. This is attributed to the actual change in the climate condition or a misrecording by the sensor during this specific period.



**Figure 32. Comparison of simulated and measured data for October 4 - 6**

Figure 32 shows the comparison of simulated and measured air temperature and relative humidity using 3-day average initialization for October 4 – 6. The following observations can be made:

1. The measured air temperature and relative humidity has a regular pattern through the 3 day simulation period with a maximum of 23°C - 25°C and minimum of 10°C - 12°C. Therefore, by initializing the model using the average of these 3 days, the model is able to predict the air temperature with an RMSE of 2.03°C and relative humidity with an RMSE of 7.65%. The correlation between simulated and measured air temperature and relative humidity is 0.94 and 0.95 respectively. This shows that there is a high degree of correlation between the simulated and measured by initializing the model using a 3-day average.

Therefore, it can be concluded that for climate conditions when the minimum and maximum air temperature variations are not above 10°C - 15°C, the ENVI-met model is able to accurately predict the air temperature and relative humidity. However, when these minimum and maximum variations exceed 15°C, a 1-day initialization and simulation is recommended to achieve simulated data comparable to measured data. It should also be noted that, there can exist climate conditions with very high variability in the daily minimum and maximum as well as between the consecutive days air temperatures. Such days are extremely difficult to predict and cannot be simulated with accuracy. These variations can most often occur in a heating dominated climate such as Pittsburgh, PA during the winter and spring seasons. However, the number of such days are negligible when compared to an annual simulation. The above conditions can be translated into rules to derive the number of ENVI-met simulations that would be required to simulate the microclimate for an annual period.

### **3.6.1. Method to derive number of ENVI-met simulations for an annual period**

Based on the analysis in Section 3.6 above, the two rules have been established to derive the number of ENVI-met simulations.

1. **Rule 1:** *If difference between maximum and minimum air temperature  $\leq 15^\circ\text{C}$ , then rule 2.*
2. **Rule 2:** *If difference between daily hourly temperature  $\leq 15^\circ\text{C}$ , then  
Simulation uses 3-day average initialization, else  
Simulation uses 1-day initialization.*

First, Rule 1 is used to eliminate the days that cannot be simulated to achieve the required degree of accuracy. Second, Rule 2 is used to provide the number of simulations that is

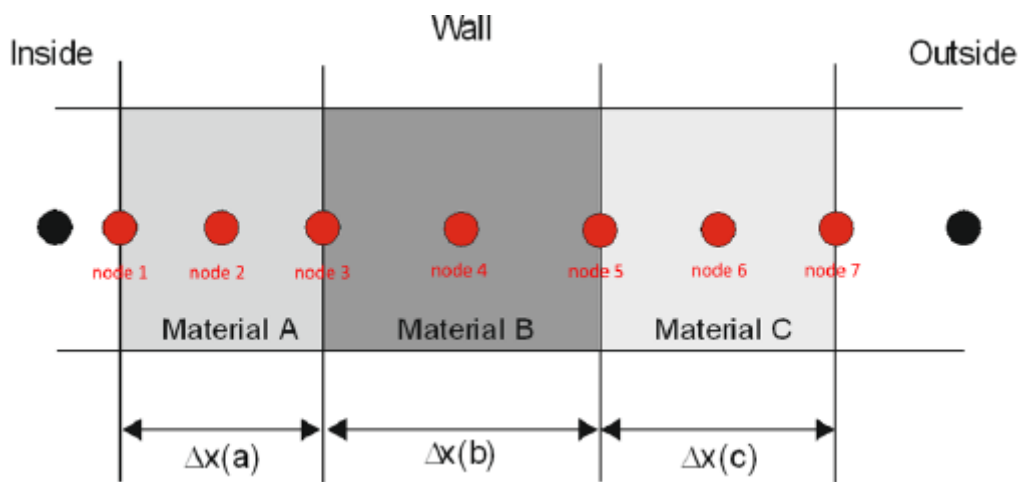
required to be conducted using a 3-day average and a 1-day initialization. Therefore, by this method, it is possible to derive the total number of ENVI-met simulations required to cover an annual period.

As an example, the above described rules was implemented to calculate the number of ENVI-met simulations that would be required to predict the microclimate for an annual period using 2016 air temperature data for Pittsburgh. Results show that: 96 simulations with 3-day average initialization and 38 simulations with 1-day initialization would be required to simulate the annual microclimate. Since Pittsburgh microclimate has seasons where it is hard to predict the microclimate, the results also show that the microclimate cannot be predicted with high degree of accuracy for 40 days of the year.

### **3.6.2. Analysis of simulated and measured façade temperature**

Sections 3.5.1 and 3.5.2 provide a detailed statistical analysis of the air temperature and relative humidity by comparing the air temperature and relative humidity with the weather station and the five experimental setup points. This constitutes for first two steps in the comparative analysis of the simulated and measured data. This section provides analysis of the simulated and measured façade temperature which is the third step for comparing the accuracy of the ENVI-met prediction. This analysis is especially important to determine the ENVI-met model accuracy using the 7-node calculation to estimate the façade temperature. Results show that the ENVI-met model is able to predict the façade temperature with a high degree of accuracy by implementing the 7-node modeling function. Given that the CSL model is a high-resolution model (2m), the maximum variation between the measured and simulated façade temperature is 7.8%, which means that the ENVI-met model is able to simulate façade temperature that closely represent measured thermographic data.

According to (Huttner, 2012), to calculate the outside and inside façade temperature and the indoor air temperature, the façade layer uses seven calculation nodes as shown in Figure 33. This allows for the construction of up to three building material layers which can vary in width and material properties. Every material can have its own physical properties (absorption, transmission, reflection, emissivity, specific heat capacity, thermal conductivity and density). As shown in Figure 33, the red dots symbolize the different nodes, located at the center and lateral borders of each material (Simon).



**Figure 33. Schematic layout of 7-node wall and roof construction in ENVI-met**  
(Simon, 2016)


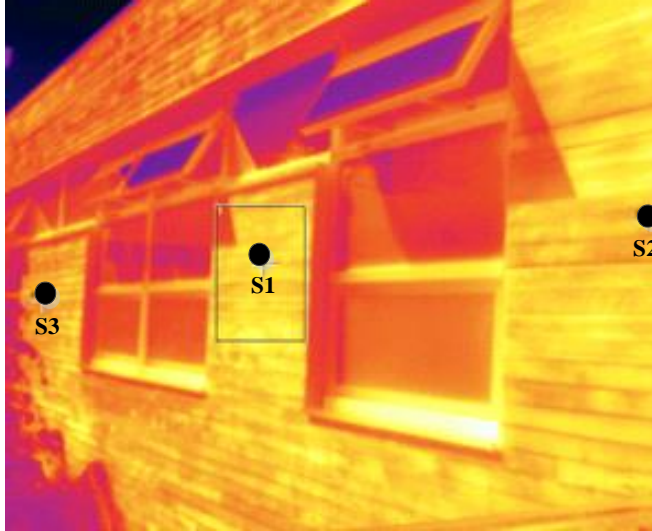
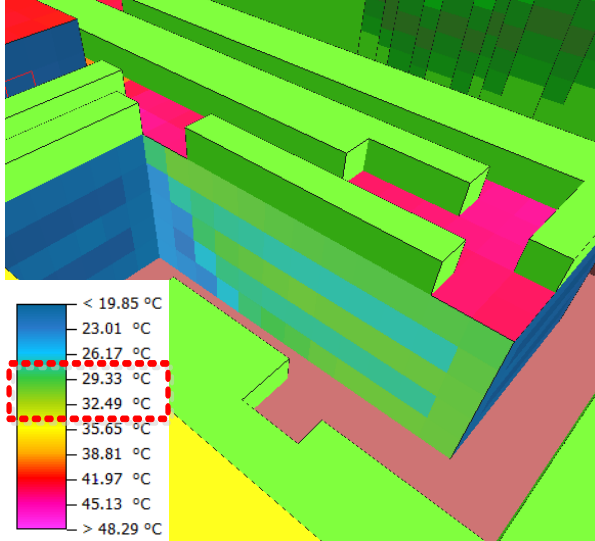
Based on this detailed façade modeling feature in ENVI-met, the 7-node criteria is used for the CSL case-study building. The material properties for the ENVI-met model are obtained from the EnergyPlus model. To evaluate the accuracy of this 7-node façade and roof modeling in ENVI-met, it is important to compare the predicted and measured façade temperatures.

The measurement was conducted using a thermographic camera on June 14, 2016. Two time periods, 10:00am and 2:00pm were selected to cover the morning and afternoon periods on a sunny day. Based on the building orientation and sun direction, the measured thermographic images were compared with simulated north and east façade at 10:00am



and the south and west façade at 2:00pm. Tables 5 & 6 show the comparison with the thermographic images for three selected spots, façade maximum and façade average temperature for the north and south facades. The table comparison for the west and east facades is documented in Appendix A.

Table 5. Comparison of simulated and measured north façade temperature

June 14, 2016 – 10:00am (North façade)		
		
Surface Temperature Measurement spot	Thermographic image - Measured (°C)	ENVI-met Simulated (°C)
Spot 1	33.23	30.17
Spot 2	32.54	31.56
Spot 3	33.53	30.61
Area Maximum	35.42	32.49 - 35.65
Area average	32.71	30.11 - 32.49

**Table 6. Comparison of simulated and measured south façade temperature**


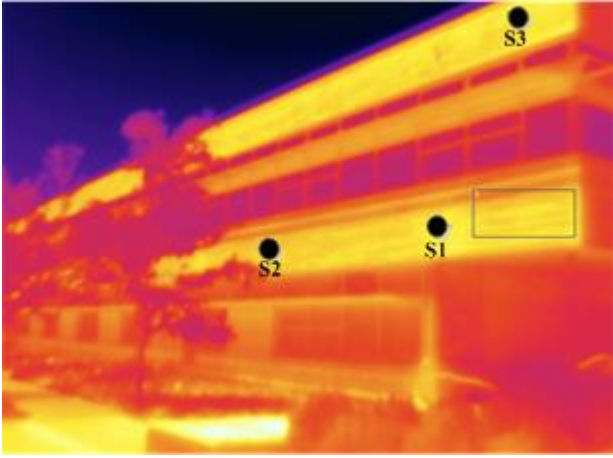
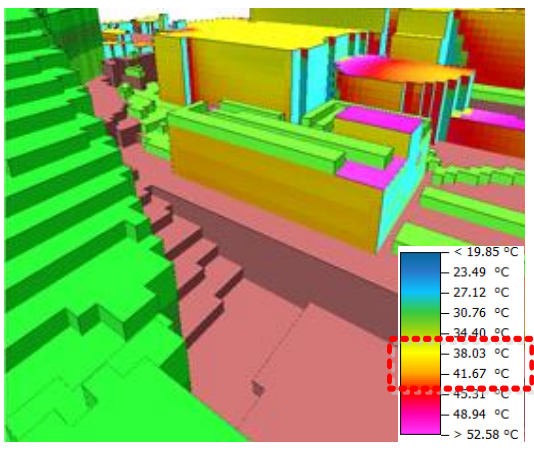
June 14, 2016 – 2:00pm (South façade)		
		
Surface Temperature Measurement spot	Thermographic image - Measured (°C)	ENVI-met Simulated (°C)
Spot 1	43.50	40.20
Spot 2	42.54	40.91
Spot 3	41.06	41.14
Area Maximum	43.73	41.67 - 45.31
Area average	40.65	38.03 - 41.67

Table 5 & 6 compares the simulated and measured data for the north and south façade at 10:00am and 2:00pm respectively. Results show that the variation in simulated and spot measured façade temperature can be attributed to the sun angle rotation and the percentage of glazing on the building versus the ENVI-met model. ENVI-met calculates the sun angle based on the latitude, longitude and the time zone and this can have a slight variation when compared to actual sun position. It should also be noted that the ENVI-met model is grid based with a model resolution of 2m. Therefore, when comparing spot façade temperatures, the model represents the temperature for entire grid which can cause slight inaccuracies.

From Table 5, it is seen that three measurement spots are selected on the thermographic image to conduct the comparison with the simulated data. Comparing spot 1, 2 and 3, it is observed that the difference between measured and simulated façade temperature is 3.03°C, 0.94°C, and 2.89°C respectively. It is also observed that though the spot measurements have a maximum variation of 3.03°C, the area maximum and average fall in between the ENVI-met simulated range and closely match the simulated data.

Similarly, Table 6 compares the simulated and measured data for the south façade at 2:00pm where three measurement spots are selected on the thermographic image to conduct the comparison. Comparing spot 1, 2 and 3, it is observed that the difference between measured and simulated façade temperature is 3.3°C, 1.6°C, and 0.14°C respectively. It is also observed that though the spot measurements have a maximum variation of 3.3°C, the area maximum and average fall in between the ENVI-met simulated range and very closely match the simulated data. Similar pattern is observed for the east and west facades (Appendix A).

Therefore, as highlighted previously, results show that the ENVI-met model is able to predict the façade temperature with a high degree of accuracy by implementing the 7-node modeling function.

### **3.7. Summary**

This chapter describes the ENVI-met model automation, setup and initialization process for the CSL case-study. The ENVI-met 3D model can be seamlessly created using ArcGIS 3D analyst functions. From the simulations for the 24 cases that represent the annual climate condition of Pittsburgh, three types of analysis were conducted to compare the accuracy of the simulated and measured data as well as to emphasize the importance of accurate model initialization.

From the initialization analysis, results show for the winter months (November – February), when the measured air temperature pattern is not regular in terms of the daily minimum and maximum, the model should be initialized with 1-day data and simulated for every 24-hour period. By initializing the model with a 3-day average data, the RMSE for air temperature and relative humidity is higher than the summer months. For the summer months (May – August), the model is able to predict the air temperature and relative humidity with a high degree of accuracy using a 3-day average initialization. This is because of the regular air temperature and relative humidity that is used to initialize the ENVI-met model. For the swing months (late March – early May and September - October), the accuracy of the simulated data depends on the pattern of the air temperature and relative humidity used to initialize the model. Results also show that by using ENVI-

met 7-node feature to accurately define the building envelope properties, the model is able to predict the façade temperature with a high degree of accuracy.

Therefore, after accurately conducting the ENVI-met simulations, the next step is to couple these results with the CSL EnergyPlus model to analyze the effect of microclimate on building energy consumption.

## **Chapter 4: Implementation of coupling method to improve building energy consumption predictions**

### **4.1. Overview**

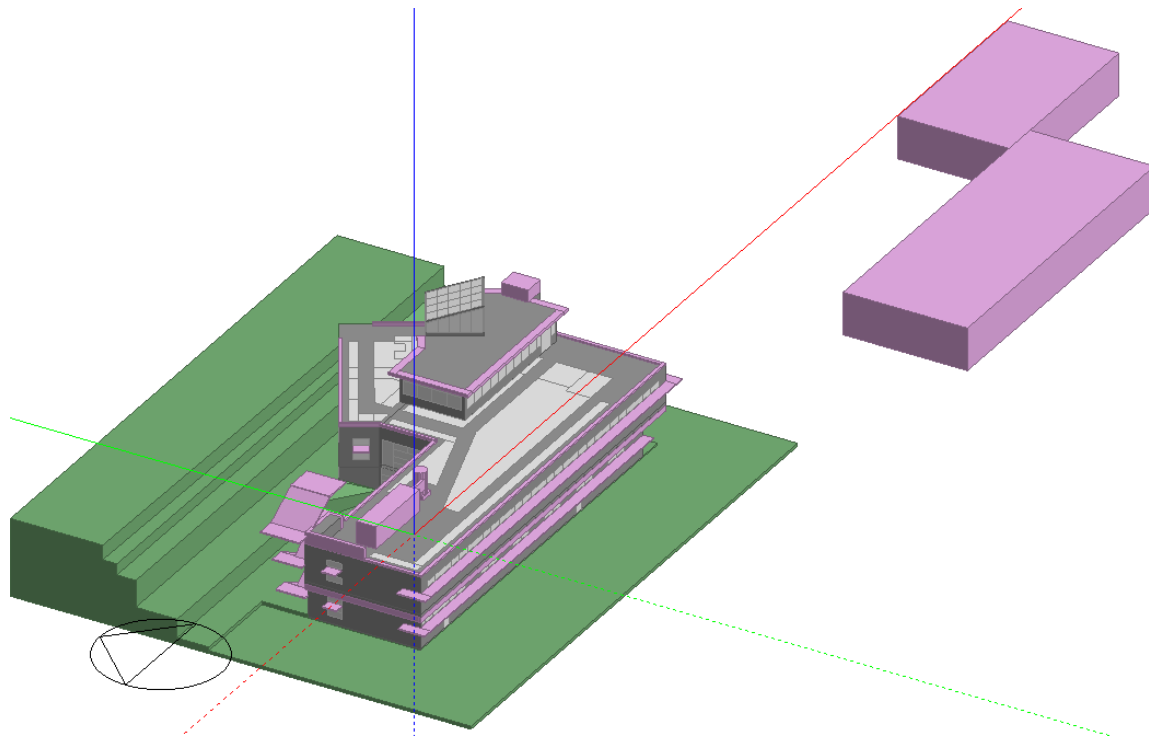
After the microclimate simulations were conducted and the model initialization analyses made as described in Chapter 3, the simulated data was coupled with the building energy simulation tool, EnergyPlus, using BCVTB as the coupling platform. As described in Chapter 3, six simulation cases—representing winter, summer, and the swing seasons—were selected to demonstrate the effects on building energy consumption of coupling the thermodynamic interactions between natural and built environments. This chapter describes the coupling of the urban microclimate with the building energy simulation tool. Section 4.1 describes the data mapping and exchange between ENVI-met and EnergyPlus. Section 4.4 details the coupling of surface boundary conditions and infiltration, and Sections 4.5 and 4.6 provide analyses of the impact of TMY3 weather data versus simulated weather data on the façade temperature and building energy consumption.

### **4.2. Building energy model description**

As a first step to coupling the microclimate simulated results with a building energy model, it is important to create an energy model that closely represents the as-built building. This research uses the energy model of the CSL case-study adapted from Zhao (2015). This detailed energy model was converted using DesignBuilder to the more recent EnergyPlus v8.5. During this conversion, care was taken to maintain the building's geometry because the building form and thermal zoning can modify the outside

microclimate conditions (i.e., wind speed, wind direction and air temperature). Therefore, the building form is an important factor in quantifying the effects of microclimate on energy consumption.

The main elements of an energy model that affect building energy consumption are the construction materials (building envelope), operational schedule, and mechanical system.

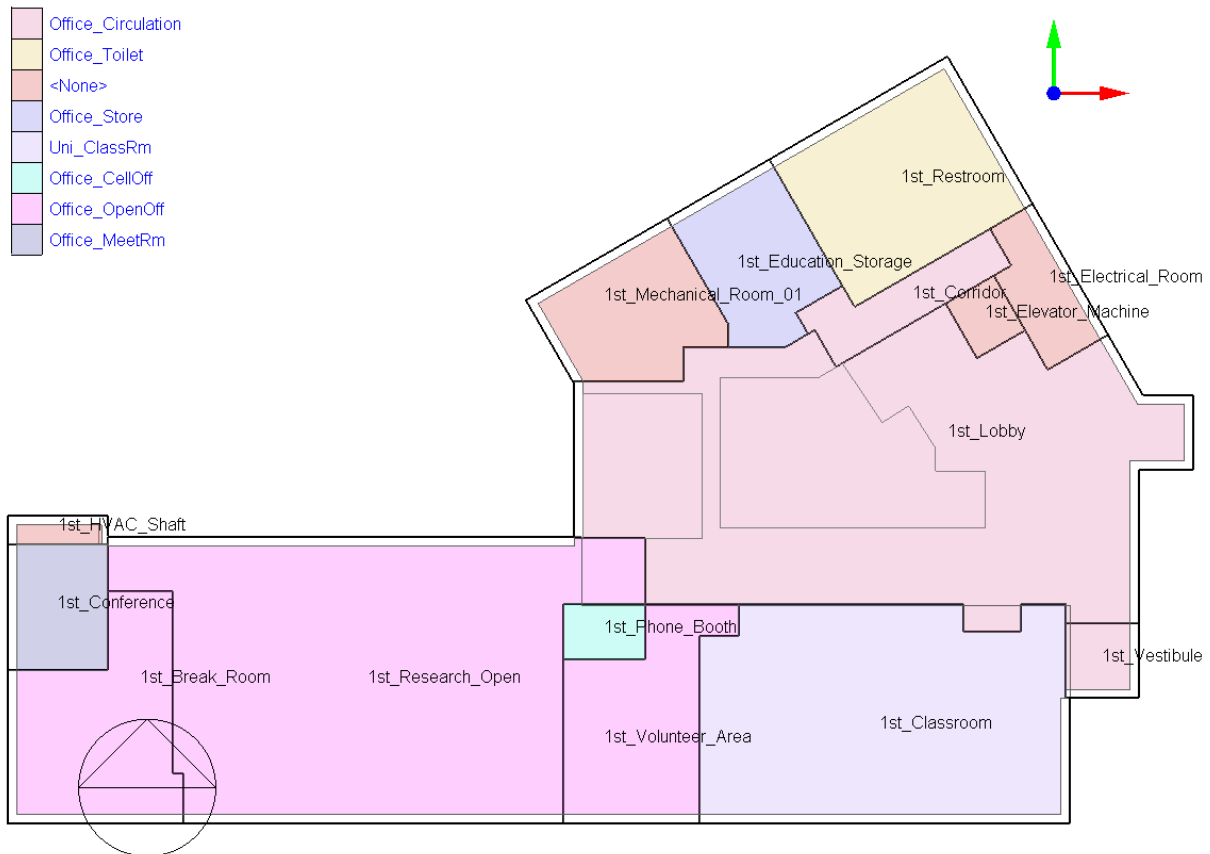


**Figure 34. DesignBuilder model of the CSL building**

The EnergyPlus model represents the as-built building in terms of building construction materials and operational schedules (Zhao, 2015). However, the HVAC system in the EnergyPlus model is a variable air volume (VAV) with reheat system (boiler and chiller), whereas the HVAC system of the CSL building is a central air handling unit (AHU) with a ground source heat pump (GSHP) and energy recovery ventilator (ERV). The under-floor air distribution (UFAD) system is used for the open-style offices, conference rooms,



and other regularly occupied spaces. A ceiling-based air distribution system is used for other spaces, such as restrooms, service areas, and mechanical and storage areas. Despite this variation between the EnergyPlus modeled HVAC and the as-built HVAC, comparable measured data was obtained, as detailed in Section 4.6. Figures 34 and 35 show the EnergyPlus model of the CSL building.



**Figure 35. First floor plan of the CSL building**

The energy model used in this thesis is based on the construction drawings for the building envelope. The HVAC system is a ASHRAE baseline system, which is a VAV with reheat, and it does not represent the as-built water source heat pump system. However, necessary steps have been taken to accurately calculate the measured cooling and heating energy

consumption from the as-built mechanical system through data mining as described in Chapter 4. This is essential to compare the coupled model energy consumption correctly.

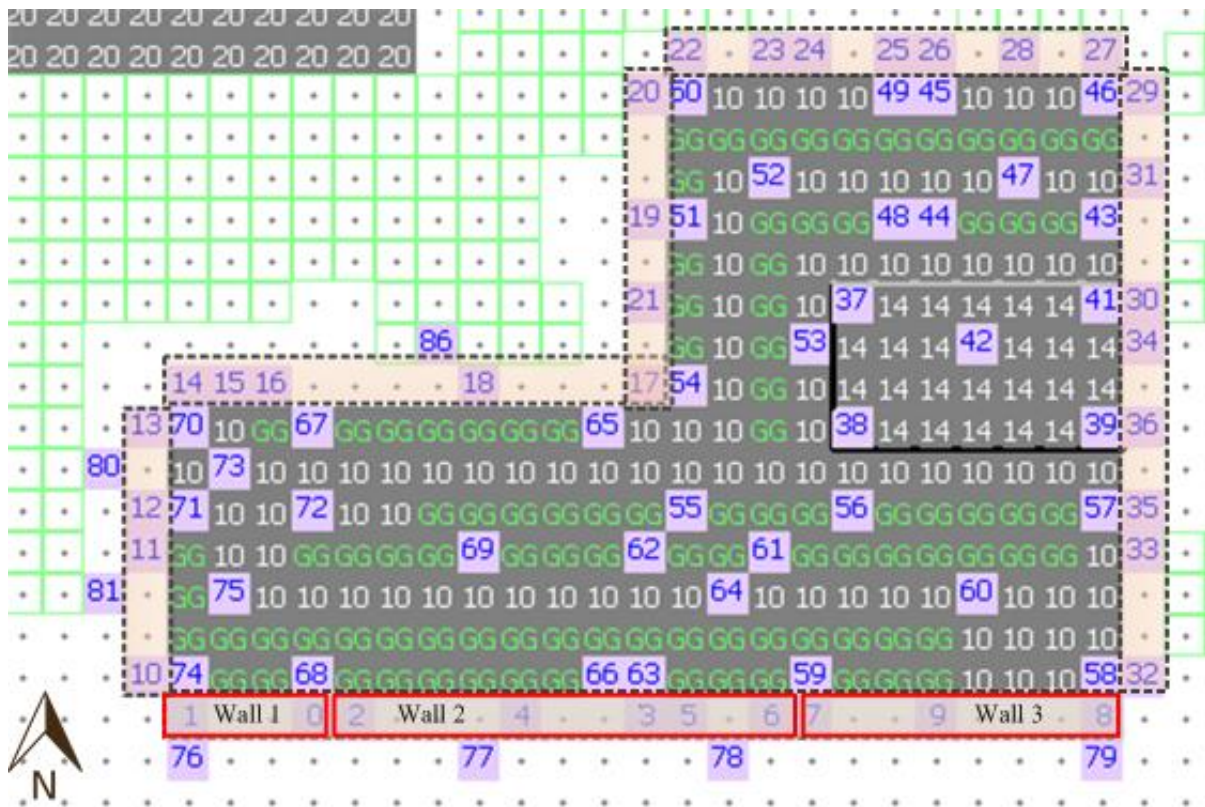
### **4.3. Data mapping and exchange between ENVI-met and EnergyPlus**

After the setup of the EnergyPlus model, the next step was to process the ENVI-met microclimate simulation results to match the EnergyPlus format accurately. As discussed in Chapter 2, Section 2.3.3.1, in ENVI-met, the 3D model geometry is based on structured grids while in the EnergyPlus building envelope, elements are considered single entities. In ENVI-met, each of these surfaces is divided into grids based on the model resolution, which is 2m for the CSL case-study building. Simulation data is recorded using the receptor function in every grid (every 2m) along the height of the building. Therefore, to transfer the simulated microclimate data from ENVI-met to EnergyPlus, each surface is treated as an individual unit (e.g., each wall and roof is a separate unit) in both tools, as shown in Figure 36.

BCVTB is used to process and calculate the air temperature and wind speed data for every surface based on the receptor information. Figure 34 shows how the data was extracted and mapped using BCVTB. As seen in the figure, the extraction process was based on the model parameters, wall and roof extraction, and the EnergyPlus processed output.

The model parameters (Figure 37) show that the simulation period is 3 days where ENVI-met simulated data is processed for the full building height ( $B_g$ ). The number of surfaces in the CSL EnergyPlus model for which ENVI-met simulated data is mapped, is 302 ( $N_r$ ). It should be noted that the  $N_r$  value for a 2-story office building is high owing to the detailed nature of the EnergyPlus model. The number of receptors required to map the

ENVI-met simulated data for the CSL building façade is 37 (Wr), as seen in Figure 36. From Figure 36, it can be seen that the data for each façade is mapped based on the EnergyPlus thermal zones (wall 1, wall 2, wall 3, etc). Figure 37 shows that the wall extractor is mapped for every wall and split based on the floor to generate the wind speed and air temperature. The same process was repeated for the roof extractors at the roof height to generate the output.



**Figure 36. Layout of receptors for recording simulated data in ENVI-met for the CSL case-study**

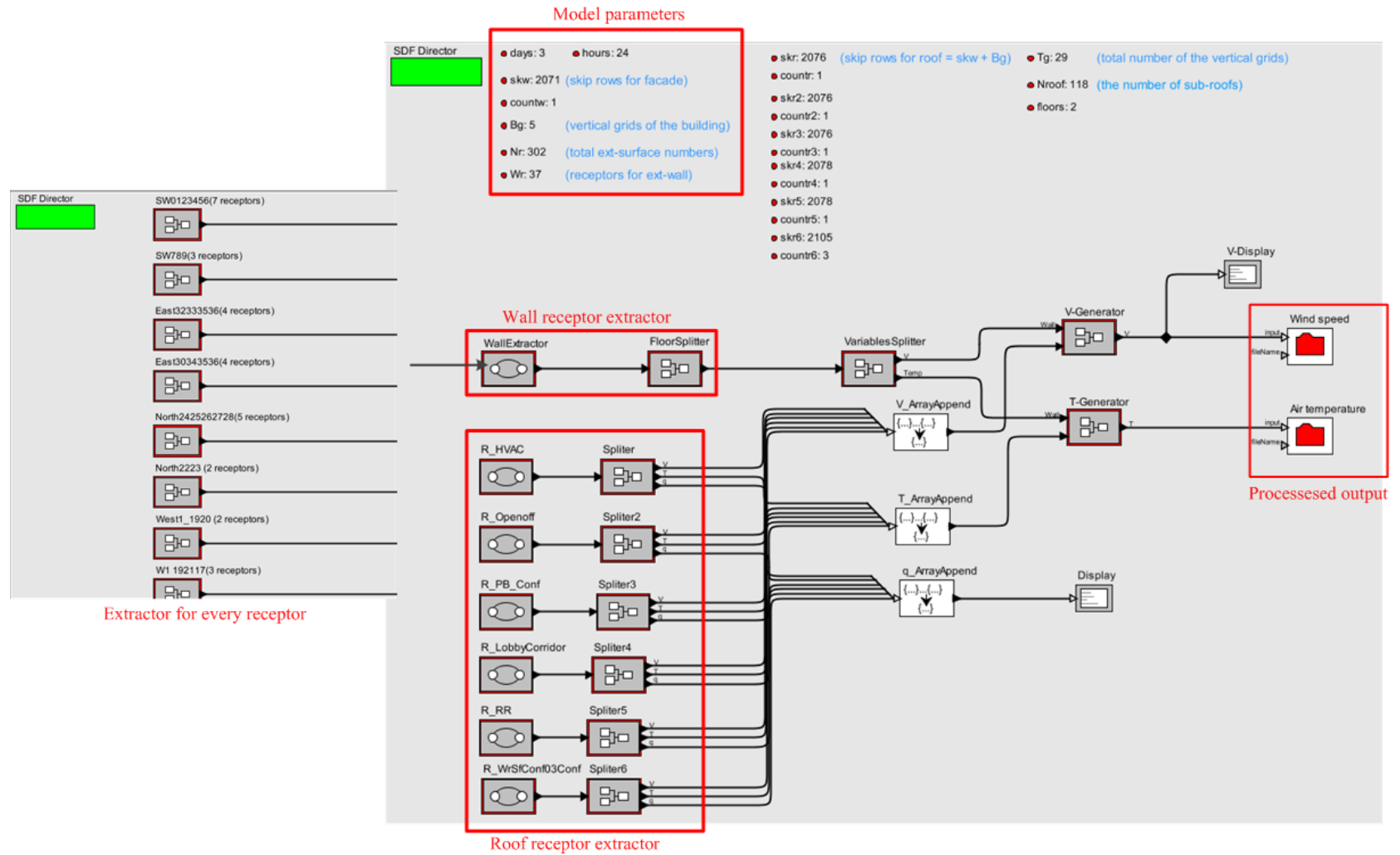


Figure 37. BCVTB module for data extraction and mapping

#### 4.4. Implementation of coupling platform

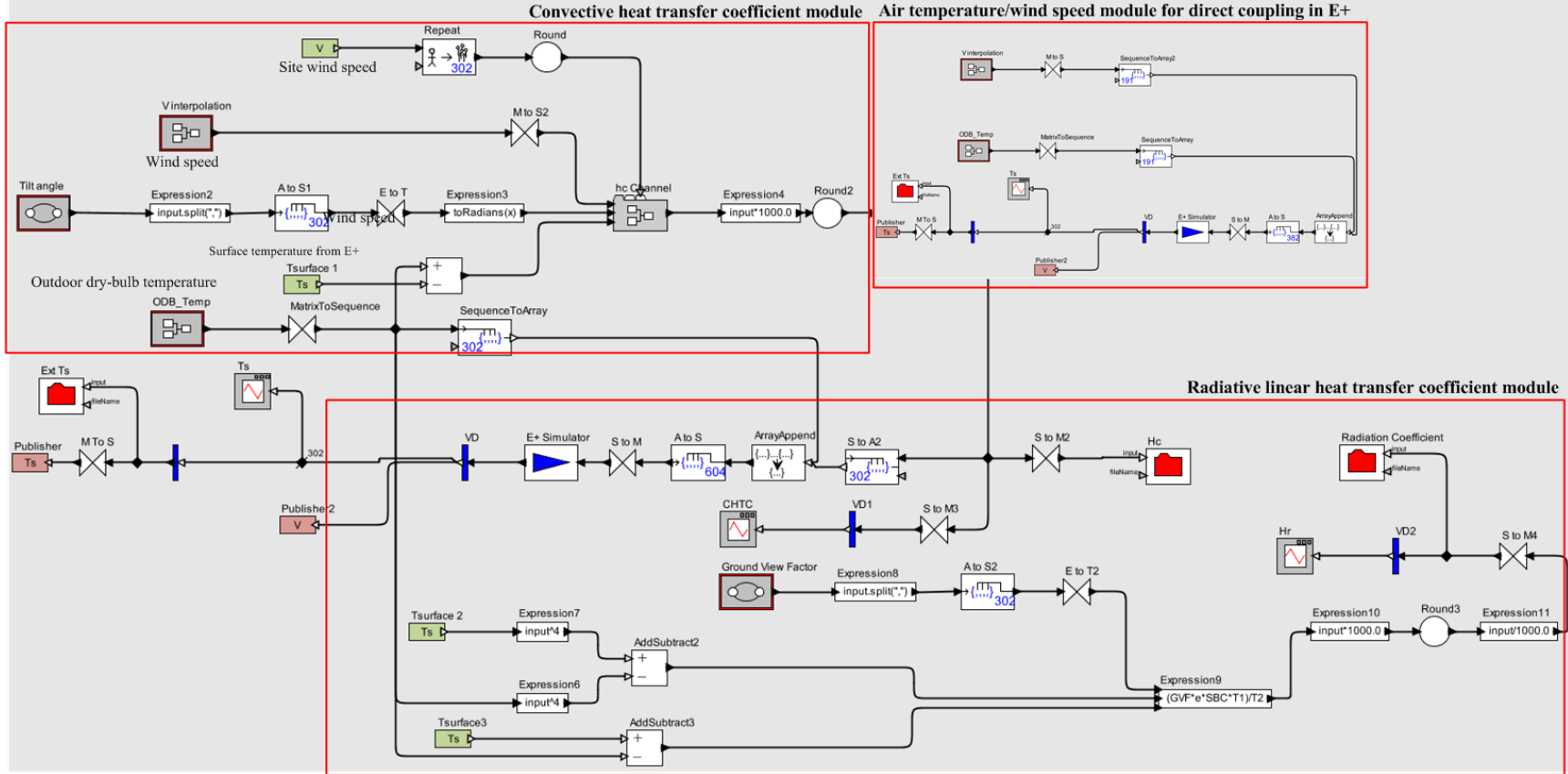
After successfully processing the ENVI-met simulated air temperature and wind speed into the EnergyPlus format for all 302 building surfaces, the next step was to implement the coupling method described in Chapter 2, Section 2.3.3.2. According to Section 2.3.3.2a, the absorbed direct and diffuse solar flux was accounted for by modeling the surrounding building in EnergyPlus (shadow calculations). The input for ground reflectance in EnergyPlus was modified using the EnergyPlus object “Site:GroundReflectance” for every simulation period based on the ENVI-met simulation results.

The next step was to couple the effects of surface boundary conditions as described in Section 2.3.3.2b, shown in Figure 38. Stage 1 implementation was the convective heat transfer coefficient ( $h_c$ ), which was calculated based on equation (4). As shown in Figure 35,  $h_c$  was calculated and overwritten in EnergyPlus using the Energy Management System (EMS) actuator “Exterior Surface Convective Heat Transfer Coefficient.” Stage 2 implementation consisted of adding the effects of the radiation linear heat transfer coefficient. However, as described in Chapter 2, the EMS External Interface data exchange between BCVTB and EnergyPlus has a limitation of 1024 values at any given time. Therefore, according to the method described in Section 2.3.3.2b, Stage 2 involves implementation and direct computation of  $h_c$  and  $h_r$  in EnergyPlus by overwriting the air temperature and wind speed using the EMS actuator, “Outdoor Air Drybulb Temperature.”

After coupling the surface boundary conditions, the next step was to couple the effects of infiltration. Following equation (5) in Section 2.3.3.2c, the effects of outdoor dry-bulb temperature and wind speed were coupled using the EMS actuator “Outdoor Air Wind Speed.”

**Coupling module parameters**

SDF Director		
Days: 3 (simulation days)	n: 0 (for V interpolation)	e: 0.9 (emissivity)
timeStep: 5*60	t: 0 (for T interpolation)	SBC: 0.0000000567 (Stefan - Boltzmann Constant)
floors: 2	m: 0 (for P interpolation)	
finalTime: Days*24*3600	Nr: 302 (number of ext-surfaces)	



**Figure 38. BCVTB coupling module for convective and radiative fluxes for the CSL case-study**

The impact of coupling the ENVI-met simulated data with the CSL EnergyPlus model is analyzed and discussed using two variables: (1) the CSL façade temperature and (2) heating and cooling energy consumption. Section 4.5 discusses the effect of coupling microclimate data on façade temperature and Section 4.6 discusses the effect of coupling microclimate data on the CSL heating and cooling energy consumption.

Façade temperature comparison is conducted for a summer and winter case simulation using typical metrological year (TMY3) weather data and simulated weather data. As previously described, TMY3 weather file represents climate conditions from previous years (1991–2005) rather than current or recent weather conditions, for which the air temperatures and wind speed are approximately 10°C and 7–10m/s higher than the measured data for 2016, respectively.

#### 4.5. Effects of coupling microclimate data on façade temperature

Figures 39–42 show the variations in façade temperature during the summer when a TMY3 weather file was used versus a simulated microclimate weather file.

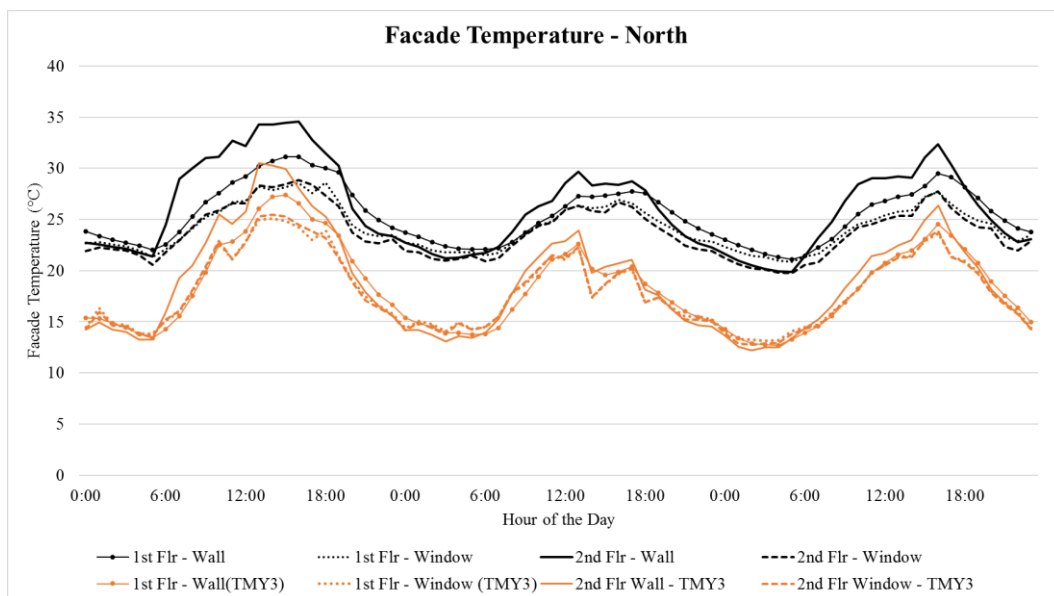
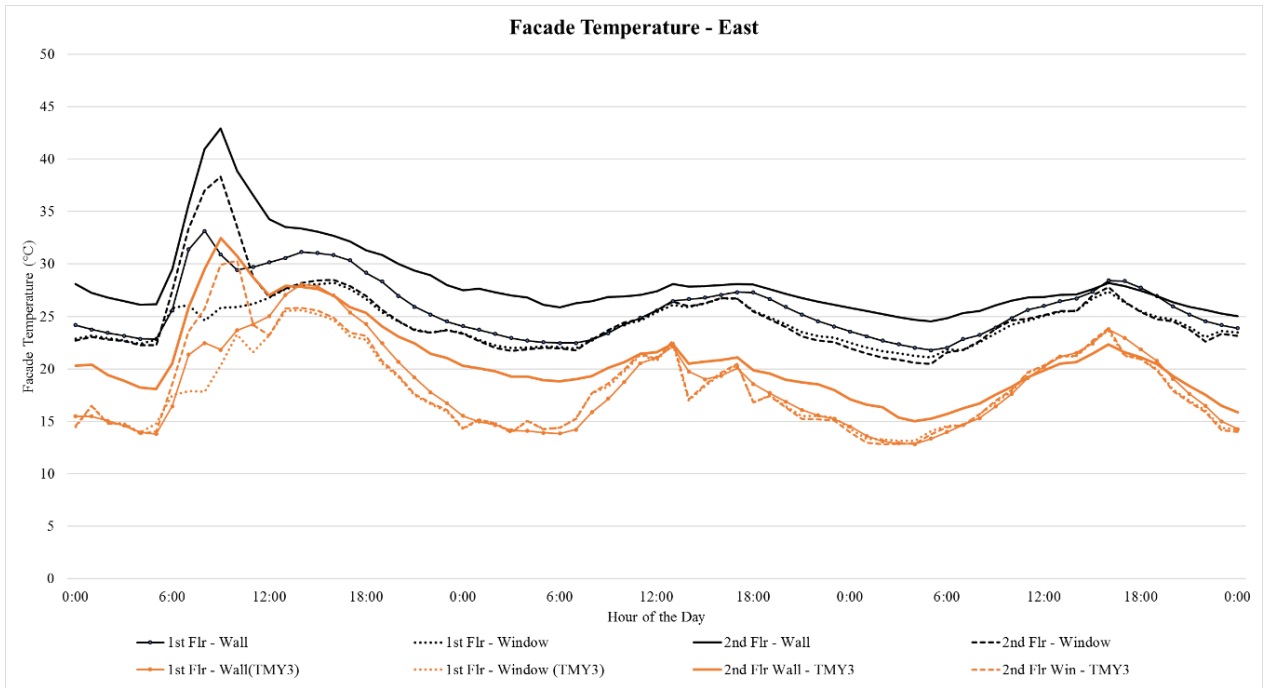
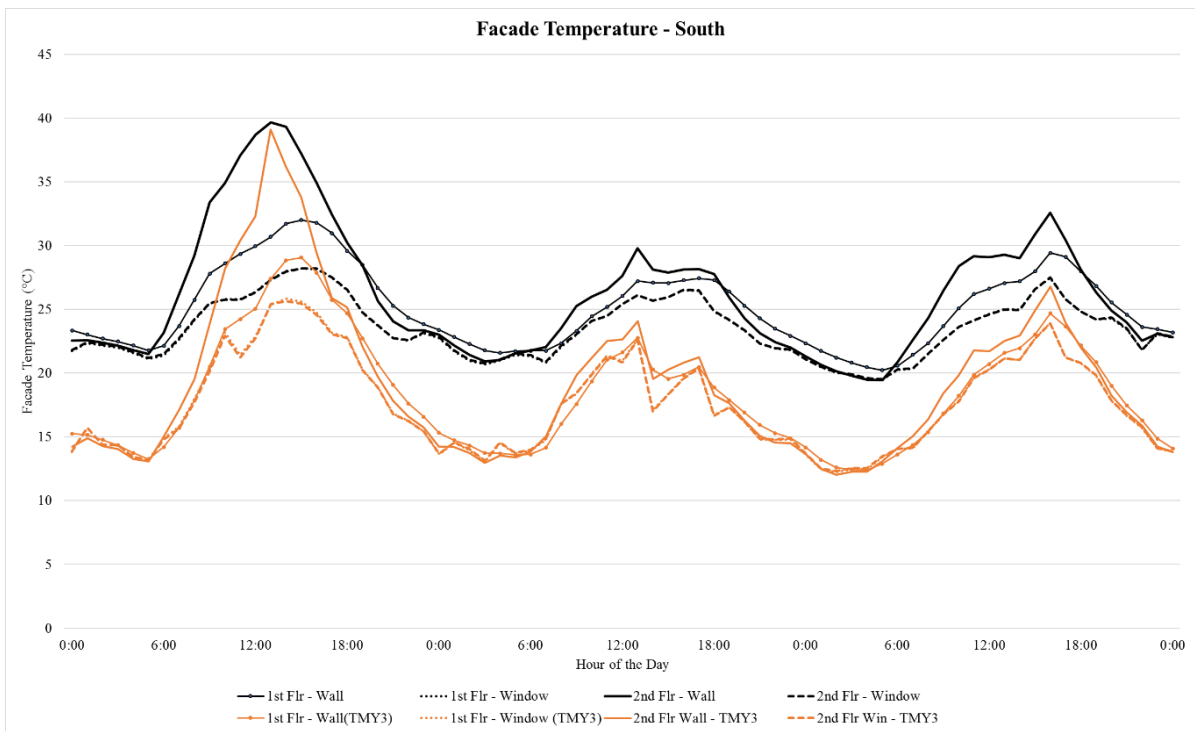


Figure 39. Comparison of north façade temperature in the summer

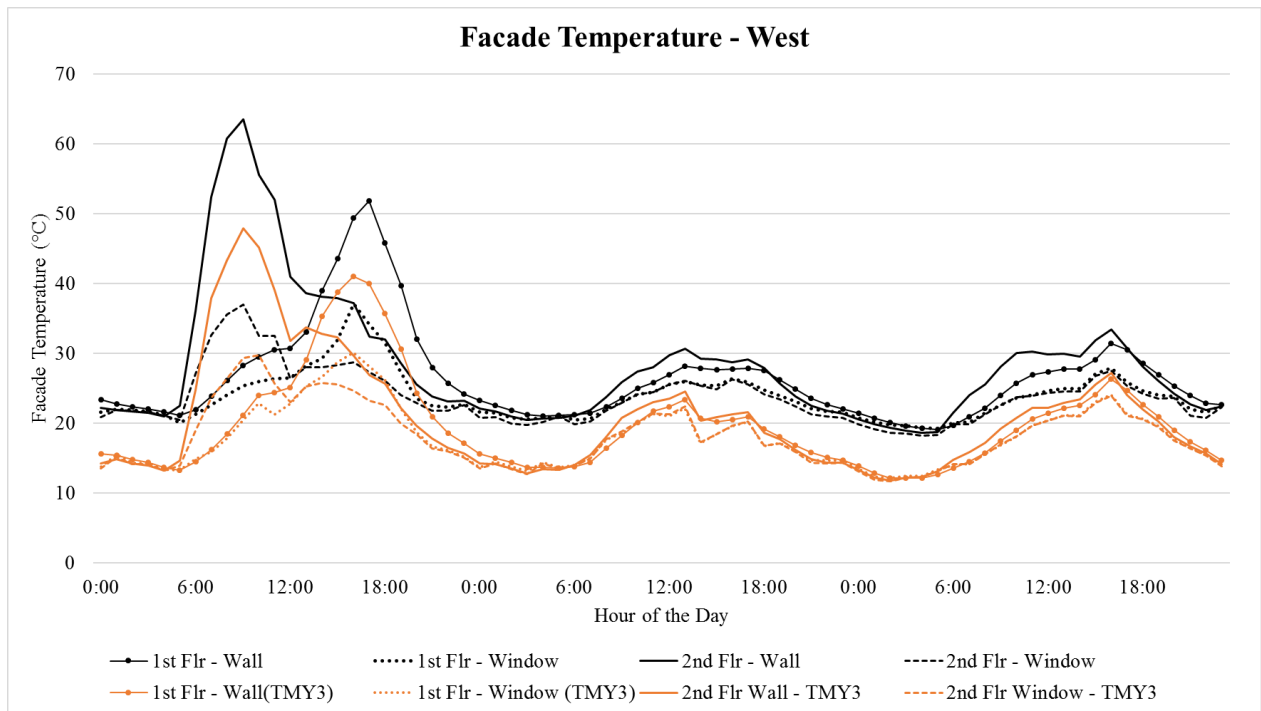


**Figure 40. Comparison of east façade temperature in the summer**



**Figure 41. Comparison of south façade temperature in the summer**





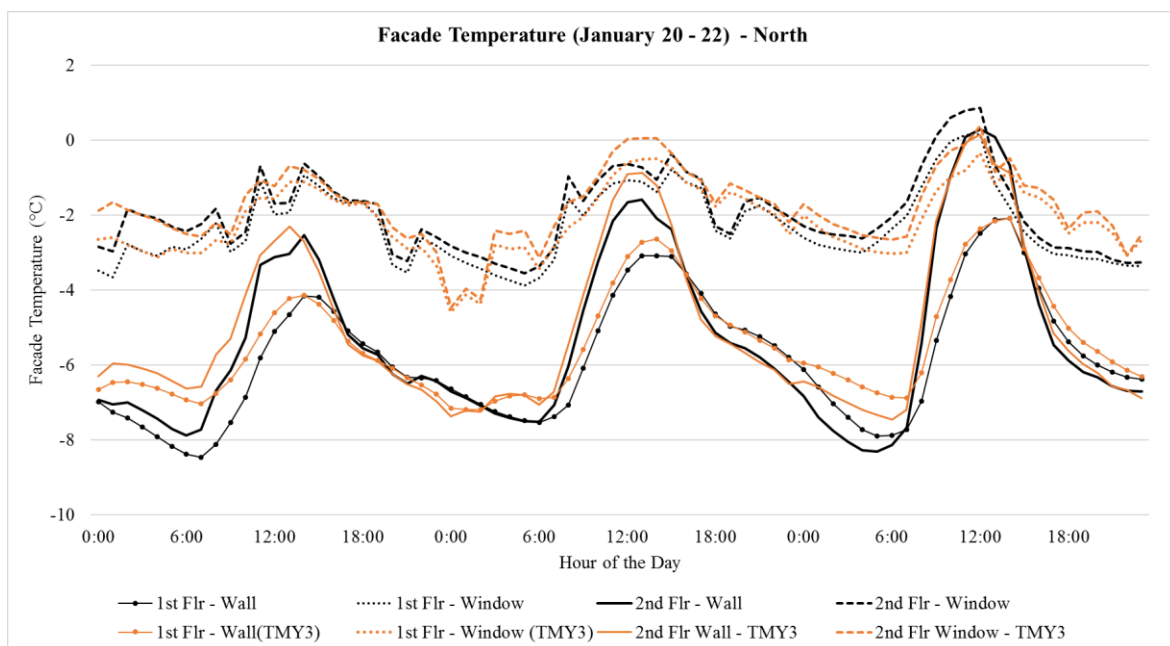
**Figure 42. Comparison of west façade temperature in the summer**

The comparison includes the first-floor wall and window and the second-floor wall and window.

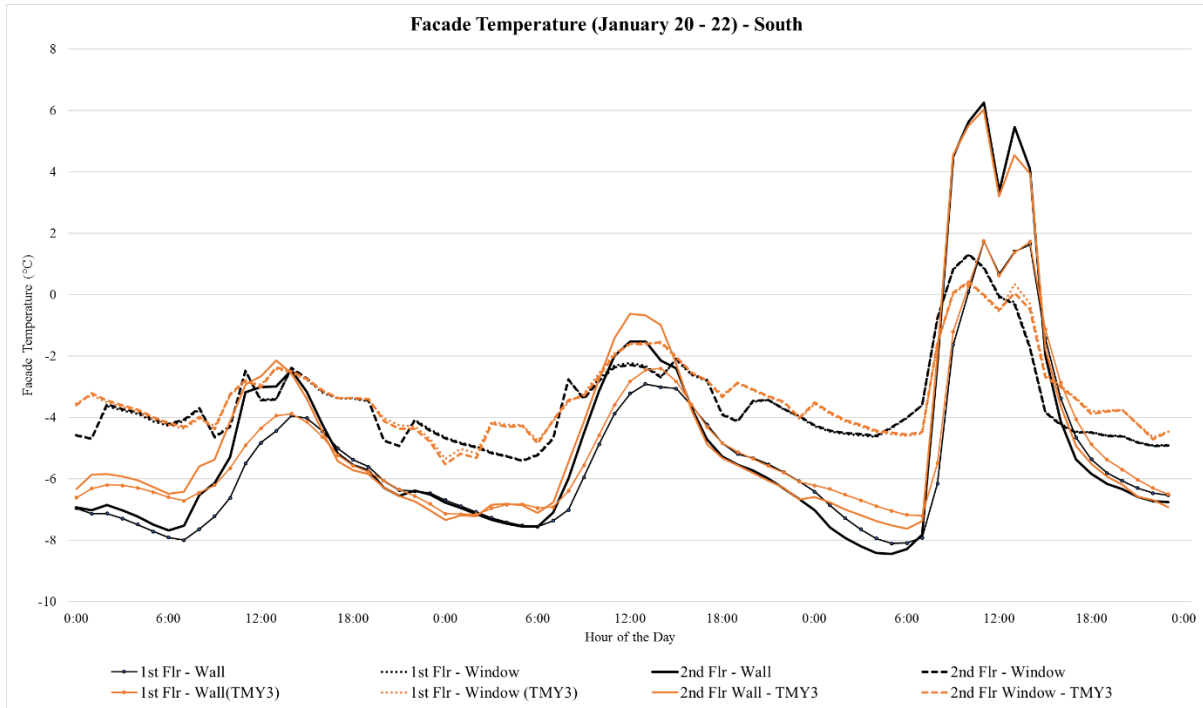
Overall, the comparisons show that TMY3 weather data does not accurately predict the façade temperatures in the summer. Results show that the highest temperature variations occur on the north and south façades, with variances of approximately 12°C–15°C for any given time of day during the 3-day simulation period. These variations are present in both walls and windows.

The east façade has the next highest variation of approximately 10°C, especially on days 2 and 3 of the simulation period. The west façade showed a variation of approximately 5°C–8°C for the simulation period. These variations are attributed to the different weather conditions defined in the TMY3 weather file as opposed to the simulated file (which represents the actual weather). It was observed that the air temperature during this period was approximately 20°C higher than that recorded in the TMY3 file. In addition, the wind

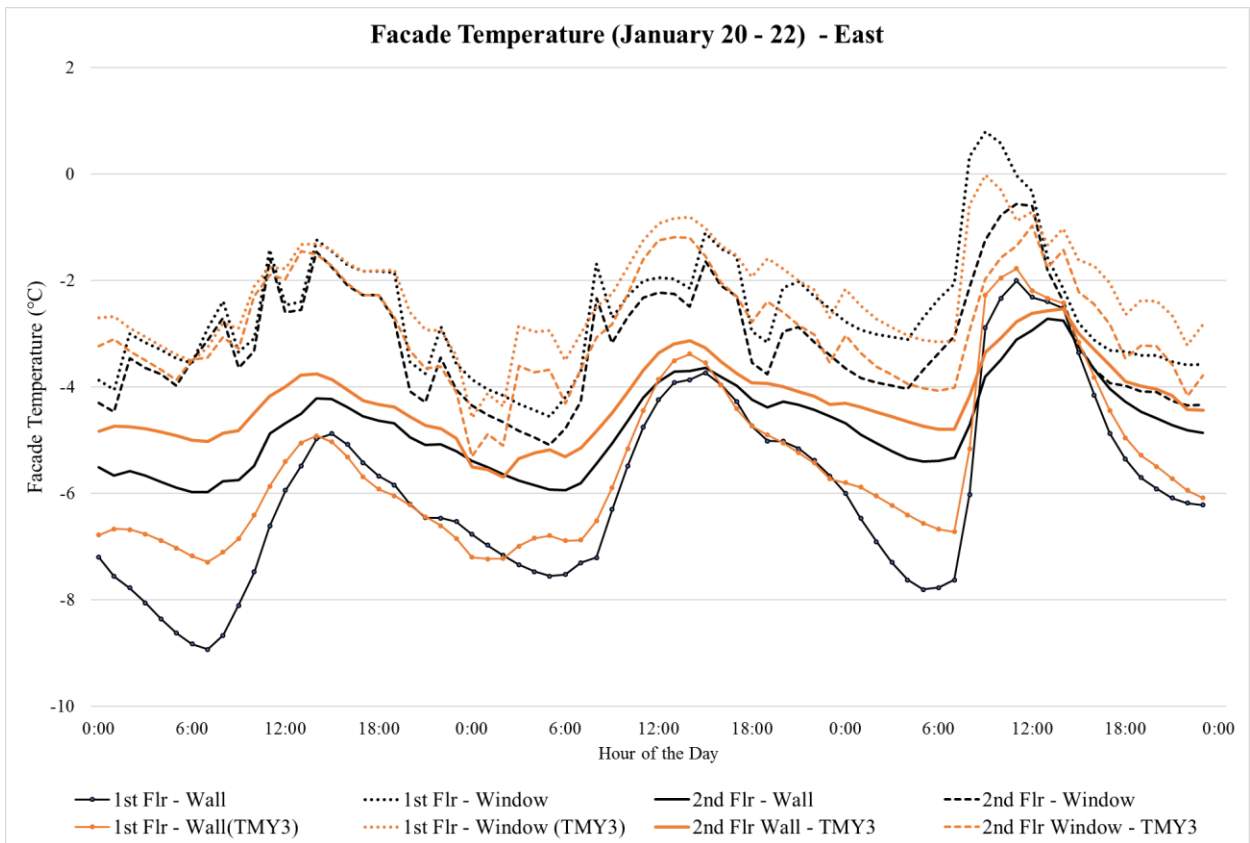
speed in the TMY3 data is much higher than in the simulated data (approximately 0 - 1m/s). It should also be noted that the north and south façades have the highest variation because they have the longest period of sun exposure and cover a larger surface area of the building envelope. Hence, during a sunny, clear day in summer, as represented by day 1 (owing to peak façade temperature), these façades are exposed to a high degree of solar radiation. Therefore, it is evident that using TMY3 weather data does not accurately represent the current weather conditions for obtaining realistic simulation results.



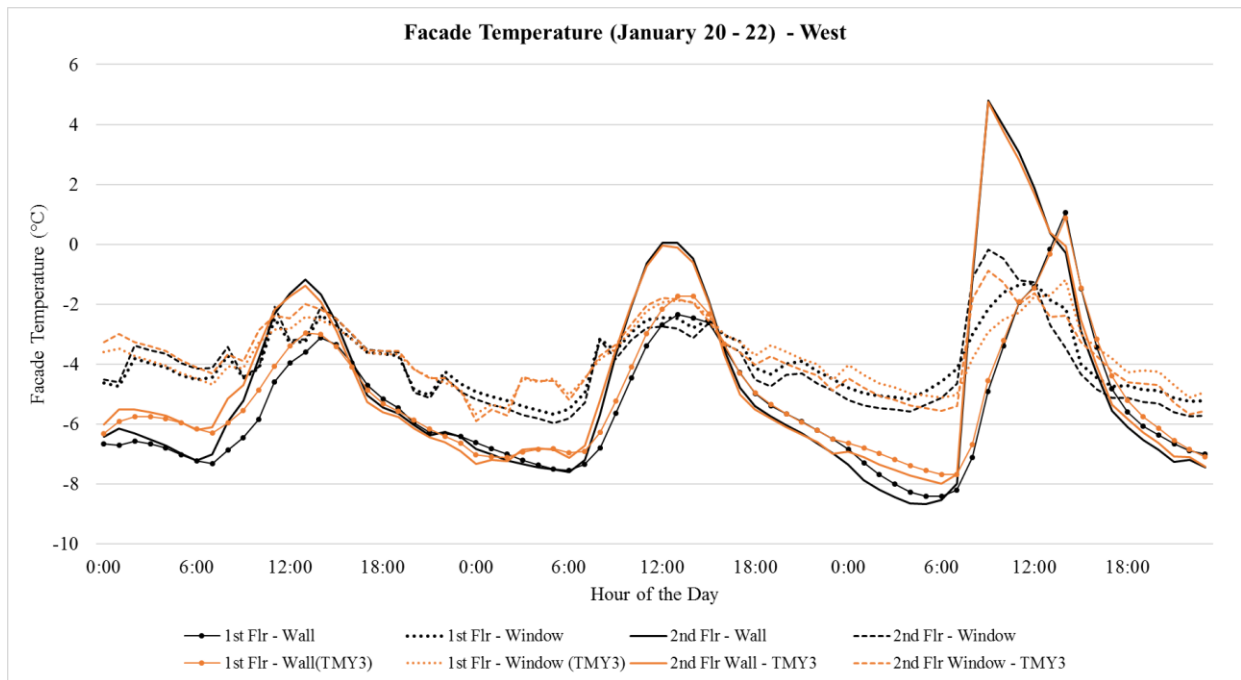
**Figure 43. Comparison of north façade temperature in the winter**



**Figure 44. Comparison of south façade temperature in the winter**



**Figure 45. Comparison of east façade temperature in the winter**



**Figure 46. Comparison of west façade temperature in the winter**

Figures 43–46 show the variations in façade temperatures during the winter from an energy model simulation that uses a TMY3 weather file versus simulated weather data. As with the summer conditions, the comparison includes the first-floor wall and window and the second-floor wall and window. Overall, comparison for the winter show a minimal variation in façade temperature when using a TMY3 weather file versus simulated weather data. This minimal variation is attributed to the cloudy sky which reduces solar radiation impact on the facades. Solar radiation has a direct impact on the façade’s solar heat gain and energy consumption. For the simulated winter period, the impact of reduced solar radiation is observed on the heating energy consumption as noted in the following section.

Results show that in the winter, minimal variation exists in the façade temperature whether one uses TMY3 weather data or simulated weather data. On the north and south façades, which have the highest duration and surface area for solar exposure, it was observed that for both walls and windows, the pattern of the façade temperature has less

variation. Similar observations can be made with the east and west façades. In addition, the highest variation of approximately 2°C–3°C occurs between the first- and second-floor walls of the east facade. Here, the temperature of the first-floor walls is lower than for the second floor, a difference that may be attributed to the effect of the water pond adjacent to the east façade. Additionally, for all facades, wall temperatures are observed to be approximately 2°C lower than the window glazing temperatures. Based on these observations, it can be concluded that the façade temperature is not greatly affected during the winter season when simulating using either TMY3 or predicted weather file. However, it should be noted that though the weather file does not demonstrate a significant impact on the façade temperature during the winter, it does affect the energy consumption prediction as discussed in Section 4.6.

In addition, analyzing the façade temperature in summer and winter can be extremely important in understanding the behavior of building materials (heat gain and thermal resistance) for conducting thermal comfort studies. Facades are one of the most significant contributors to the building energy consumption and the comfort parameters in any building. Optimal façade design is essential to understand: orientation, geometry and massing of the building to respond to solar position; shading devices and natural ventilation potential to control cooling energy consumption, improved thermal comfort and air quality; lighting controls for artificial lighting and daylighting strategies; and exterior wall insulation to optimize heating and cooling energy consumption. Therefore, understanding the seasonal variation in façade temperature when simulating with TMY3 and simulated weather data is essential.

## 4.6. Effects of coupling microclimate on building energy consumption

After successfully coupling the surface boundary conditions and the infiltration, it is necessary to compare the effects of these thermodynamic interactions on building energy consumption. This section uses three steps to provide a comparative analysis of the effects of the thermodynamic interactions between the built and the natural environment on building energy consumption: (1) changing the weather file to measured and simulated data, (2) incorporating the effects of surface boundary conditions (convective and radiative heat flux), and (3) incorporating the effects of building infiltration.

The energy consumption of steps 1, 2 and 3 is also compared with the measured energy consumption of the CSL building. As mentioned in the CSL case-study description of the HVAC system, a water-source heat pump (WSHP) supplies the heating and cooling. However, the EnergyPlus model has a VAV system. Therefore, it is important first to estimate and convert the CSL measured heating and cooling energy consumption so that it is comparable to the EnergyPlus simulated energy consumption.

CSL sub-meters the electrical consumption for its Berner AHU units, which include supply fan, exhaust fan, heat recovery wheel motor, and the water source heat pump unit. Through data mining, it was possible to disaggregate and estimate the energy consumption for the WSHP, which generates heating/cooling to the building. After the compressor energy consumption was derived, an estimation of the overall COP of 3.2–3.5 for the WSHP (without the water pump) was used (Brandi) to estimate the heating and cooling use. This estimated heating and cooling use was then compared to the VAV system boiler and chiller energy consumption.

The following points summarize the constraints during the microclimate modeling, energy modeling and data acquisition phase of the CSL case study:

1. **HVAC system:** As described above, the modelled HVAC system in EnergyPlus is a simplified VAV system and does not represent actual building HVAC system which is a WSHP. Therefore, an alternative approach has been taken to calculate the measured heating and cooling energy consumption as described above.
2. **Simulation period:** The simulation period (3-day) for every season has been selected based on the regularity of the air temperature and relative humidity pattern. Therefore, this 72-hour period should not be assumed as a representative pattern for the entire season. Rather, the simulation results show that the coupled model successfully predicts the microclimate and the heating/cooling energy consumption for this 3-day period.
3. **CSL building surroundings:** For the ENVI-met microclimate modeling, the surrounding vegetation and building construction has been modelled to closely represent the existing conditions. However, due to ENVI-met limitations due to grid-based modeling and specifying building construction layers (three layers maximum), it is possible that the ENVI-met model does not represent the exact physical site and building conditions which can impact thermodynamic interactions between the natural and the built environment.

The following charts show the comparison of the heating and cooling energy consumption for the six simulation cases (winter, summer, and swing seasons) using TMY3 and measured/simulated weather data. As noted previously, the TMY3 weather file represents climate conditions from previous years (1991–2005) rather than current or recent weather

conditions, for which the air temperatures and wind speed are approximately 10°C and 7–10m/s higher than the 2016 measured data, respectively. These are the three take-aways

Figures 47 and 48 compare the coupled effects of the urban microclimate on building energy consumption using TMY3 and simulated weather data for January 20–22 and February 20–22 respectively. Since these periods are considered winter, the heating energy consumption is compared based on the various stages of coupling the microclimate effects.

From the comparative analysis, it was found that the simulated ENVI-met–EnergyPlus coupled model for CSL is able to predict the heating energy consumption with an accuracy of 14%–20% of the measured consumption. Additionally, it was found that the predicted heating and cooling energy consumption are in very close agreement when comparing the simulation results that use ENVI-met simulated weather file with the CSL measured weather file. Lastly, similar to the previous discussion in Section 4.5, the TMY3 weather file does not represent the current microclimate conditions accurately enough to predict the energy consumption.

For winter, Figure 47 shows an increase in heating energy consumption by approximately 63% and 54% for the TMY3 weather file versus measured/simulated weather data. For February 20–22, Figure 48 shows a decrease of 42% to 53% in heating energy consumption. These increases/decreases are attributed to the high degree of variation in the climate variables (air temperature, relative humidity, wind speed) in a TMY3 weather file and measured/simulated weather file. For January, measured/simulated air temperature was colder—and for February, warmer—when compared to TMY3 air temperature.



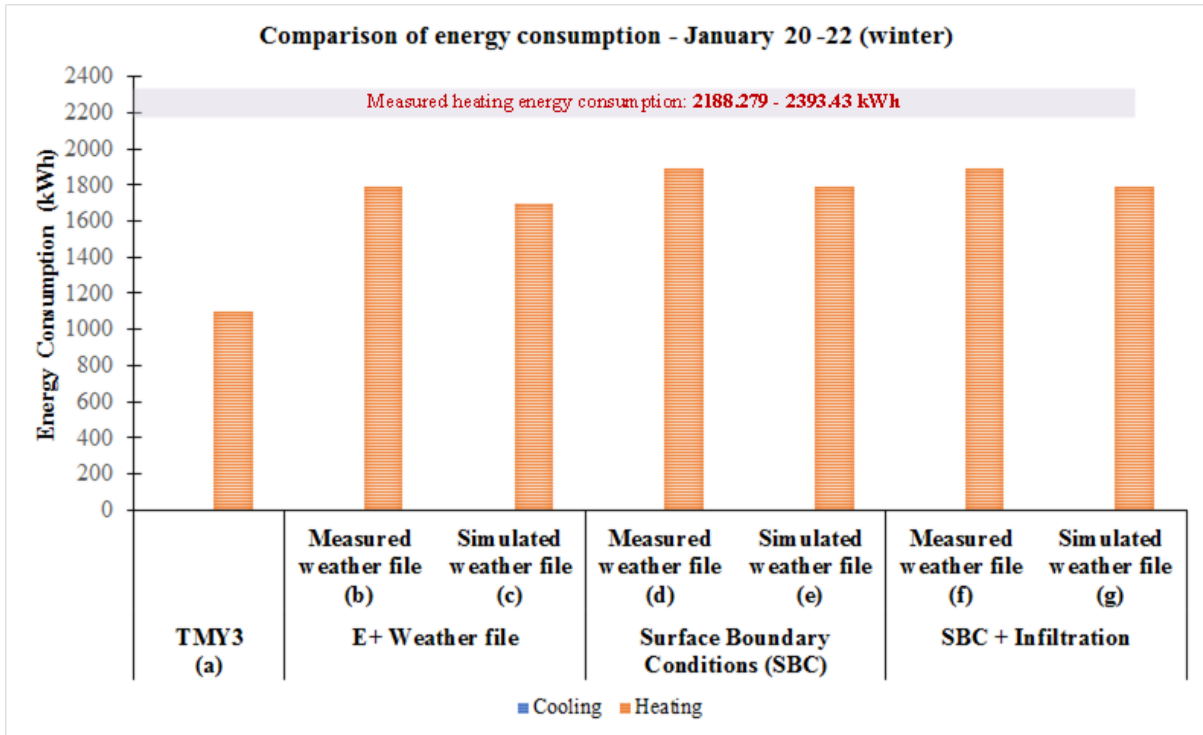


Figure 47. Comparison of building energy consumption in the winter

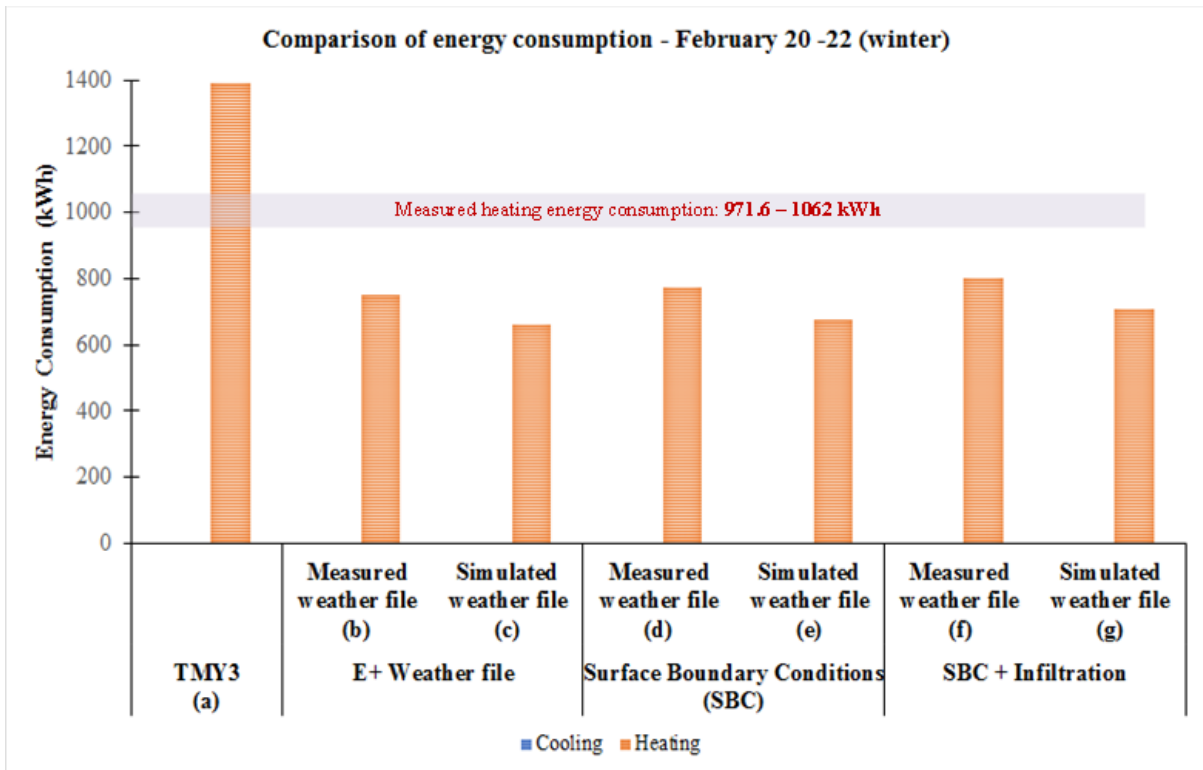
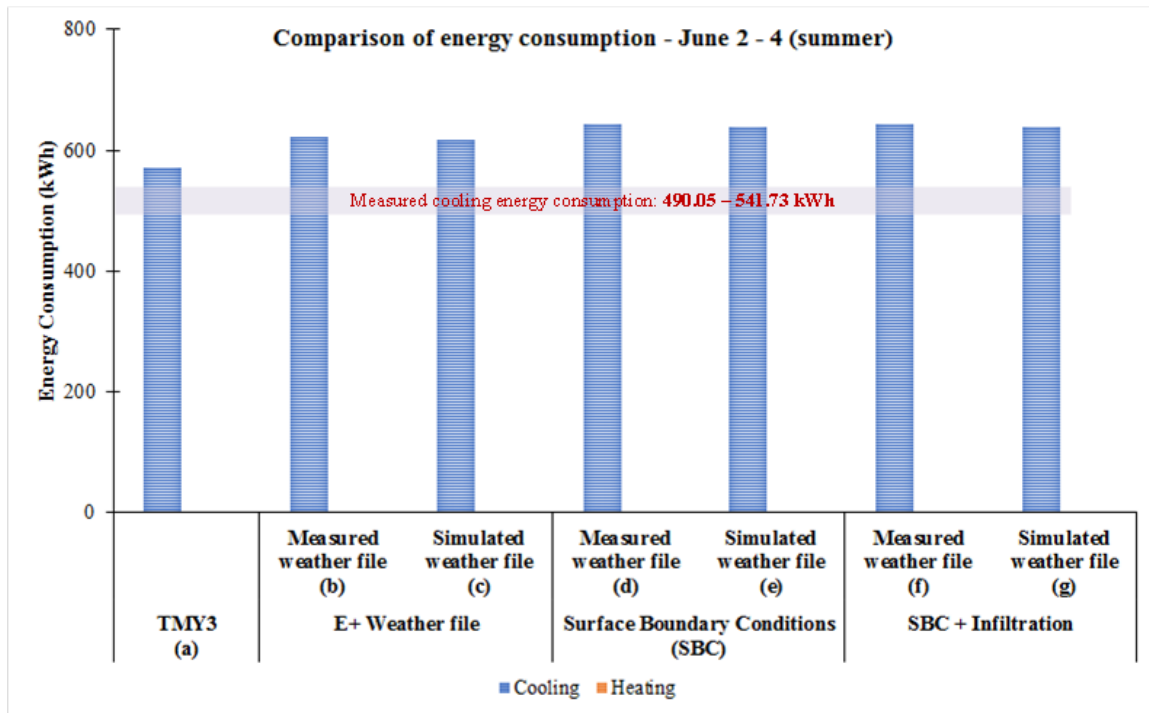


Figure 48. Comparison of building energy consumption in the winter

Figures 47 and 48 also show that convective and radiative heat flux and infiltration affect building energy consumption minimally if the energy model already uses the simulated weather file. This minimal effect is because the simulated weather file already considers the effect of wind speed, air temperature, and surface temperature, which are the primary factors that affect surface boundary conditions and infiltration. It should also be noted that this increase in energy consumption is for a 3-day period. Therefore, predictions of energy consumption for a heating-dominated climate can be exponentially high.

Figures 47 and 48 further show that the coupled EnergyPlus model is able to predict heating energy consumption with an accuracy of 14–20% of the measured heating energy consumption. Therefore, it can be concluded that using current microclimate conditions results in estimating the heating energy consumption with a high degree of accuracy.

Figures 49 and 50 compare the coupled effects of the urban microclimate on cooling energy consumption using TMY3 and measured/simulated weather data for June 2–4 and August 15–17, respectively.

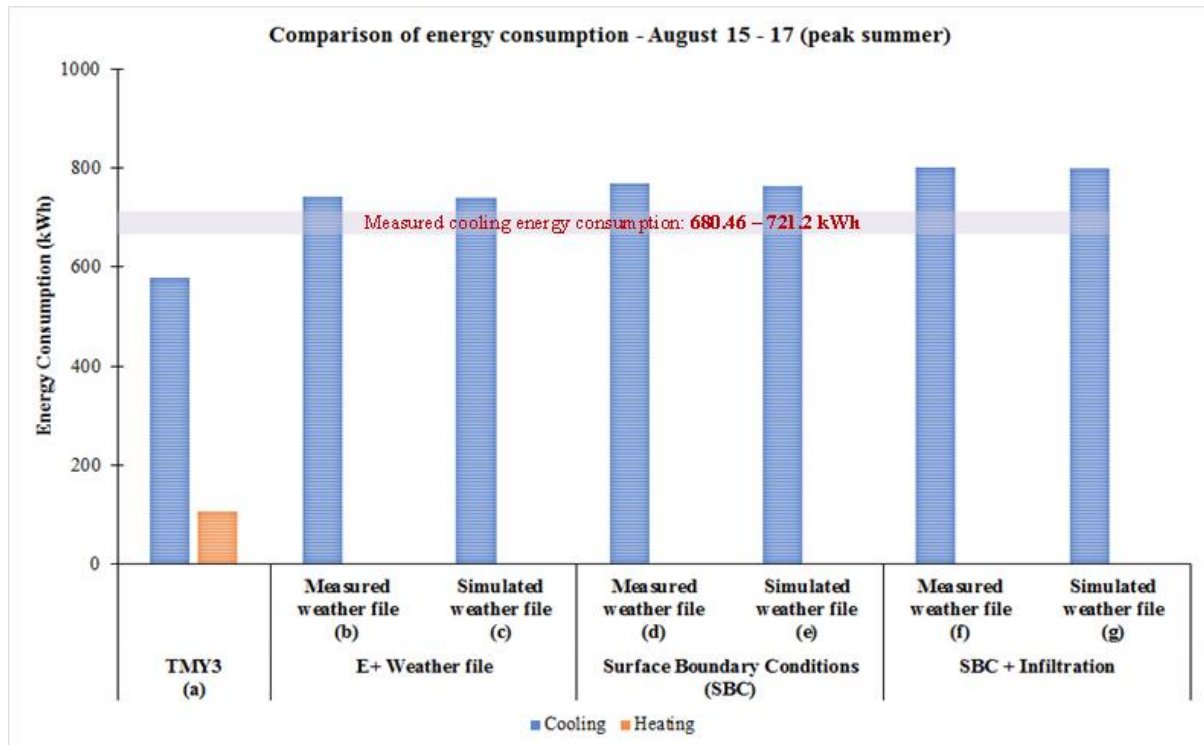


**Figure 49. Comparison of building energy consumption in the summer**

Overall results for the summer period indicate a greater increase in cooling energy consumption during peak summer (August) than during the start of summer (June) when comparing simulations using TMY3 weather and measured/simulated weather. For this summer period, coupling surface boundary conditions and infiltration has a minimal increase on cooling energy consumption (4%–8%) if the simulations take the microclimate effects into account. Additionally, it was observed that the ENVI-met–EnergyPlus coupled model is able to predict the cooling energy consumption with an accuracy of 10%–14%.

For June 2–4, the start of the summer period, there is minimal increase in cooling energy consumption when using a TMY3 weather file versus measured/simulated data (8%–9%).

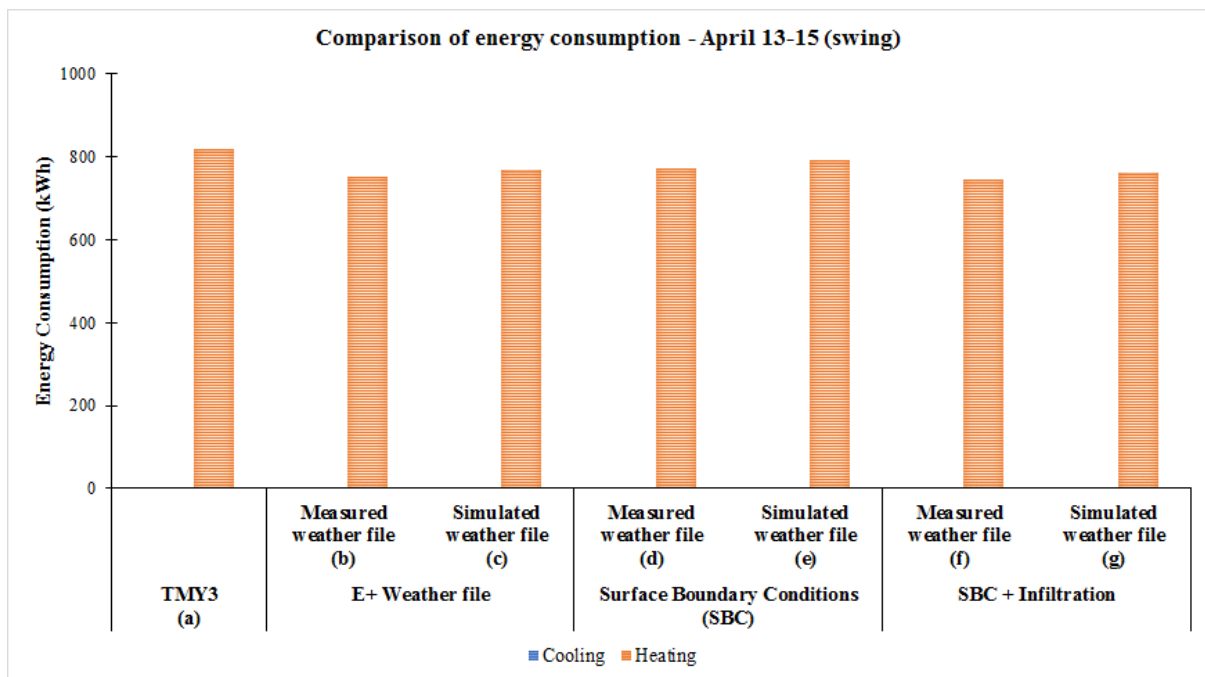
A similar trend is observed for August 15–17 where the increase in cooling energy consumption is higher (approximately 28%) than in June owing to peak summer conditions (i.e., heat and humidity).



**Figure 50. Comparison of building energy consumption in the summer**

A temperature difference of approximately 10°C–12°C for the simulation period in June and August was noted when the TMY3 and measured/simulated air temperature were compared. However, in June, only a minimal increase in the cooling energy consumption was observed. This minimal increase in cooling energy consumption in June may be attributed to various factors, such as the urban form, vegetation, radiative effects, and relatively lower air temperatures and humidity than in peak summer conditions. The location of the CSL building is not considered an urban setting, although the building is in the city. The building is surrounded by dense vegetation in summer. In addition, a water body on the east side of the building helps cool the surrounding environment. The combined effect of the vegetation and the water body helps to reduce the heat trapping

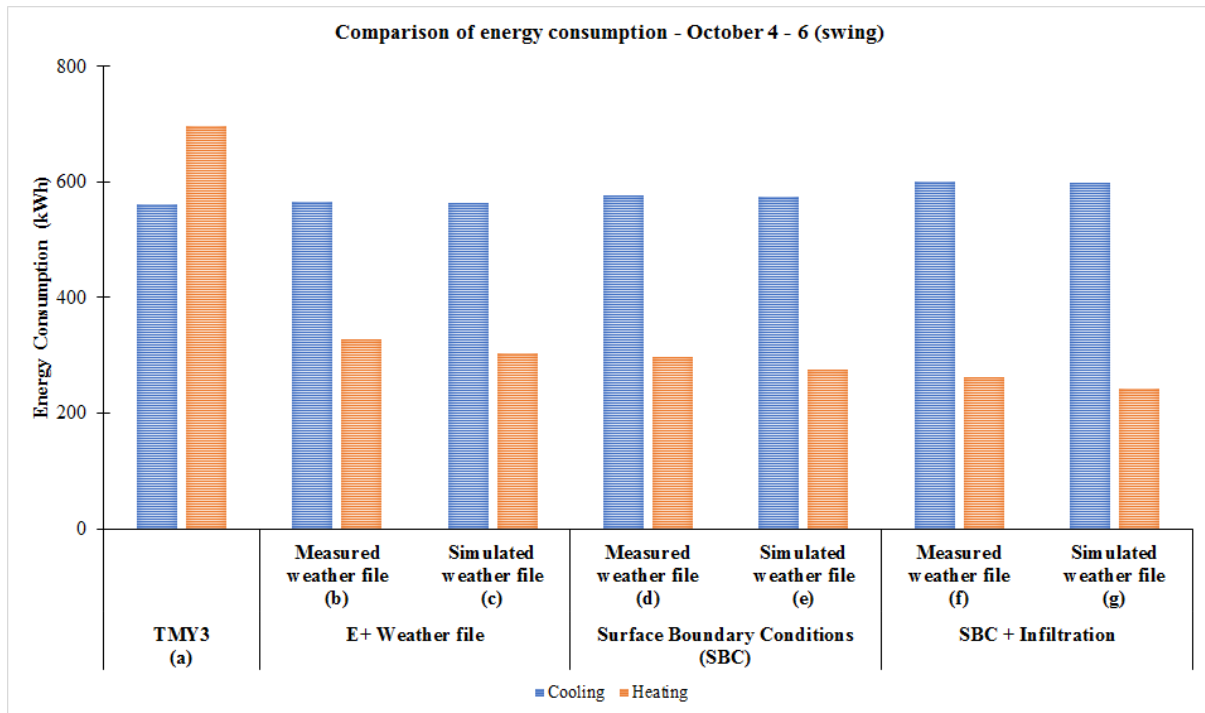
that would otherwise occur in a dense urban environment. However, the increase in cooling energy consumption in August (Figure 50) is observed to be higher than in June. This is because August is considered peak summer condition, when the relative humidity is much higher than in June. The relative humidity for this simulation period is between 80% and 90% whereas it is 40–50% in June. Therefore, more energy is required to dehumidify and cool the air before the air is circulated within the building. Similar to the winter results, the TMY3 weather data here do not accurately represent the current microclimate conditions, especially during peak summer conditions. Figures 49 and 50 further show that the coupled EnergyPlus model is able to predict the cooling energy consumption with an accuracy of 10–14% of the measured cooling energy consumption.



**Figure 51. Comparison of building energy consumption in a swing period**

Figures 51 and 52 compare the coupled effects of the urban microclimate on the heating and cooling energy consumption using TMY3 and measured/simulated weather data for April 13–15 and October 4–6, respectively. It should be noted that swing seasons are harder to predict because of the high variability in the daily and hourly climate conditions.

Results show that similar to winter and summer conditions, the EnergyPlus model either over or under predicts the heating/cooling energy consumption if TMY3 weather data are used.



**Figure 52. Comparison of building energy consumption in a swing period**

Figure 51 shows that for April, heating energy consumption decreases by 6%–8% when simulating the energy model using TMY3 and measured/simulated weather data. In addition, if the EnergyPlus model takes the simulated microclimate into account, the effect of surface boundary conditions and infiltration on heating energy consumption is observed to be minimal (1%–3%). Figure 52 for October, which shows both heating and cooling energy consumption, demonstrates a minimal increase in cooling energy consumption (< 1%) but a significant decrease in heating energy consumption (52%–56%). This significant decrease may be attributed to the warmer air temperatures during October 2016 versus October 1999 (TMY3). Results also show that coupling the effects

of convective/radiative heat flux and infiltration with the energy model has a minimal effect on building energy consumption if the energy model already uses the simulated weather file.

The variations in the microclimate and their effects on building heating and cooling energy consumption are higher during a swing season, especially in Pittsburgh, PA. This may be attributed to several factors, such as the wind speed and direction, vegetation, and extreme ranges in air temperature and humidity. These extreme conditions also vary every year, hence making microclimate predictions more difficult. However, these periods occur for only approximately 3–4 months in a year.

**Table 7. Percentage difference in heating/cooling energy consumption using TMY3, measured and simulated weather data**

Comparison criteria/ Simulation period	Jan 20-22 (winter) Heating	Feb 20-22 (winter) Heating	Jun 2-4 (summer) Cooling	Aug 15-17 (summer) Cooling	Apr 13-15 (swing) Heating	Oct 4-6 (swing) Cooling/ Heating	
	% difference						
a with b	62.89	46.07 ↓	8.88	28.40	8.15 ↓	0.81	52.79 ↓
a with c	54.63	52.55 ↓	8.08	27.83	6.06 ↓	0.38	56.42 ↓
b with d	5.52	3.29	3.59	3.42	2.87	2.1	9.91 ↓
c with e	5.48	2.82	3.50	3.21	3.02	2.03	9.30 ↓
b with f	5.46	7.29	3.59	7.99	1.06 ↓	6.26	19.90 ↓
c with g	5.42	7.32	3.51	7.86	1.02 ↓	6.14	20.19 ↓

As has been discussed, Table 6 provides a focused snapshot of the comparative analysis of the percent increase and decrease when comparing the predicted heating and cooling energy consumption by using, (a) TMY3 weather file, (b) CSL weather station measured weather data and, (c) ENVI-met simulated weather data. The table also compares the percent difference in the heating and cooling energy consumption when using measured and simulated weather files when coupling the effects of surface boundary conditions and infiltration for the six cases.

## 4.8. Summary

This chapter describes the coupling of ENVI-met simulated data with the CSL EnergyPlus model to calculate the surface boundary conditions (convective and radiative heat fluxes) and infiltration. After the coupling process, a comparative analysis was conducted in three steps to determine the effects of these thermodynamic interactions on building energy consumption (Section 4.6). A comparative analysis was also carried out to discuss the effects of TMY3 weather data and simulated weather data on building façade temperature (Section 4.5).

Results indicate that TMY3 weather data does not accurately represent the current weather conditions to provide realistic predictions of the façade temperature and the inaccuracy is more evident in summer than in winter. For summer, the results show that the highest temperature variation occurs on the north and south façades as compared to the east and west facades with approximately 12°C–15°C variation for any given time of the day during the 3-day simulation period. The air temperature during this period showed an increase of approximately 20°C in comparison to the TMY3 file which directly affects the façade temperature. In addition, the wind speed in the TMY3 data is much higher than in the simulated. As discussed in Section 4.6, although not a high degree of variation in façade temperature was observed for the winter, it does affect the heating energy consumption.

Section 4.6 compares the heating and cooling energy consumption for summer, winter, and swing seasons. For winter, the heating consumption varied according to the outside air temperature when measured/simulated data were used in comparison to TMY3 weather data. Additionally, it was found that the ENVI-met–EnergyPlus coupled model



for CSL is able to predict the heating energy consumption with an accuracy of 14%–20% of the measured consumption. For summer, the results indicate a higher increase in cooling energy consumption during peak summer (August) than during the start of summer (June) when comparing TMY3 weather simulations and measured/simulated weather. In addition, the coupled effects of surface boundary conditions and infiltration minimally increase cooling energy consumption (4%–8%) if the simulation weather file takes microclimate effects into account. Additionally, the ENVI-met–EnergyPlus coupled model was able to predict the cooling energy consumption with an accuracy of 10%–14%. For the swing season, results show that, similar to winter and summer conditions, with the TMY3 weather data, the EnergyPlus model either over or under predicts the heating/cooling energy consumption. It should also be noted that heating and cooling energy consumption is harder to predict during the swing season.

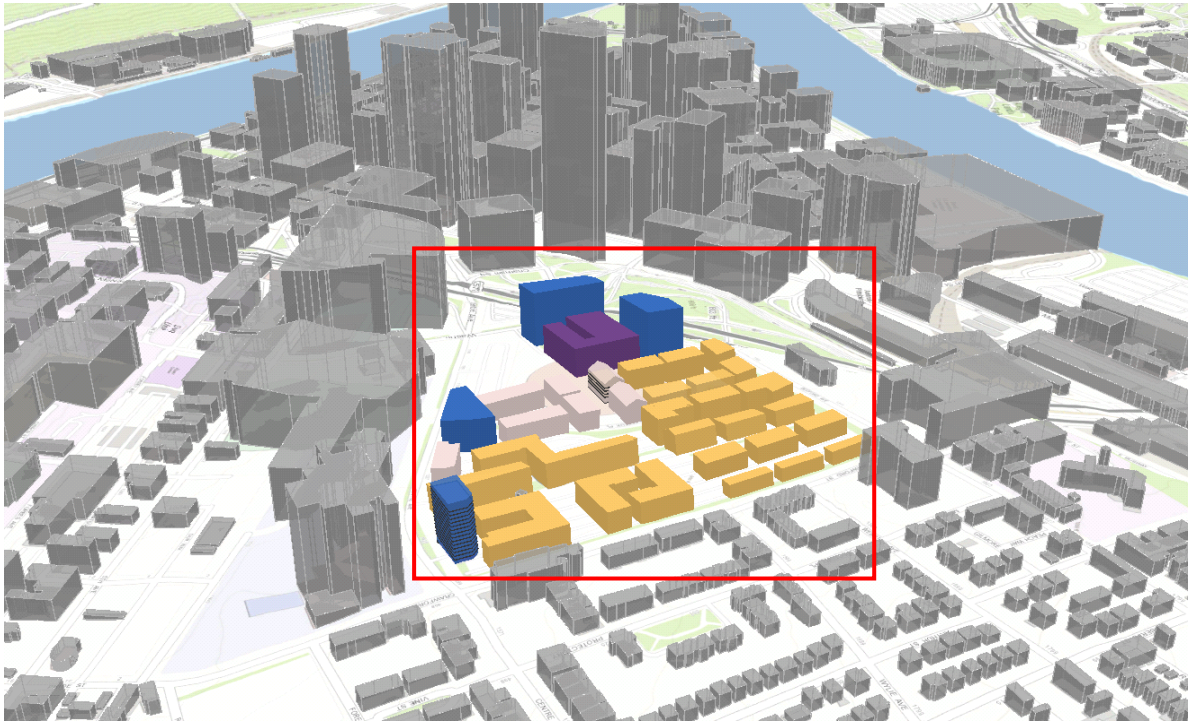
# **Chapter 5: Design case implementation of the coupling method to improve building energy consumption predictions**

## **5.1. Overview**

Chapter 4 demonstrated that using a TMY3 weather file to predict building energy consumption may not provide results that represent current microclimate conditions. Therefore, it is important to understand the impact of coupling urban microclimate effects for a design case during the conceptual design stage. This chapter details the coupling of surface boundary conditions and infiltration on a design case located in downtown Pittsburgh, PA. Section 5.2 describes the design case; Section 5.3 provides details on the setup of the ENVI-met microclimate model and the EnergyPlus model; and Section 5.4 compares energy consumption between the coupled and decoupled models. As described in the previous chapter, the simulation was conducted for the same six cases representing the winter, summer, and swing-season conditions.

## **5.2. Design case – Lower Hill District mixed-use redevelopment**

The coupling method described in Chapter 2 was implemented on a 28-acre mixed-use redevelopment site (Lower Hill District Redevelopment) that is located in downtown Pittsburgh, PA, USA. This redevelopment plan proposes a mix of residential, commercial, and community buildings with open spaces. As shown in Figure 53, the plan consists of 36 buildings of varying land uses, such as residential (multi-family/townhouses), commercial, retail, hotel, and community spaces.



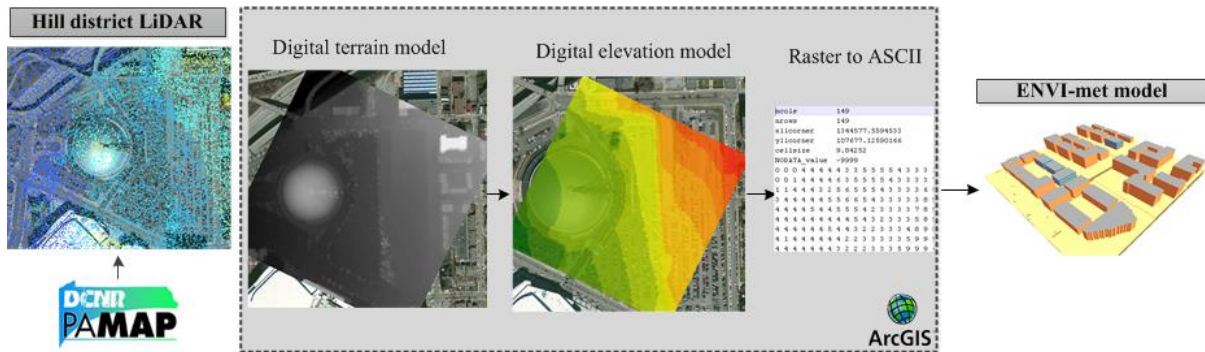
**Figure 53. Lower Hill District study area (design case)**

Figure 53 shows the study area for this thesis, which was selected with an eye toward not compromising the model resolution and having a domain size that would include the surroundings, as well as the computational resources available to conduct the microclimate simulations. The coupling method was implemented on Building G1, which has retail on the first floor and multi-family dwellings for the upper floors.

### **5.3. ENVI-met microclimate model and EnergyPlus model description**

As described in Chapter 2, Section 2.3.1, and Chapter 3, Section 3.4, the first step to conducting an ENVI-met simulation is to generate the microclimate model from ArcGIS. LiDAR data was obtained for the Lower Hill District from the Pennsylvania Department of Conservation and Natural Resources (PA DCNR). The next step was to generate the Digital Terrain Model (DTM) and Digital Surface Model (DSM) to derive the respective site elevation and building elevation using the 3D analyst function in ArcGIS. The Digital

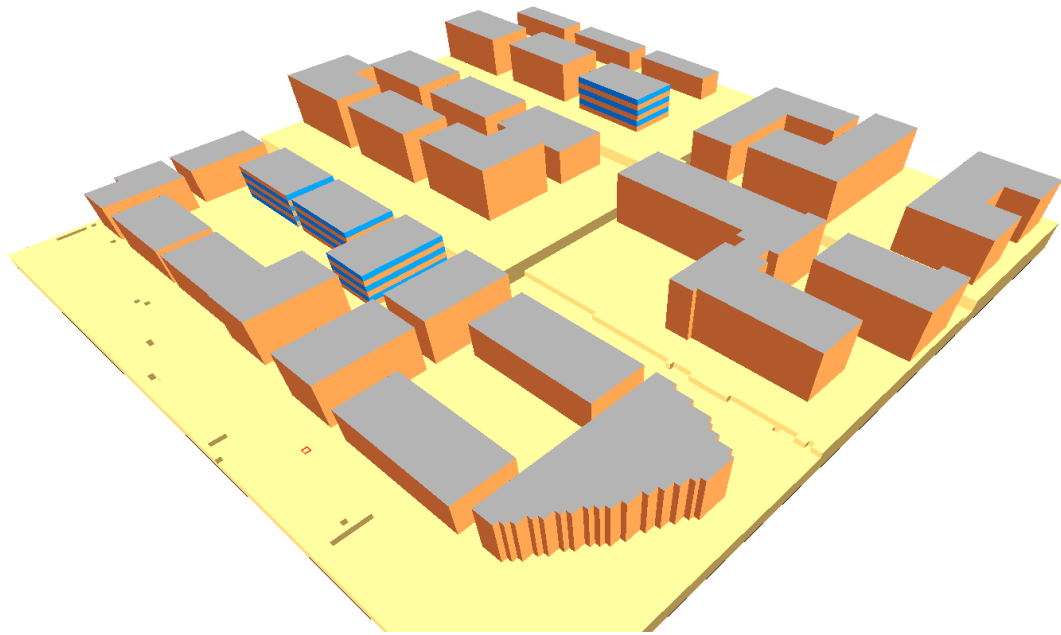
Elevation Model and the building model was then converted into ASCII text format, which is used directly as input to the ENVI-met area input file to generate the ENVI-met microclimate model (Figure 54).



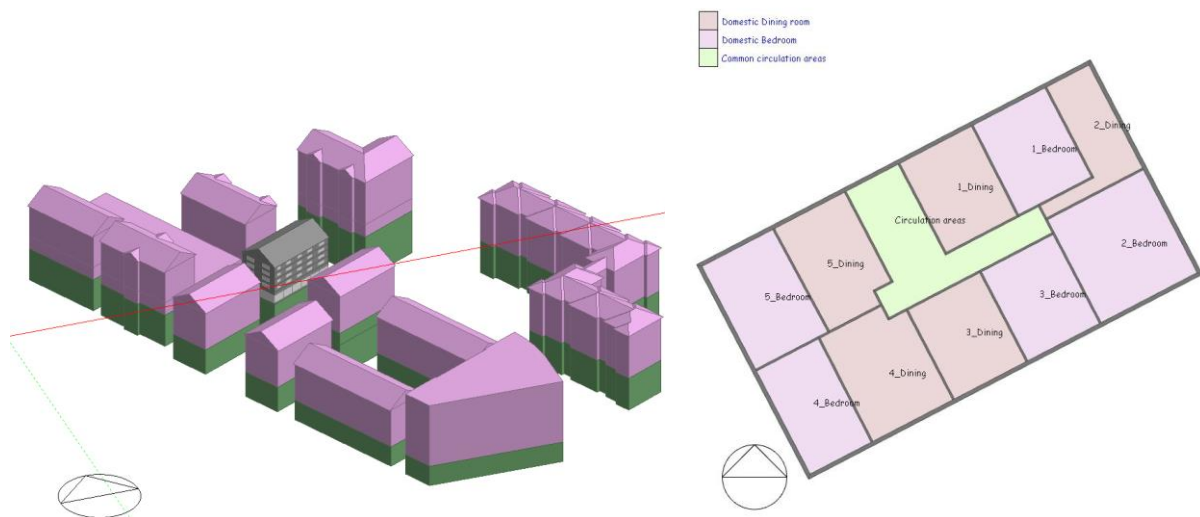
**Figure 54. Automation of ENVI-met microclimate model for the Lower Hill District**

Figure 55 shows the ENVI-met model domain for the Lower Hill District design case that is used to conduct the microclimate simulations. The domain size is 150mx150m with a 3m grid resolution.

The energy model is developed from the SketchUp models provided by Urban Design Associates (UDA). Other model details provided by UDA are site zoning, building geometries, building areas for each residential unit, offices and retail spaces, and the number of residential units and building heights. The EnergyPlus model was created based on ASHRAE 90.1 2010 “Energy Standard for Buildings except Low-Rise Residential Buildings” and the Department of Energy (DOE) Reference Models for New Construction. Figure 56 shows the layout and floor plan of Building G1 (DesignBuilder model), which is used for the coupling energy analysis.



**Figure 55. ENVI-met model domain for the Lower Hill District design case**



**Figure 56. DesignBuilding (EnergyPlus) model of Building G1**

#### **5.4. Analysis of Building Energy consumption**

After a successful coupling of the surface boundary conditions and the infiltration, the next step is to conduct a comparative analysis on the effects of these thermodynamic interactions on building energy consumption. The following charts show a comparison of the heating and cooling energy consumption, using both TMY3 and measured/simulated

weather data. The measured weather data used for the comparison is from the CSL on-site weather station data because the Lower Hill District is a design case that does not have an on-site weather station. Therefore, CSL being the closest weather station to the Lower Hill District site, it better represents the annual microclimate and thus was used for the comparative analysis. Similar to the CSL case study, this section provides a comparative analysis of the effects of the thermodynamic interactions on the built environment and hence on building energy consumption for six cases (winter, summer, swing seasons) in three steps: (1) changing the weather file to measured and simulated data, (2) incorporating the effects of surface boundary condition (convective and radiative heat flux), and (3) incorporating the effects of building infiltration.

Figures 57–62 compare the heating and cooling energy consumption using TMY3 and measured/simulated weather data. The charts also provide a comparative analysis of the percentage increase/decrease in energy consumption when simply incorporating the microclimate simulated weather data versus the coupling parameters.

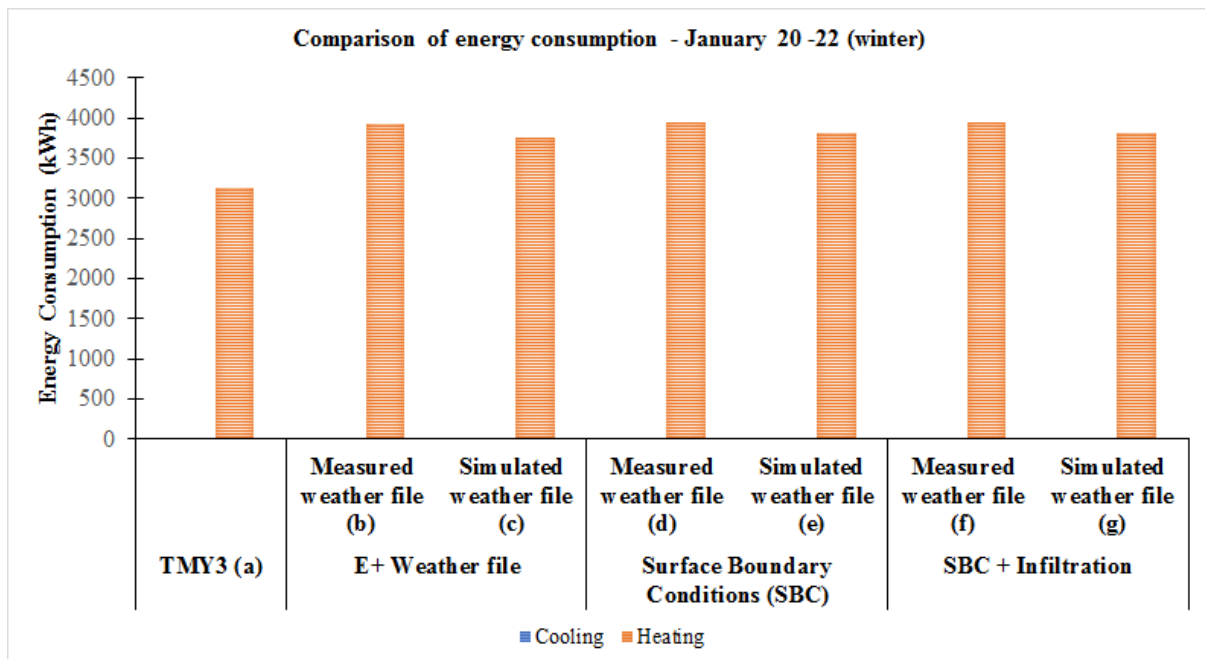
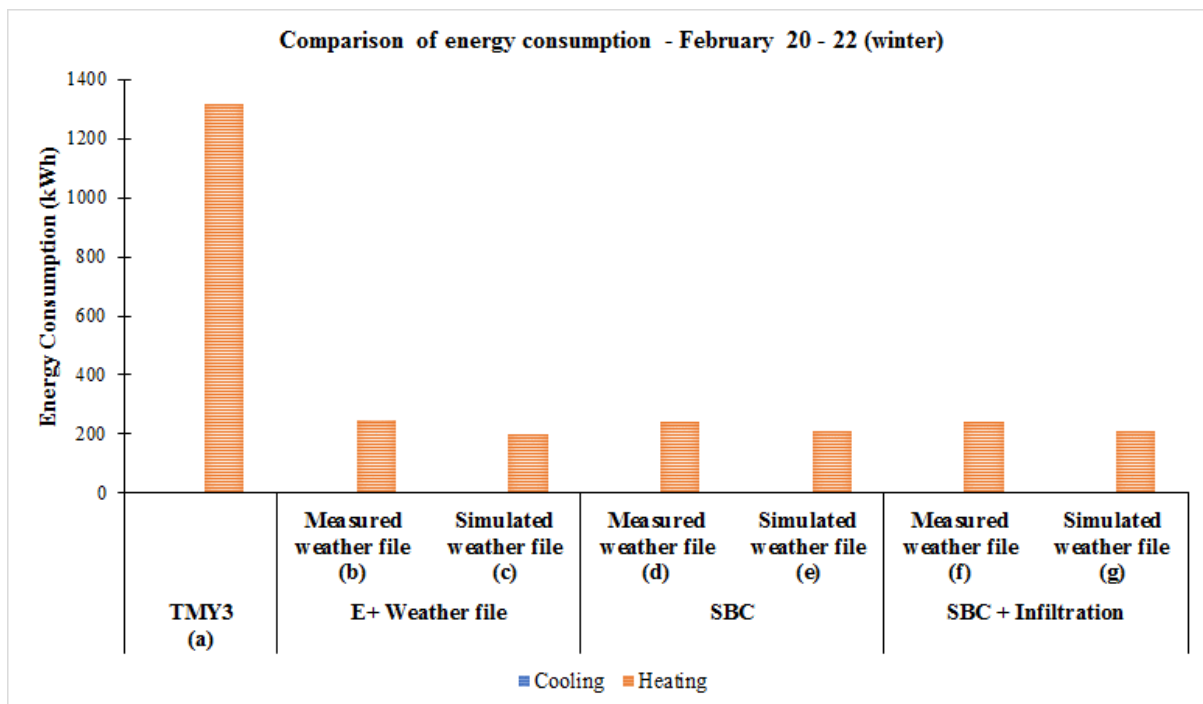


Figure 57. Comparison of building energy consumption in the winter

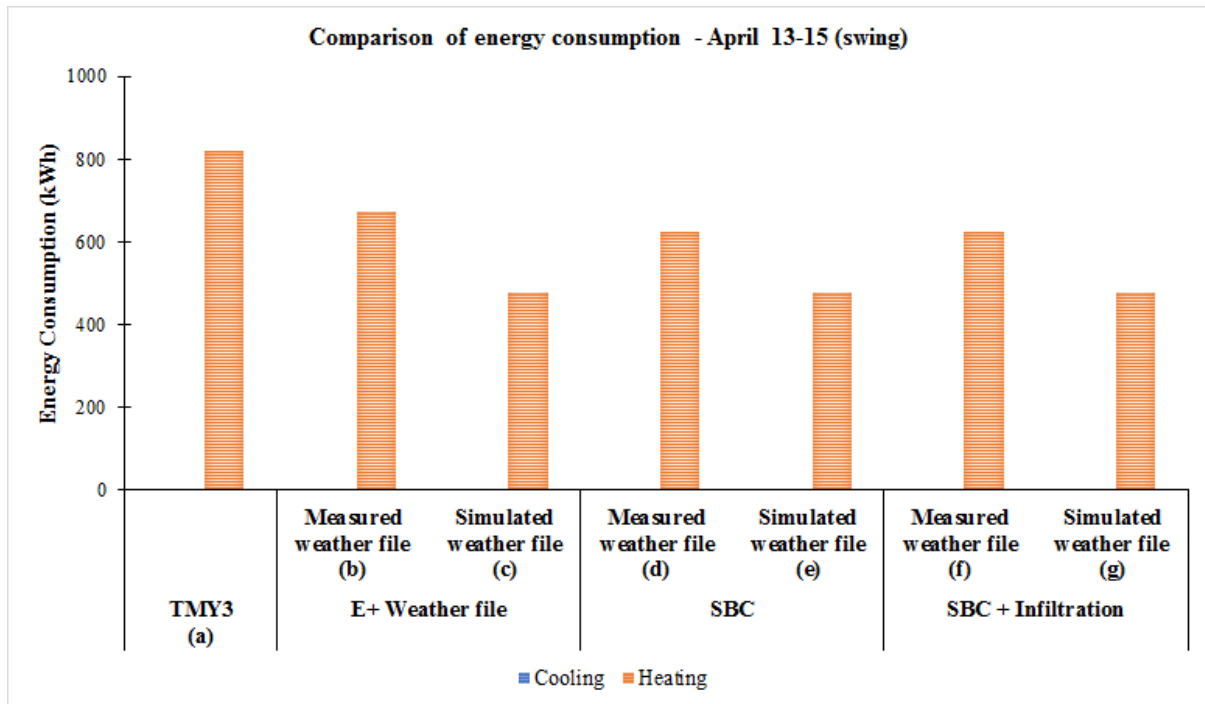
Figures 57 and 58 compare the coupled effects of the urban microclimate on heating energy consumption using TMY3 and measured/simulated weather data for January 20–22 and February 20–22, respectively. Figures 57 and 58 show an increase of 20%–25% and a decrease of 81%–85% when using TMY3 weather versus measured/simulated weather data to predict the heating energy consumption. Similar to the discussion in Section 4.6 for the CSL case study, this increase/decrease in heating energy consumption may be attributed to the high degree of variation in the climate variables (air temperature, relative humidity, wind speed) in a TMY3 weather file versus a measured/simulated weather file. For January, the measured/simulated air temperature was colder—and for February, warmer—when compared to TMY3 air temperature.



**Figure 58. Comparison of building energy consumption in the winter**

In addition, Figures 57 and 58 show that convective and radiative heat flux and infiltration have a minimal effect on building energy consumption if the energy model already uses a simulated weather file. The effect is minimal because the simulated weather file already allows for wind speed and air temperature, which in turn affect the surface temperature

used to calculate the convective and radiative fluxes. Similar to the CSL case study, because of outdoor air temperature variation, increases and decreases in heating energy consumption are not captured by using TMY3 weather data for energy simulation.



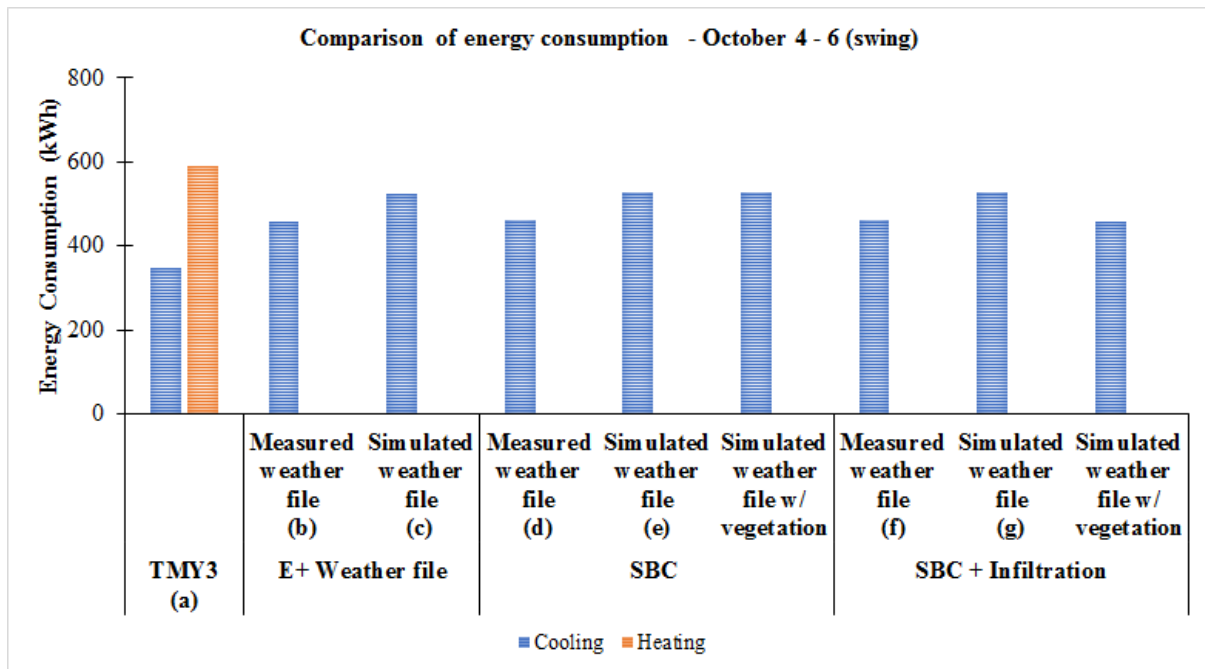
**Figure 59. Comparison of building energy consumption in a swing period**

Figures 59 and 60 compare the coupled effects of the urban microclimate on building energy consumption for April 13–15 and October 4–6, respectively, which are considered swing season dates in Pittsburgh. Results show that April and October swing seasons differ in terms of heating and cooling energy consumption. Overall results indicate that using TMY3 weather data either overestimates heating energy consumption or underestimates cooling energy consumption for the swing seasons.

Figure 59 shows a decrease of 18%–42% in heating energy consumption. Figure 60 shows an increase of 33%–52% in cooling energy consumption when using TMY3 data versus measured/simulated. This increase/decrease in heating energy consumption, especially using simulated weather data, can be attributed to the urban surroundings, which cause

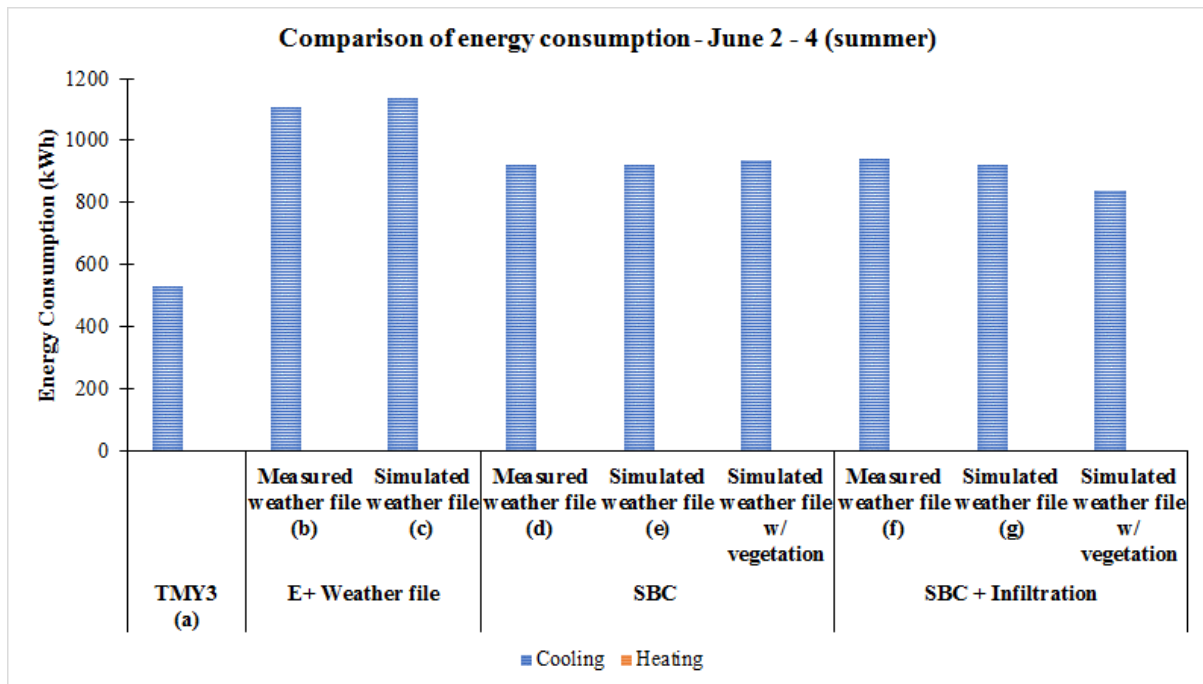


different wind speeds and higher air temperatures compared to the location of the CSL building.



**Figure 60. Comparison of building energy consumption in a swing period**

For October, when using simulated weather data, predictions show that there is no heating energy consumption when compared to the use of TMY3 weather data. Another important observation is the presence and impact of vegetation on cooling energy consumption. The coupled model shows a decrease of 13% when compared to the decoupled model with on-site vegetation. Therefore, it is evident that vegetation helps in cooling the urban environment, thereby reducing cooling energy consumption. This result again emphasizes the importance of accounting for local and current climate conditions versus using TMY3 weather for energy simulation.

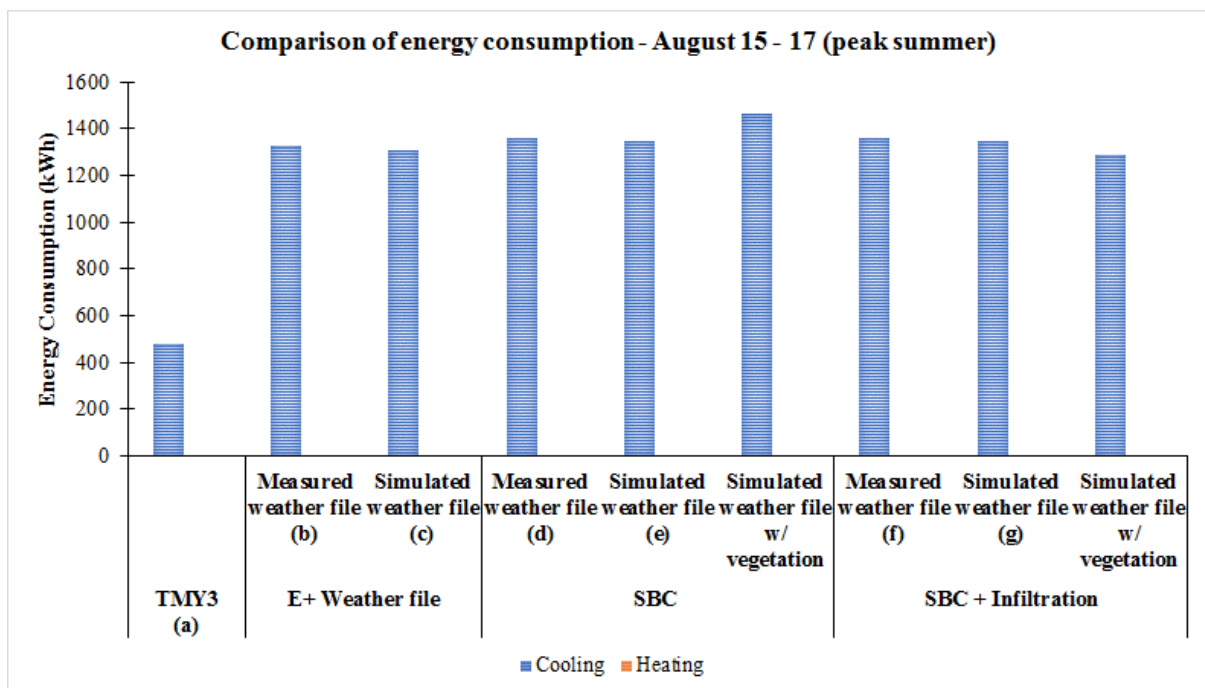


**Figure 61. Comparison of building energy consumption in the summer**

Figures 61 and 62 compare the coupled effects of the urban microclimate on the cooling energy consumption for June 2–4 and August 15–17, dates that occur in summer periods in Pittsburgh. Similar to previous comparisons, the results show that if TMY3 weather data is used, the model is unable to predict accurately the cooling energy consumption. Figures 61 and 62 show an increase of approximately 110% and 175% when using TMY3 as compared to measured/simulated weather data. Note that the increase in cooling energy consumption is much higher for the Hill District as compared to the CSL case. The reason is that the Hill District site is surrounded by dense buildings and does not have any vegetation or water body to cool the outside air temperature. Owing to the dense network of buildings surrounding the Lower Hill District, radiation from the building surfaces and

other hard surfaces (i.e., asphalt, paving, concrete) increases the air temperature, thus also increasing cooling energy consumption in summer.

For the month of June, the coupled EnergyPlus model predicts a decrease of approximately 18% and 25% in the cooling energy consumption as compared to a decoupled model and in the presence of vegetation. However, for August, results show that the coupled model has an increase of approximately 3% without vegetation and a decrease of 1% with vegetation.



**Figure 62. Comparison of building energy consumption in the summer**

Although the effects of the coupled model and the vegetation have varying impacts on cooling energy consumption, the overall conclusion is that the use of TMY3 data underestimates the cooling energy consumption by more than 100%. This is especially important for a design case like the Lower Hill District when stake holders rely on energy simulations to estimate peak loads for HVAC system sizing and to evaluate the feasibility

of district systems and project phasing. Therefore, the design case reinforces the importance of coupling the effects of the urban microclimate when predicting building energy consumption.

**Table 8. Percentage difference in heating/cooling energy consumption using TMY3, measured and simulated weather file**

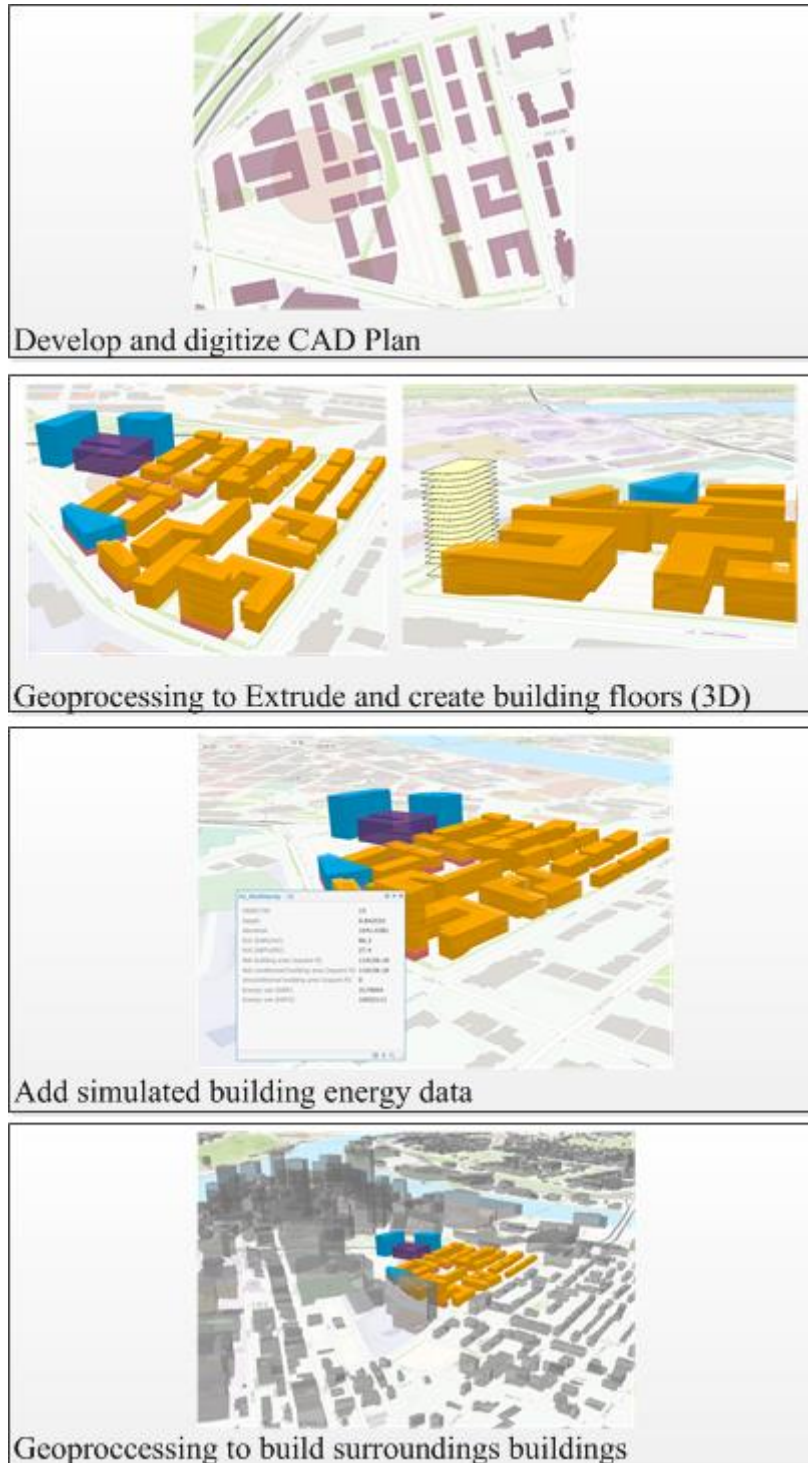
Comparison criteria/ Simulation period	Jan 20-22 (winter) Heating	Feb 20-22 (winter) Heating	Jun 2-4 (summer) Cooling	Aug 15-17 (summer) Cooling	Apr 13-15 (swing) Heating	Oct 4-6 (swing) Cooling/ Heating	
	% difference						
a with b	25.67	81.11 ↓	108.80	178.09	17.94 ↓	0.81	52.79 ↓
a with c	19.70	84.63 ↓	113.81	173.69	41.87 ↓	0.38	56.42 ↓
b with d	5.17	2.15 ↓	16.85 ↓	2.45	7.32	2.1	9.91 ↓
c with e	1.73	5.07	18.62 ↓	2.97	0.15	2.03	9.30 ↓
b with f	0.15	2.15	15.12 ↓	2.45	7.32 ↓	6.26	19.90 ↓
c with g	1.86	5.07	18.62 ↓	2.97	0.16 ↓	6.14	20.19 ↓

As has been discussed, Table 7 provides a focused snapshot of the comparative analysis of the percent increase and decrease when comparing the predicted heating and cooling energy consumption by using, (a) TMY3 weather file, (b) CSL weather station measured weather data and, (c) ENVI-met simulated weather data. The table also compares the percent difference in the heating and cooling energy consumption when using measured and simulated weather files when coupling the effects of surface boundary conditions and infiltration for the six cases.

## 5.5. Visualization Method (Design Decision Support)

It is then important to communicate the energy consumption data as the results of such coupling to the project stakeholders, which include the design, mechanical, developer, and financial teams. As seen in the Lower Hill District case, this information is especially important during the design phase of a building or urban development to assist designers and engineers in selecting appropriate building materials, determining the size of the HVAC system, calculating energy use, estimating return on investment, and conducting the comparative estimates of MTCO<sub>2</sub> (carbon dioxide) associated with district thermal and district tri-generation (heat, cool and electric power) versus stand-alone systems. In addition, energy consumption can assist with decisions about conducting parametric studies on the impact of microclimate on building energy consumption based on land use, vegetation, and building layout and orientation.

By using ArcGIS Pro and Web GIS it is possible to visualize building level energy consumption that can be shared online with the project stakeholders. This simulated energy data can be visualized in a 3D environment that also provides a realistic conceptualization of the site and its surroundings. Visualizing on the web is important specifically because it streamlines the decision-making process for project stakeholders by providing accurate building specific data. It enables not only simulated building energy data visualization, but, also district level design decision. It also eliminates the need for project stakeholders to install the ArcGIS software on their computers.



**Figure 63. Development of DDS method using ESRI's Web Scene**

Figure 63 demonstrates the implementation of visualization in ArcGIS Pro using 3D analyst tools. As described in the figure, the 2D CAD plan of the Lower Hill District and its surroundings is digitized in ArcGIS. The digitized polygons are extruded using actual building heights. After the buildings are extruded, the simulated energy data is recorded

as feature attributes. The recorded attributes of the simulated energy data are then configured using the pop-up function which are then viewed by clicking each building feature.

## **5.6. Importance of the Design Decision Support (DDS)**

Figures 64-68 demonstrate the visualization features of the ESRI Story map. Figures 64 and 65 illustrates the simulated energy results that can be visualized as time based, building type based and scale based data. The time-based data provides annual and monthly natural gas and electricity consumption for every building on the site. The scale based output provides data from a macro level (site scale) to a micro level (building floor scale). The building level data provides details on the energy consumption and peak loads.

Figure 66 provides details on the building construction materials used for performing the building energy simulations. This building materials information is especially important to an architect during the design stage. Figure 67 and 68 show the use of story map to identify land use zoning as well as annual daylight and shadow analysis.

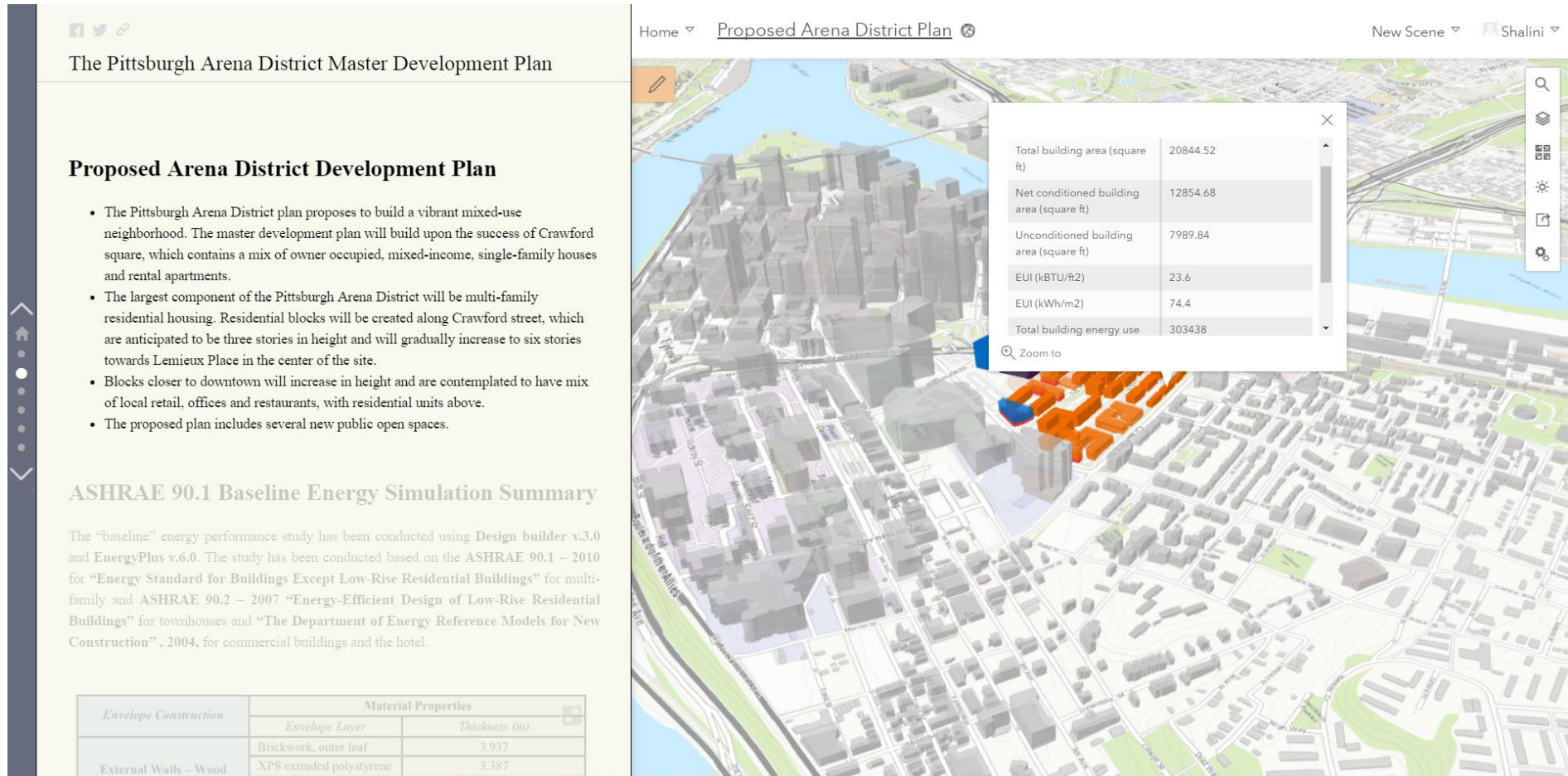
When dealing with urban scale projects, communicating simulated energy data for the various buildings can be a cumbersome and error prone process. Putting together all the simulated data in a structured database with graphical representation serves as the most effective method of communication. The design decision support tool is especially important to:

1. **Urban planners and architects:** Site topography, land use patterns, building form, daylight and shadow analysis are crucial factors during the conceptual design stage. The DDS method helps visualize important urban design principles like adjacent neighborhoods and placement of buildings, pedestrian and vehicle

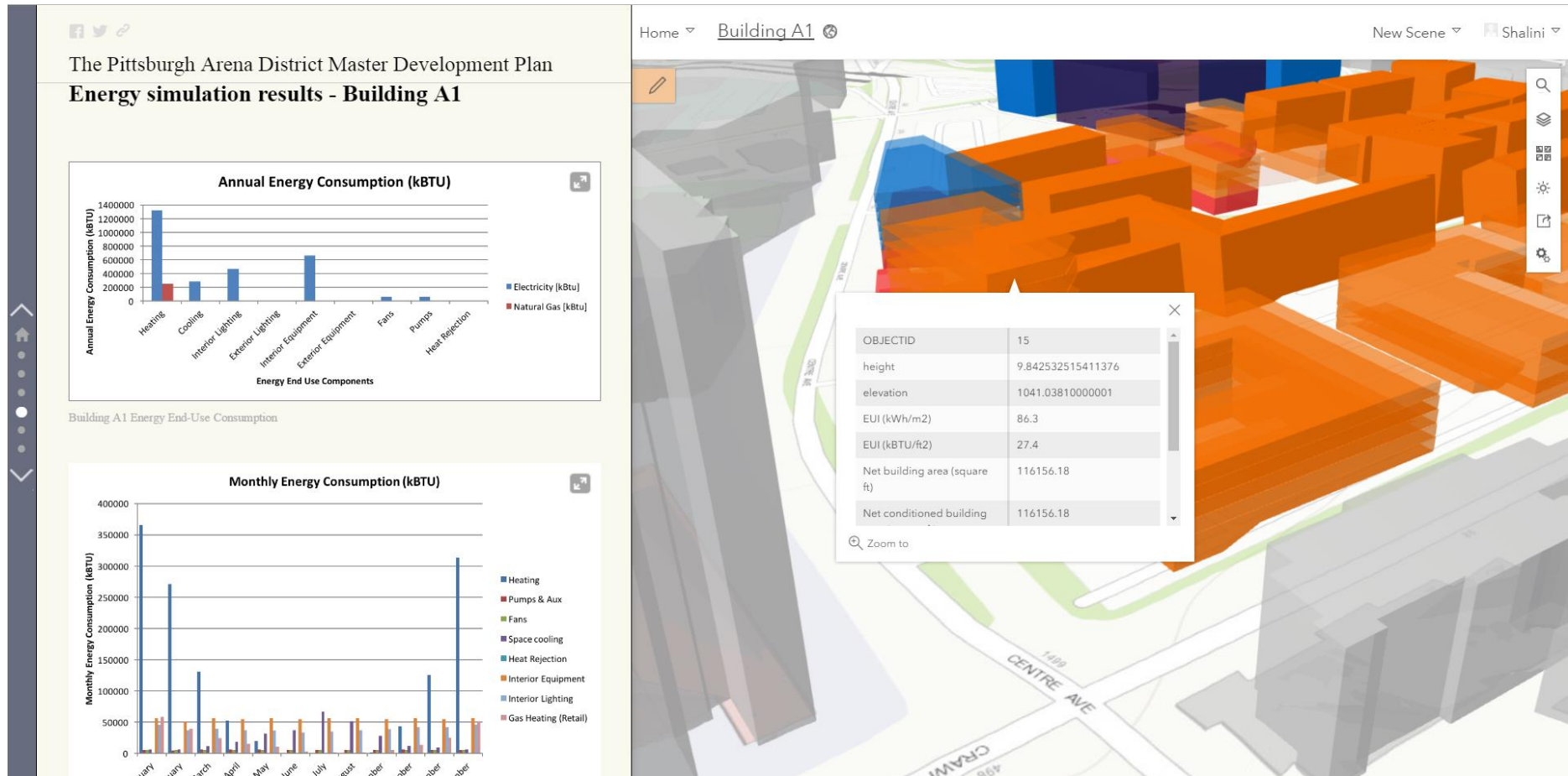
connectivity, and preserve and enhance view corridors into downtown. The method also assists architects to understand the building form and envelope performance.

2. **Mechanical engineers:** The Story map helps effectively communicate all the urban level simulated data systematically. The method serves as an effective design decision support tool for assessing potential project impacts in terms of energy consumption. This method helps in analyzing the peak loads for heating and cooling on an urban scale and assessing the feasibility of district systems with respect to sizing and combined heat and power systems.
3. **Financial stakeholders:** The method helps in analyzing potential neighborhood parties that may be interested in investing in the district systems to get an optimal load for the maximum benefits from the district system.





**Figure 64. Visualization of simulated energy consumption data using ArcGIS Pro and Web Scene**



**Figure 65. Visualization of annual and monthly energy consumption data from building level to floor level**

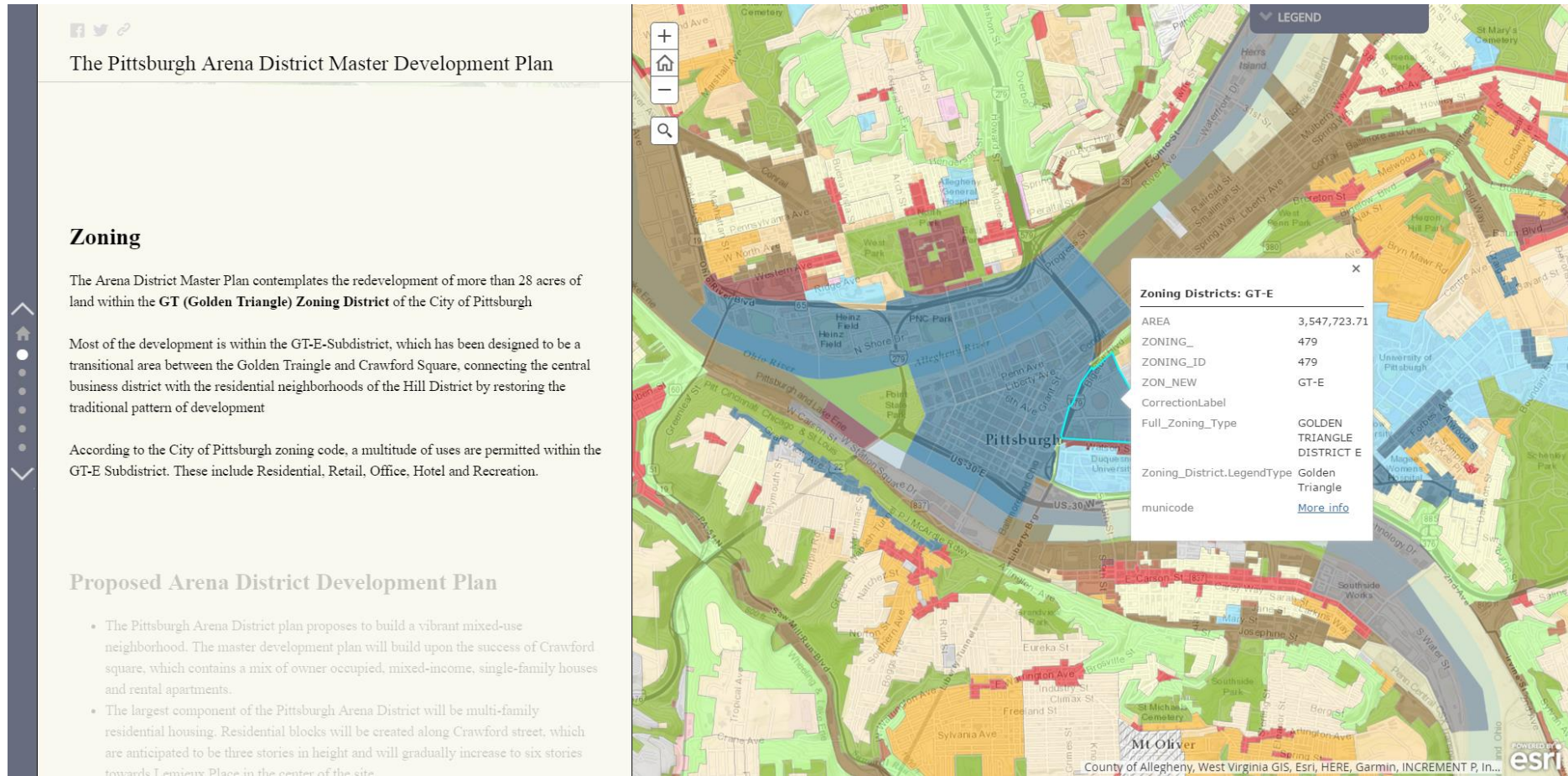
The Pittsburgh Arena District Master Development Plan  
**ASHRAE 90.1 Baseline Energy Simulation Summary**

The “baseline” energy performance study has been conducted using **Design builder v.3.0** and **EnergyPlus v.6.0**. The study has been conducted based on the **ASHRAE 90.1 – 2010** for “Energy Standard for Buildings Except Low-Rise Residential Buildings” for multi-family and **ASHRAE 90.2 – 2007** “Energy-Efficient Design of Low-Rise Residential Buildings” for townhouses and “The Department of Energy Reference Models for New Construction”, 2004, for commercial buildings and the hotel.

Envelope Construction	Material Properties	
	Envelope Layer	Thickness (m)
External Walls – Wood Stud Construction (Top 4 stories)	Brickwork, outer leaf	3.937
	XPS extruded polystyrene	3.387
	Wood – Dry hardwood	3.937
	Gypsum plastering	0.512
U-value (Btu/hft <sup>2</sup> F)		0.051
U-value (W/m <sup>2</sup> K)		0.284
External Walls – CMU block with brick veneer siding (Lower stories)	Brickwork, outer leaf	3.937
	XPS extruded polystyrene	2.291
	Concrete block (medium)	3.937
	Gypsum plastering	0.512
U-value (Btu/hft <sup>2</sup> F)		0.079
U-value (W/m <sup>2</sup> K)		0.448
Internal Walls – Lightweight 2x25mm gypsum plasterboard with 100mm cavity	Gypsum Plasterboard	0.984
	Air gap 10mm	3.937
	Gypsum Plasterboard	0.984
	U-value (Btu/hft <sup>2</sup> F)	
U-value (W/m <sup>2</sup> K)		1.641
External Floor – Slab on grade	Urea Formaldehyde foam	3.421
	Cast concrete (dense)	3.937
	Floor/Roof Screed	2.756



**Figure 66. ESRI’s Story map provides detail on the energy simulation input parameters**



**Figure 67. Story map provides details on the zoning criteria for the Lower Hill District**



**Figure 68. Story map provides daylight and shadow analysis for the Lower Hill District**

## 5.6. Summary

This chapter demonstrates the implementation of the coupling method on a design case to emphasize to the design industry the importance of taking into account the urban microclimate effects when predicting building heating and cooling energy consumption. This industry applicability is discussed using the 28-acre Lower Hill District Redevelopment site, by implementing the coupling method on a mixed-use building.

Results show for the winter period, due to the high degree of variation in the outdoor air temperature, there is an increase (20%-25%) and decrease (81%-85%) in the heating energy consumption which is not captured by using TMY3 weather data for energy simulation. For the summer and swing seasons, it was observed that the effects of the coupled model and the vegetation has a varied impact on the cooling energy consumption.

However, the overall conclusion is that TMY3 weather data either over estimates or under estimates since the data is from 1999-2005 rather than more recent and site-specific weather data. This is especially important for a design case like the Lower Hill District when stake holders rely on energy simulations to accurately predict the peak loads for HVAC system sizing, evaluate the feasibility of district systems and project phasing. Therefore, the design case provides another reinforcement that it is important to couple the effects of the urban microclimate when predicting building energy consumption. It can also be concluded that detail surface level coupling is not required to accurately predict the energy consumption if the EnergyPlus weather file accounts for the ENVI-met simulations microclimate data for the weather parameters.

The chapter also demonstrates ESRI's Story Map as a powerful tool used for Design Decision Support for project stakeholders.

## **Chapter 6: Conclusion**

### **6.1. Summary of findings**

This dissertation has demonstrated a coupling method to quantify the effects of thermodynamic interactions between the natural and the built environment on building energy consumption. This coupling method had been implemented on a case-study and a comparative analysis was conducted to study the microclimate effects on façade temperature and building heating and cooling energy consumption. Next, to demonstrate the industry applicability, the coupling method was implemented on a mixed-use redevelopment project. A comparative analysis of the coupled energy model prediction was then conducted with ASRAE 90.1 2010 prediction of the building heating and cooling energy consumption. Finally, the simulated energy consumption is visualized using a Web GIS platform that serves as design-decision-support for project stake holders.

#### **6.1.1. Hypothesis testing results**

The hypotheses of this thesis were:

- A coupled urban microclimate and building energy model can improve the prediction of building heating and cooling energy consumption.
- The microclimate model must be correctly initialized to obtain results that are comparable to measured data.

The hypotheses were tested throughout the various stages using the case-study building.

Chapter 2 presented the overall thesis method for (1) automating the ENVI-met microclimate model, (2) coupling the microclimate model data with the EnergyPlus model

in terms of surface boundary conditions and infiltration and (3) visualizing the simulated energy data using Web Scene Viewer and Story Maps.

Chapter 3 demonstrated the ENVI-met model automation, setup and initialization process for the CSL case-study. The ENVI-met 3D model can be seamlessly created using geoprocessing functions in ArcGIS Pro. From the initialization analysis conducted for 24 cases, results show for the winter months (November-February), when the measured air temperature pattern is not regular in terms of the daily minimum and maximum, the model should be initialized with 1-day data and simulated for every 24-hour period. For the summer months (May-August), the model is able to predict the air temperature and relative humidity with a high degree of accuracy using a 3-day average initialization. For the swing months (late March-early May and September-October), the accuracy of the simulated data depends on the pattern of the air temperature and relative humidity used to initialize the model. Results also show that by using ENVI-met 7-node feature to accurately define the building envelope properties, the model is able to predict the façade temperature with a high degree of accuracy.

Chapter 4 demonstrated the coupling of ENVI-met simulated data with the CSL EnergyPlus model to compare the effects of the microclimate on building heating and cooling energy consumption. The effects of the coupled model were compared using the CSL façade temperatures and the CSL heating and cooling energy consumption. Results showed using TMY3 weather data does not accurately predict façade temperature during the summer as compared to the winter period. Although, only minimal variation is observed in façade temperature for the winter season, it was found that using TMY3 does affect the prediction of heating energy consumption.



For the comparison of the heating and cooling energy consumption, results show that using TMY3 weather data can under predict or over predict for the winter, summer and swing seasons. This variation largely depends on the outdoor air temperature, wind speed and relative humidity. In addition, it can be concluded that detailed coupling of the surface boundary conditions and infiltrations is not required if the simulated microclimate is taken into account in the EnergyPlus weather file. Therefore, since a detailed surface level coupling is not necessary, the ENVI-met model resolution can be reduced because only one receptor point is required to generate the site-specific weather data. This reduction in the ENVI-met model resolution can greatly decrease the simulation time required to conduct the ENVI-met simulations.

Chapter 5 shows the industry applicability of the coupling method on a design case using the Lower Hill District redevelopment site. Similar to the CSL case-study, results show that the accuracy of the building heating and cooling prediction depend to a great extent on the EnergyPlus weather data. Using a site-specific microclimate weather file provides more accurate predicts than TMY3 weather data. Additionally, the chapter also demonstrates the visualization of the simulated energy data on the Web Scene and Story Map platform. This communication method for urban scale simulated data provides a more structured and systematic way to organize and display the simulated data especially for large developments like the lower hill district. By using the structured database and sharing using Web GIS it is possible to reduce data management errors and serve as a powerful decision support tool for city planners, mechanical system designers and other project stakeholders.

## 6.2. Industry applicability

This section describes the industry applicability of the proposed coupling method. Taking into account the effects of the changing microclimate is especially important for architects, landscape architects, mechanical engineers, urban planners and policy makers and investors and financial institutions.

**Architects and Landscape Architects:** For architects, microclimate predictions (ENVI-met simulations) is useful (1) to assess the behavior of façade and surface material selection; (2) to understand the spatial and temporal distribution of solar radiation and wind; (3) to study the impact of greening technologies (green roofs, green walls, vegetation areas); and (4) to understand the impact of the outside microclimate on the indoor air temperature.

**Mechanical engineers:** For mechanical engineers, the coupling of the microclimate effects with the building energy model is extremely important to accurately estimate the building heating and cooling energy consumption and understand the peak consumption for a given building. This accurate estimation is important to size HVAC systems and assess the feasibility of district systems for large development projects like the Lower Hill District.

**Urban planners and policy makers:** Urban areas are highly complex systems with numerous interactions between the natural and the built environment. Keeping in mind climate change and global warming on a larger scale, it is important for urban planners and policy makers to understand how this larger scale phenomena affects the wind pattern, local climate and air quality. For a design case like the Lower Hill District, it is especially important to understand the solar access, natural ventilation strategies, green spaces and

material selection. All these factors have a direct impact on the behavior of the building system and more specifically the HVAC system.

**Investors and financial institutions:** Large-scale projects like the Lower Hill District, requires the attention of investors if the project is phased. The sizing of the mechanical system plays a vital role in the decision making for project phasing. In addition, a development that is designed keeping in mind global implications and minimizes the use of energy resources automatically attracts investors.

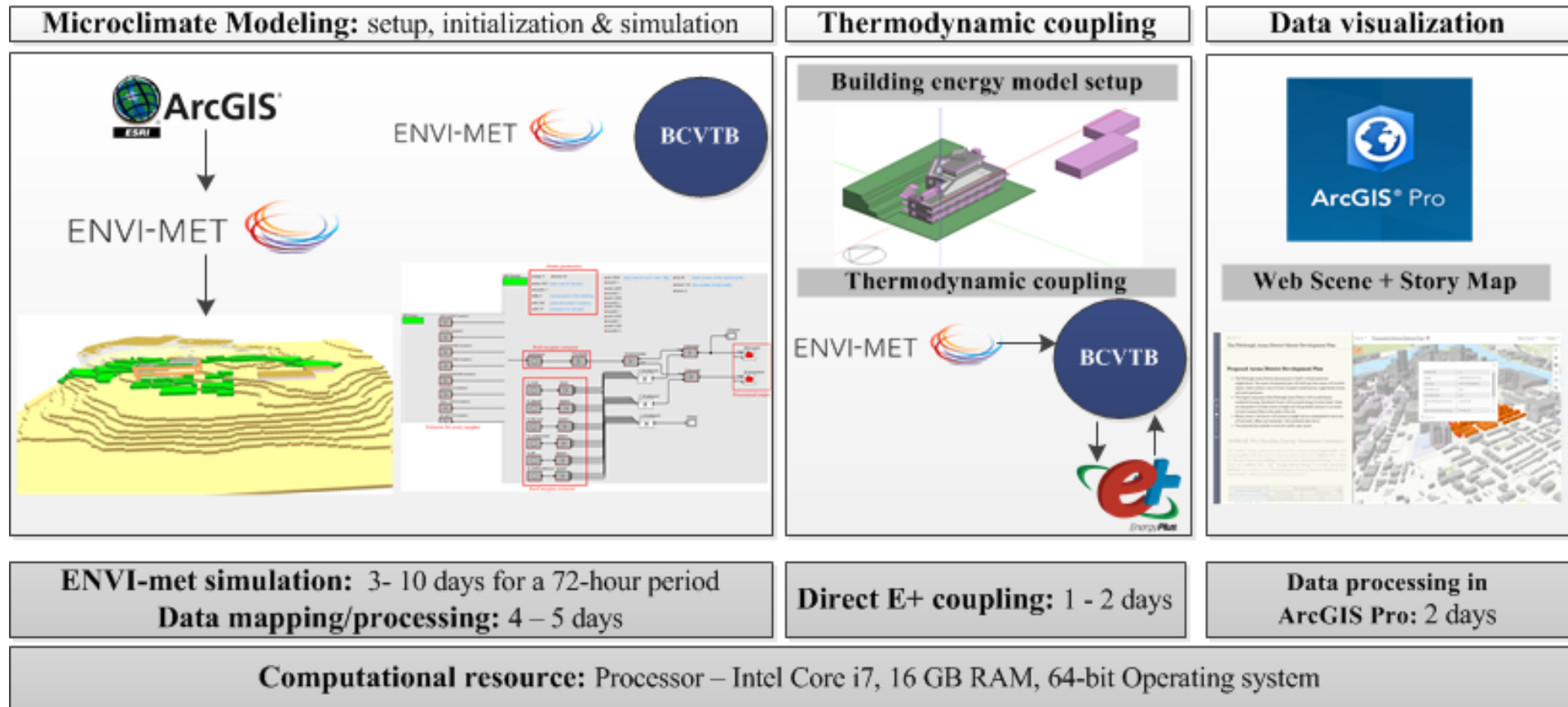


Figure 69. Industry applicability to implement the coupling method during conceptual design

### 6.3. Limitations

This section discusses the limitations of the method presented in this thesis. The first two limitations relate to the adoption of the coupling method by the design industry. The third limitation relates to obstacles of implementing the coupling module. Figure 69 details time and computational resource that are required to implement the coupling on a design case/

1. **Simulation time and computational resources:** The desktop configuration used for this thesis is an Intel Core i7, 64-bit operating system with a 16GB RAM. In order to complete one ENVI-met microclimate simulation for a 3-day period continuously, a high-resolution model incorporating all elements of the built environment (terrain, vegetation, surrounding buildings) takes approximately 8 – 10 days on a fairly high configuration windows desktop. If the same model is simulated for every 24 hours individually it takes 2 – 3 days to complete the simulations running simultaneously. Even the 2 -3-day time resource is considered a long waiting period for the industry stakeholders in comparison to an EnergyPlus simulations which takes only a few hours to complete the energy simulation. Industry stakeholders expect results within minutes if not seconds. Therefore, this is one of the main challenges when advocating to the industry to implement the coupling of the microclimate with the EnergyPlus model for energy prediction.
2. **Expert knowledge:** In depth knowledge of the usage of ENVI-met, BCVTB and EnergyPlus is required to implement this coupling method. Even if the coupling is implemented as direct coupling within EnergyPlus, knowledge of the EnergyPlus objects and input/output variables is extremely important to implement the coupling.

3. **Software limitations:** EnergyPlus Energy Management Actuators that are used to couple data from external sources have a limitation of 1024 values at a given simulation time. Therefore, for a building with many surfaces, it is not possible to directly couple ENVI-met simulated data with EnergyPlus without changing the number of values for data exchange within the EnergyPlus source code. However, modifying the EnergyPlus source code can be a cumbersome process and hence it is recommended to either simplify the EnergyPlus model (reduced number of surfaces) or couple the effects of the microclimate directly within EnergyPlus.

#### 6.4. Future work

This dissertation has presented a method to couple the effects of the microclimate with the building energy simulation tool EnergyPlus to accurately predict the building heating and cooling energy consumption. However, in the future, the method and its robustness can be improved to overcome the limitations discussed above.

1. Extended microclimate predictions for building controls and energy model calibration: The predicted microclimate parameters such as air temperature, relative humidity, global solar radiation, can be extended for an annual time period. This annual microclimate prediction can serve as inputs parameters for building control and building energy model calibration studies.
2. To reduce the ENVI-met simulation time specially to extend the microclimate predictions for an annual period, the proposed rule-based method in Chapter 3 can be expanded to include more weather variables such as wind speed, relative humidity, wind direction, and direct and diffuse solar radiation. After expanding this rule-based method to estimate the number of microclimate simulations required for an annual period, representative days can be selected and simulated

to cover the entire year. Then, through data mining, a method can be derived that can use representative simulated days for annual microclimate predictions. Therefore, this data mining method can eliminate the time-consuming ENVI-met simulations but also achieve high-fidelity weather data that would be based on representative ENVI-met simulations.

3. The ArcGIS and Web Scene visualization method can be extended to directly map EnergyPlus simulated results. EnergyPlus simulation provides hourly simulation results for every thermal zone. For engineers and designers, this is useful information to understand the building loads according to thermal zones. Therefore, by using python scripts and APIs in ArcGIS Pro, mapping and visualizing the high-fidelity simulated energy data is possible.

This page is intentionally left blank



## References

- Allegrini, J., Dorer, V., & Carmeliet, J. (2012). Analysis of convective heat transfer at building façades in street canyons and its influence on the predictions of space cooling demand in buildings. *Journal of wind engineering and industrial aerodynamics*, 104, 464-473.
- Allegrini, J., Dorer, V., & Carmeliet, J. (2012). Influence of the urban microclimate in street canyons on the energy demand for space cooling and heating of buildings. *Energy and Buildings*, 55, 823-832.
- Allegrini, J., Kämpf, J. H., Dorer, V., & Carmeliet, J. (2013). Modelling the urban microclimate and its influence on building energy demands of an urban neighbourhood. In *Proceedings of CISBAT 2013 Cleantech for Smart Cities and Buildings* (Vol. 2, No. EPFL-CONF-195701, pp. 867-872). EPFL Solar Energy and Building Physics Laboratory (LESO-PB).
- Ambrosini, D., Galli, G., Mancini, B., Nardi, I., & Sfarra, S. (2014). Evaluating mitigation effects of urban heat islands in a historical small center with the ENVI-Met® climate model. *Sustainability*, 6(10), 7013-7029.
- Asawa, T., Hoyano, A., & Nakaohkubo, K. (2008). Thermal design tool for outdoor spaces based on heat balance simulation using a 3D-CAD system. *Building and Environment*, 43(12), 2112-2123.
- Autodesk, Inc. *Project Dasher*. 2017. 6 February 2017.  
<https://www.autodeskresearch.com/projects/dasher>

Autodesk. *Autodesk Design Academy - AU Workshop*. 3 December 2016.

<http://auworkshop.autodesk.com/printpdf/1070>

Barnaby, C. S., & Crawley, D. B. (2011). Weather data for building performance simulation. *Building Performance Simulation for Design and Operation*, 37-55.

Berthou, T., Duplessis, B., Rivière, P., Stabat, P., Casetta, D., & Marchio, D. (2015). Smart-E: a tool for energy demand simulation and optimization at the city scale. *Building Simulation 2015*.

Bouyer, J., Inard, C., & Musy, M. (2011). Microclimatic coupling as a solution to improve building energy simulation in an urban context. *Energy and Buildings*, 43(7), 1549-1559.

Brandl, H. (2006). Energy foundations and other thermo-active ground structures. *Geotechnique*, 56(2), 81-122.

Bruse, M., & Fler, H. (1998). Simulating surface–plant–air interactions inside urban environments with a three dimensional numerical model. *Environmental Modelling & Software*, 13(3), 373-384.

Bruse, M. ENVI-met documentation.16.04.2016, 2004a.

<http://www.envi-met.com/documents/Envimet30.PDF>

Bueno, B., Norford, L., Pigeon, G., & Britter, R. (2011). Combining a detailed building energy model with a physically-based urban canopy model. *Boundary-layer meteorology*, 140(3), 471-489.

Bueno, B., Pigeon, G., Norford, L. K., Zibouche, K., & Marchadier, C. (2012). Development and evaluation of a building energy model integrated in the TEB scheme.

Bueno, B., Pigeon, G., Norford, L. K., & Zibouche, K. (2011). Development and evaluation of a building energy model integrated in the TEB scheme. *Geoscientific Model Development Discussions*, 4(4), 2973-3011.

Building components and building elements – thermal resistance and thermal transmittance – calculation method (ISO 6946: 2007), German version EN ISO 6946.

CHATZIDIMITRIOU, A., LIVERIS, P., BRUSE, M., & TOPLI, L. Urban Redevelopment and Microclimate Improvement.

Center for Computational Technologies Private Limited. *simulationHub*. 6 February 2017.

<https://www.simulationhub.com/>

Clarke, J. A. (2001). *Energy simulation in building design*. Routledge.

Chen, L., Ng, E., An, X., Ren, C., Lee, M., Wang, U., & He, Z. (2012). Sky view factor analysis of street canyons and its implications for daytime intra-urban air temperature differentials in high-rise, high-density urban areas of Hong Kong: a GIS-based simulation approach. *International Journal of Climatology*, 32(1), 121-136.

Conry, P., Sharma, A., Potosnak, M. J., Leo, L. S., Bensman, E., Hellmann, J. J., & Fernando, H. J. (2015). Chicago's heat island and climate change: bridging the scales via dynamical downscaling. *Journal of Applied Meteorology and Climatology*, 54(7), 1430-1448.

Crawley, D. B., Hand, J. W., Kummert, M., & Griffith, B. T. (2008). Contrasting the capabilities of building energy performance simulation programs. *Building and environment*, 43(4), 661-673.

Crawley, D. B. (2008). Estimating the impacts of climate change and urbanization on building performance. *Journal of Building Performance Simulation*, 1(2), 91-115.

Daniel, Staley. *Urban heat islands – What are they and why are they a big deal?* 01 March 2017.

<https://blog.oup.com/2015/08/urban-heat-islands/>

Defraeye, T., Blocken, B., & Carmeliet, J. (2011). Convective heat transfer coefficients for exterior building surfaces: Existing correlations and CFD modelling. *Energy Conversion and Management*, 52(1), 512-522.

ENVI-MET. *ENVI-met Model Architecture*. 2 March 2017.

<http://www.envi-met.info/hg2e/doku.php?id=intro:modelcnept>

ESRI, Environmental Systems Research Institute. *ArcGIS Pro - Help*. 19 April 2017.

<https://pro.arcgis.com/en/pro-app/help/sharing/overview/web-scene-layer.htm>

ESRI, Environmental Systems Research Institute. *Story Maps*. 19 April 2017.

<https://storymaps.arcgis.com/en/>

Giridharan, R., & Kolokotroni, M. (2009). Urban heat island characteristics in London during winter. *Solar Energy*, 83(9), 1668-1682.

Gros, A., Bozonnet, E., & Inard, C. (2014). Cool materials impact at district scale— Coupling building energy and microclimate models. *Sustainable Cities and Society*, 13, 254-266.

Group, Urban Heat Island. *Urban Heat Island Group*. 16 January 2017.

<http://www.urbanheatislands.com/>

Gusson, C. S., & Duarte, D. H. (2016). Effects of Built Density and Urban Morphology on Urban Microclimate-Calibration of the Model ENVI-met V4 for the Subtropical Sao Paulo, Brazil. *Procedia Engineering*, 169, 2-10.

Hamilton, John. *Bloomington.gov*. 2017.

[https://bloomington.in.gov/documents/viewDocument.php?document\\_id=7061](https://bloomington.in.gov/documents/viewDocument.php?document_id=7061)

Hassid, S., Santamouris, M., Papanikolaou, N., Linardi, A., Klitsikas, N., Georgakis, C., & Assimakopoulos, D. N. (2000). The effect of the Athens heat island on air conditioning load. *Energy and Buildings*, 32(2), 131-141.

He, J., & Hoyano, A. (2009). A 3D CAD-based simulation tool for prediction and evaluation of the thermal improvement effect of passive cooling walls in the developed urban locations. *Solar energy*, 83(7), 1064-1075.

Howard, B., Parshall, L., Thompson, J., Hammer, S., Dickinson, J., & Modi, V. (2012). Spatial distribution of urban building energy consumption by end use. *Energy and Buildings*, 45, 141-151.

Huttner, S. (2012). Further development and application of the 3D microclimate simulation ENVI-met. *Johannes Gutenberg-Universität, Mainz*.

Huttner, S., & Bruse, M. (2009, June). Numerical modeling of the urban climate—a preview on ENVI-met 4.0. In *7th International Conference on Urban Climate ICUC-7, Yokohama, Japan* (Vol. 29).

Ihara, T., Kikegawa, Y., Asahi, K., Genchi, Y., & Kondo, H. (2008). Changes in year-round air temperature and annual energy consumption in office building areas by urban heat-island countermeasures and energy-saving measures. *Applied Energy*, 85(1), 12-25.

Karaguzel, O. T. (2013). *Simulation-Based Parametric Analysis of Building Systems Integrative Solar Photovoltaics* (Doctoral dissertation, Carnegie Mellon University).

Kapsomenakis, J., Kolokotsa, D., Nikolaou, T., Santamouris, M., & Zerefos, S. C. (2013). Forty years increase of the air ambient temperature in Greece: The impact on buildings. *Energy Conversion and Management*, 74, 353-365.

Kikegawa, Y., Genchi, Y., Kondo, H., & Hanaki, K. (2006). Impacts of city-block-scale countermeasures against urban heat-island phenomena upon a building's energy-consumption for air-conditioning. *Applied Energy*, 83(6), 649-668.

Kolokotroni, M., Davies, M., Croxford, B., Bhuiyan, S., & Mavrogianni, A. (2010). A validated methodology for the prediction of heating and cooling energy demand for buildings within the Urban Heat Island: Case-study of London. *Solar Energy*, 84(12), 2246-2255.

Kolokotroni, M., Ren, X., Davies, M., & Mavrogianni, A. (2012). London's urban heat island: Impact on current and future energy consumption in office buildings. *Energy and buildings*, 47, 302-311.

Kolokotroni, M., Giannitsaris, I., & Watkins, R. (2006). The effect of the London urban heat island on building summer cooling demand and night ventilation strategies. *Solar Energy*, 80(4), 383-392.

Lahme, E., & Bruse, M. (2003, September). Microclimatic effects of a small urban park in densely built-up areas: measurements and model simulations. In *Fifth International Conference on Urban Climate (ICUC5) Lodz* (pp. 1-5).

Lam, K. (2012). Sustainability Performance Simulation Tools for Building Design. In R. A. Meyers, *Encyclopedia of Sustainability, Science and Technology* (pp. 10192-10260). Springer.

LBNL, Simulation Research Group. *Building Controls Virtual Test Bed*. 27 March 2017.

<http://simulationresearch.lbl.gov/projects/building-controls-virtual-test-bed>

Magli, S., Lodi, C., Lombroso, L., Muscio, A., & Teggi, S. (2015). Analysis of the urban heat island effects on building energy consumption. *International Journal of Energy and Environmental Engineering*, 6(1), 91-99.

Malys, L., Musy, M., & Inard, C. (2015). Microclimate and building energy consumption: Study of different coupling methods. *Advances in Building Energy Research*, 9(2), 151-174.

Masson, V. (2000). A physically-based scheme for the urban energy budget in atmospheric models. *Boundary-layer meteorology*, 94(3), 357-397.

Masson, V., Grimmond, C. S. B., & Oke, T. R. (2002). Evaluation of the Town Energy Balance (TEB) scheme with direct measurements from dry districts in two cities. *Journal of applied meteorology*, 41(10), 1011-1026.

Mavrogianni, A., Davies, M., Batty, M., Belcher, S. E., Bohnenstengel, S. I., Carruthers, D., ... & Giridharan, R. (2011). The comfort, energy and health implications of London's urban heat island. *Building Services Engineering Research and Technology*, 32(1), 35-52.

Nations, United. "World Urbanization Prospects." Highlights., 2014.

NREL. *National Solar Radiation Data Base: 1991-2005 Update: Typical Meteorological Year 3*. 20 March 2017.

[http://rredc.nrel.gov/solar/old\\_data/nsrdb/1991-2005/tmy3/](http://rredc.nrel.gov/solar/old_data/nsrdb/1991-2005/tmy3/)

Oke, T. R. (1973). City size and the urban heat island. *Atmospheric Environment* (1967), 7(8), 769-779.

Oke, T. R. (1982). The energetic basis of the urban heat island. *Quarterly Journal of the Royal Meteorological Society*, 108(455), 1-24.

Oxizidis, S. I. M. E. O. N., Dudek, A. V., & Papadopoulos, A. M. (2008). A computational method to assess the impact of urban climate on buildings using modeled climatic data. *Energy and Buildings*, 40(3), 215-223.

Padsala, R., & Coors, V. (2015, November). Conceptualizing, Managing and Developing: A Web Based 3D City Information Model for Urban Energy Demand Simulation. In *UDMV* (pp. 37-42).

Page, J., Basciotti, D., Pol, O., Fidalgo, J. N., Couto, M., Aron, R., ... & Fournié, L. (2013, August). A multi-energy modeling, simulation and optimization environment for urban energy infrastructure planning. In *Proceedings of the 13th conference of international building performance simulation association, Chambéry, France* (pp. 26-28).

Pillai, S. S., & Yoshie, R. (2013). Flow Velocity and Surface Temperature Effects on Convective Heat Transfer Coefficient from Urban Canopy Surfaces by Numerical Simulation. *Journal of Urban and Environmental Engineering (JUEE)*, 7(1).

Peng, C., & Elwan, A. F. (2012). Bridging outdoor and indoor environmental simulation for assessing and aiding sustainable urban neighbourhood design. *International Journal of Architectural Research*, 6(3), 72-90.

Pennsylvania State University & National Center for Atmospheric Research, UCAR *MM5 Community model*. 5 01 2016.

<http://www2.mmm.ucar.edu/mm5/mm5-home.html>

Pigeon, G., Moscicki, M. A., Voogt, J. A., & Masson, V. (2008). Simulation of fall and winter surface energy balance over a dense urban area using the TEB scheme. *Meteorology and Atmospheric Physics*, 102(3), 159-171.

Ptolemaeus, Claudius. (2014). *System Design, Modeling, and Simulation - Using Ptolemy II*. Manual. Mountain View: Creative Commons.

Ramesh, Shalini, et al. (2013) "Urban Energy Information Modelling: An interactive platform to communicate simulation-based high fidelity building energy analysis using Geographical Information Systems (GIS)." *Proceedings of Building Simulation*. Chambéry: International Building Performance Simulation Association (IBPSA), 1136-1143.

Ramesh, S., & Lam, K. P. (2015). Urban Energy Information Modeling—A Framework for Coupling Macro-Micro Factors Affecting Building Energy Consumption.

*Proceedings of Building Simulation*. Hyderabad: International Building Performance Simulation Association (IBPSA), 601-608.

Robinson, D., Haldi, F., Kämpf, J., Leroux, P., Perez, D., Rasheed, A., & Wilke, U. (2009, July). CitySim: Comprehensive micro-simulation of resource flows for sustainable urban planning. In *Proc. Building Simulation* (pp. 1614-1627).

Rong, F. (2006). *Impact of urban sprawl on US residential energy use* (Doctoral dissertation).

Salata, F., Golasi, I., de Lieto Vollaro, R., & de Lieto Vollaro, A. (2016). Urban microclimate and outdoor thermal comfort. A proper procedure to fit ENVI-met simulation outputs to experimental data. *Sustainable Cities and Society*, 26, 318-343.

Santamouris, M. (2014). On the energy impact of urban heat island and global warming on buildings. *Energy and Buildings*, 82, 100-113.

Santamouris, M., Papanikolaou, N., Livada, I., Koronakis, I., Georgakis, C., Argiriou, A., & Assimakopoulos, D. N. (2001). On the impact of urban climate on the energy consumption of buildings. *Solar energy*, 70(3), 201-216.

Schoetter, Robert, Aude Lemonsu and Valéry Masson. (2015). *The Town Energy Balance (TEB): An urban surface parametrisation developed at Météo France*. Toulouse, France: CNRM-GAME.

Shi, Y., Ren, C., Zheng, Y., & Ng, E. (2016). Mapping the urban microclimatic spatial distribution in a sub-tropical high-density urban environment. *Architectural Science Review*, 59(5), 370-384.

Schrag, Mary. *Green Building Alliance*. 06 March 2017.

<https://www.go-gba.org/tag/philipps-conservatory-and-botanical-gardens/>

Simon, H. (2016). *Modeling urban microclimate: development, implementation and evaluation of new and improved calculation methods for the urban microclimate model ENVI-met* (Doctoral dissertation, Mainz, Univ., Diss., 2016).

Sun, Y., & Augenbroe, G. (2014). Urban heat island effect on energy application studies of office buildings. *Energy and Buildings*, 77, 171-179.



The Department of Energy (DOE). (2015). "EnergyPlus Documentation - Engineering Reference, The Reference to EnergyPlus Calculations." Reference Guide.

The Department of Energy (DOE). (2015). "EnergyPlus Documentation - Input Output Reference: The Encyclopedic Reference to EnergyPlus Input and Output." Reference Guide.

Thomas, D., Miller, C., Kämpf, J., & Schlueter, A. (2014). Multiscale co-simulation of EnergyPlus and CitySim models derived from a building information model. In *Bausim 2014: Fifth German-Austrian IBPSA Conference*.

United Nations. (2015, July 29). *Sustainable Development Goals*. Retrieved January 3, 2017, from Department of Public Information, United Nations:  
<http://www.un.org/sustainabledevelopment/blog/2015/07/un-projects-world-population-to-reach-8-5-billion-by-2030-driven-by-growth-in-developing-countries/>

U.S. Energy Information Administration (EIA). *Independent statistics and Analysis*.2  
March 2017

<https://www.eia.gov/>

Wang, Y., & Akbari, H. (2015). Development and application of 'thermal radiative power' for urban environmental evaluation. *Sustainable Cities and Society*, 14, 316-322.

Wang, Y., Berardi, U., & Akbari, H. (2016). Comparing the effects of urban heat island mitigation strategies for Toronto, Canada. *Energy and Buildings*, 114, 2-19.

Western Pennsylvania Regional Data Center. *WPRDC*. 24 April 2017.

<https://www.wprdc.org/>

Wetter, M. (2011). Co-simulation of building energy and control systems with the Building Controls Virtual Test Bed. *Journal of Building Performance Simulation*, 4(3), 185-203.

Wetter, Michael. *Building Controls Virtual Test Bed*. Manual. (2016). Berkeley: Lawrence Berkeley National Laboratory (LBNL).

Wilcox, S., & Marion, W. (2008). *Users manual for TMY3 data sets* (pp. 4-5). Golden, CO: National Renewable Energy Laboratory.

Yaghoobian, N., & Kleissl, J. (2012). An indoor–outdoor building energy simulator to study urban modification effects on building energy use–Model description and validation. *Energy and Buildings*, 54, 407-417.

Yang, X., Zhao, L., Bruse, M., & Meng, Q. (2012). An integrated simulation method for building energy performance assessment in urban environments. *Energy and Buildings*, 54, 243-251.

Yang, X., Zhao, L., Bruse, M., & Meng, Q. (2013). Evaluation of a microclimate model for predicting the thermal behavior of different ground surfaces. *Building and Environment*, 60, 93-104.

Zhao, J. (2015). Design-Build-Operate Energy Information Modeling for Occupant-Oriented Predictive Building Control.


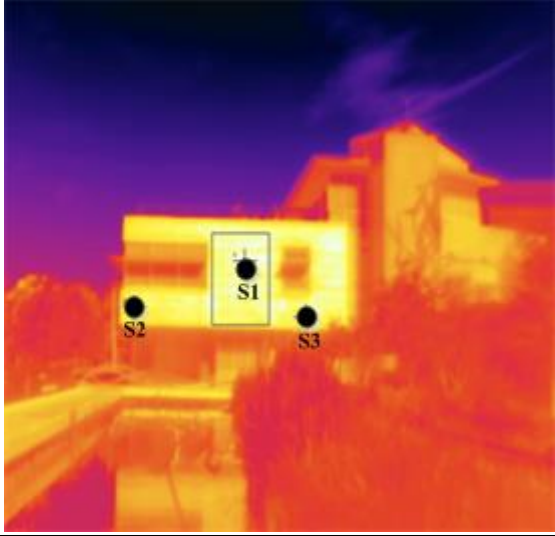
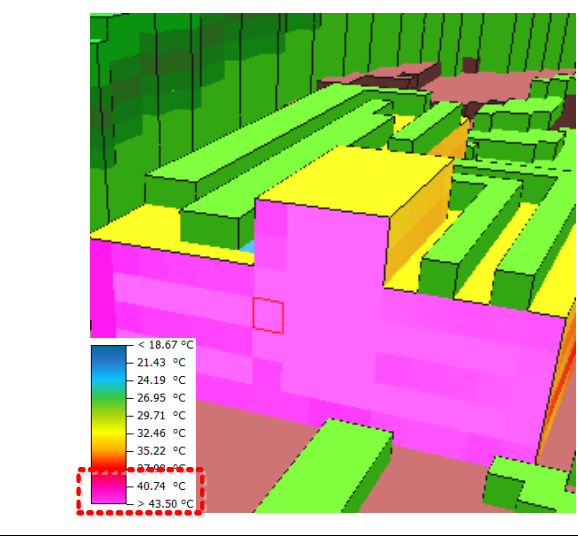
This page is intentionally left blank



## Appendices


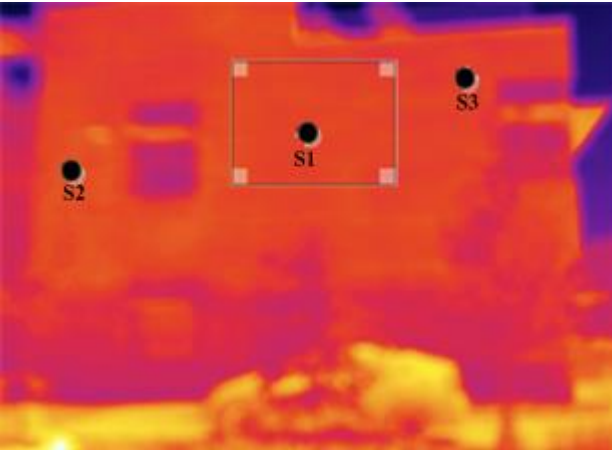

## Appendix A: Analysis of façade temperature for CSL case-study

### Comparison of simulated and measured east façade temperature

June 14, 2016 – 10:00am (East façade)		
		
Surface Temperature Measurement spot	FLIR Camera Measured (°C)	ENVI-met Simulated (°C)
Spot 1	43.2	44.67
Spot 2	39.3	40.03
Spot 3	40.4	42.5
Area Maximum	45.1	43.50 – 46.26
Area average	42.4	40.74 – 43.50

### Comparison of simulated and measured west façade temperature

June 14, 2016 – 2:00pm (West façade)

		
Surface Temperature Measurement spot	FLIR Camera Measured (°C)	ENVI-met Simulated (°C)
Spot 1	29.6	31.63
Spot 2	29.2	31.35
Spot 3	30.2	32.89
Area Maximum	30.2	31.01 – 34.73
Area average	29.5	31.73 – 33.2

## Appendix B: Synthesized workflow to implement visualization platform

**Step 1:** Develop & import CAD file of the Lower Hill District and the surroundings buildings

**Step 2:** Digitize the CAD plan for the Lower Hill District

- Use geoprocessing tool **Create feature class** to create polygon features that are z-enabled.
- On the Edit tab, use the **Create** button to digitize the CAD plan for the Lower Hill District buildings. This step is repeated for every building in the Lower Hill District.

**Step 3:** Convert 2D digitized CAD plan into 3D MultiPatch features

- Use geoprocessing tool **Extrude Feature** from the Facility tools toolbox to create 3D multipatch features by providing the building height for each building.

**Step 4:** Obtain 3D floor level details

- Use geoprocessing tool **Split floors** from the Facility tools toolbox to create floors from the 3D building multipatch. The floor are split by providing precise floor height for every floor of the building.

**Step 5:** Input simulated energy consumption data

- Use the **Add Field** button in the feature attribute table, to input the building level or floor level simulated energy data. This step is repeated for every building in the Lower Hill District.

**Step 6:** Develop 3D model of surrounding buildings using Pittsburgh3D shape file.

- On the **Appearance** tab, select **max height** extrusion to extrude the surrounding buildings based on the height attribute.

**Step 7:** Create Scene layer Package for Web Scene

- Use geoprocessing tool **Create Scene Layer Package** to generate a scene layer package (.slpk) from the input multipatch features.

**Step 8:** Upload scene layer package files to **ArcGIS Online** > My Content

